

NIST GCR 99-776

**THE EFFECT OF MINUTE WATER DROPLETS
ON A SIMULATED SPRINKLER LINK
THERMAL RESPONSE**

**F. Gavelli, P. Ruffino,
G. Anderson, M. di Marzo**

NIST

**United States Department of Commerce
Technology Administration
National Institute of Standards and Technology**

NIST GCR 99-776

**THE EFFECT OF MINUTE WATER DROPLETS
ON A SIMULATED SPRINKLER LINK
THERMAL RESPONSE**

Prepared for

**U.S. Department of Commerce
Building and Fire Research Laboratory
National Institute of Standards and Technology
Gaithersburg, MD 20899**

By

**F. Gavelli, P. Ruffino,
G. Anderson, M. di Marzo
University of Maryland
College Park, MD 20742**

June 1999

Issued July 1999



U.S. Department of Commerce

William M. Daley, *Secretary*

Technology Administration

Gary R. Bachula, *Acting Under Secretary for Technology*

National Institute of Standards and Technology

Raymond G. Kammer, *Director*

Notice

This report was prepared for the Building and Fire Research Laboratory of the National Institute of Standards and Technology under Grant number 60NANB8D0012. The statement and conclusions contained in this report are those of the authors and do not necessarily reflect the views of the National Institute of Standards and Technology or the Building and Fire Research Laboratory.

**THE EFFECT OF MINUTE WATER DROPLETS ON A
SIMULATED SPRINKLER LINK THERMAL RESPONSE**

F. Gavelli
P. Ruffino
G. Anderson
M. di Marzo

Department of Mechanical Engineering
University of Maryland
College Park, MD 20742

Submitted to the Building and Fire Research Laboratory,
National Institute of Standards and Technology
as the final report of Grant #60 NANB8D0012
for the period February 15, 1998 to May 1, 1999

June, 1999

EXECUTIVE SUMMARY

This report presents the derivation of an improved model for the prediction of the transient thermal response of a ceiling-mounted fire detection sprinkler link in the event of a fire. The model expands the range of applicability of the current approach to include the presence of minute water droplets being carried by the hot gas plume. This situation has been observed experimentally in situations where a fire develops in an enclosed space equipped with an array of sprinklers: the activation of the first sprinkler releases a fine water spray, part of which is entrained by the rising plume and affects the operation of the surrounding devices.

A new test facility has been built in order to verify the proposed model, as well as to investigate, in a controlled environment, the effect of the water droplets on different sprinkler links. The experimental results indicate that the model is able to describe the transient response of a sprinkler link immersed in a two-phase flow of hot gas and water droplets, and the assumptions made in deriving such model have been verified. Compatibility with the current sprinkler response model, in the absence of water droplets in the stream, has also been verified. Finally, numerical values have been obtained for the constants introduced with the proposed model. Future enhancements of the instrumentation capabilities will allow to broaden the range of conditions that can be tested.

TABLE OF CONTENTS

EXECUTIVE SUMMARY	i
TABLE OF CONTENTS	1
LIST OF FIGURES	3
NOMENCLATURE	4
1. INTRODUCTION	5
2. THEORETICAL FRAMEWORK.....	7
2.1. RESPONSE TIME INDEX (RTI) MODEL.....	7
2.2. EVAPORATIVE COOLING.....	9
2.2.1. DROPLET COLLECTION EFFICIENCY.....	11
2.2.2. MODIFIED SPRINKLER RESPONSE MODEL.....	14
3. FACILITY AND INSTRUMENTATION	15
3.1. FACILITY SETUP	15
3.1.1. BLOWER	18
3.1.2. GAS BURNER	19
3.1.3. WATER SPRAY NOZZLES	20
3.1.4. TEST SECTION AND SIMULATED SPRINKLER LINK.....	22
3.2. INSTRUMENTATION SETUP.....	23
3.2.1. TEMPERATURE MEASUREMENTS	24
3.2.2. OPTICAL MEASUREMENTS.....	25
4. EXPERIMENTS.....	26
4.1. REFORMULATION OF THE PROBLEM.....	27
4.2. EXPERIMENTAL PROCEDURE	28
4.3. TEST MATRIX	29
4.4. DATA ANALYSIS.....	31
4.4.1. MEASURE OF THE RESPONSE TIME INDEX	31

4.4.2. GAS VELOCITY MEASUREMENT	33
4.4.3. WATER VOLUMETRIC FRACTION MEASUREMENT	33
4.4.4. GAS TEMPERATURE MEASUREMENT	38
4.4.5. CALCULATION OF C.....	39
4.5. DETERMINATION OF THE DELAY TIME.....	41
5. CONCLUSIONS	42
6. REFERENCES	43
7. APPENDIX – STANDARDIZED TEST REPORTS.....	44

LIST OF FIGURES

Figure 1. Different types of ceiling-mounted fire sprinklers.....	5
Figure 2. Heat transfer between hot gas and fire sprinkler.....	7
Figure 3. Diagram for the evaporative cooling model.....	10
Figure 4. Potential flow solution for the gas around the sprinkler link.....	11
Figure 5. Trajectory of water droplets approaching the sprinkler link.....	13
Figure 6. Collection efficiency as a function of the droplet inertia term.....	14
Figure 7. Layout of the facility.....	16
Figure 8. Flow field across the circular orifice.....	17
Figure 9. Dayton blower.....	18
Figure 10. Natural gas burner.....	19
Figure 11. Gas burner control diagram.....	20
Figure 12. Water spray setup.....	21
Figure 13. PJ8 spray nozzle.....	22
Figure 14. Diagram of the test section.....	23
Figure 15. Thermocouple location.....	24
Figure 16. Optical setup for velocity and liquid fraction measurements.....	25
Figure 17. Snapshot of the water droplets in the gas stream.....	26
Figure 18. Measure of RTI from a dry test.....	32
Figure 19. RTI values for different tests.....	32
Figure 20. Picture of the droplets crossing the test section (negative).....	33
Figure 21. Droplet Size Distribution for the PJ8 Nozzle.....	34
Figure 22. Droplet Size Distribution for the PJ10 Nozzle.....	35
Figure 23. Normalized droplet volume versus the number of droplets.....	36
Figure 24. Variation of n_0 with the gas velocity.....	37
Figure 25. Water spray distribution through the test section.....	37
Figure 26. Temperatures profile along the duct, in dry and in wet conditions.....	38
Figure 27. Transient link temperature during wet and dry tests.....	40
Figure 28. Values of C for the different tests.....	41
Figure 29. Time delay.....	42

NOMENCLATURE

A	surface area [m ²]
Bi	Biot number
c	specific heat [J/(kg K)]
D	diameter [m]
G	water mass flux [kg/(m ² s)]
h	convective heat transfer coefficient [W/(m ² K)]
k	thermal conductivity [W/(m K)]
L	sprinkler link length [m]
Nu	Nusselt number
Pr	Prandtl number
Re	Reynolds number
T	absolute temperature [K]
U	free-stream gas velocity [m/s]
V	volume [m ³]

Subscripts

d	water droplet
g	gas
s	sprinkler link

Greek symbols

α	thermal diffusivity [m ² /s]
β	water volumetric fraction
ε	camera shutter speed [s]
Λ	latent heat of vaporization [kJ/kg]
ν	viscosity [m ² /s]
ρ	density [kg/m ³]
ξ	collection efficiency

Acronyms

RTI	Response Time Index
TC	Thermocouple

1. INTRODUCTION

Fire detection systems are installed in residential and commercial buildings to protect them and their occupants from fire. One of the most important characteristics of a fire detection system is the capability to detect a fire in the early stages, when it is still small. An early detection of the fire is important for two main reasons: first, because it allows more time for the evacuation of the occupants; second, because it increases the chances of successfully suppressing the fire before extensive damage is caused.

Different types of fire sprinklers are commercially available. The operating principle of these devices is based on the fact that the hot gas plume, generated by the fire, rises towards the ceiling and then spreads away from the fire location. In presence of a fire, therefore, a ceiling-mounted sprinkler will soon be engulfed by the hot gases. These fire sprinklers carry a small link, made of a temperature sensitive material, which constitutes the sensing component: when the hot gas reaches the sprinkler, the link is rapidly heated up until it fails. Upon breaking, the link causes the activation of a pressurized water spray, which is released into the space to try and extinguish the fire. Figure 1 shows some examples of commercially available fire sprinklers.

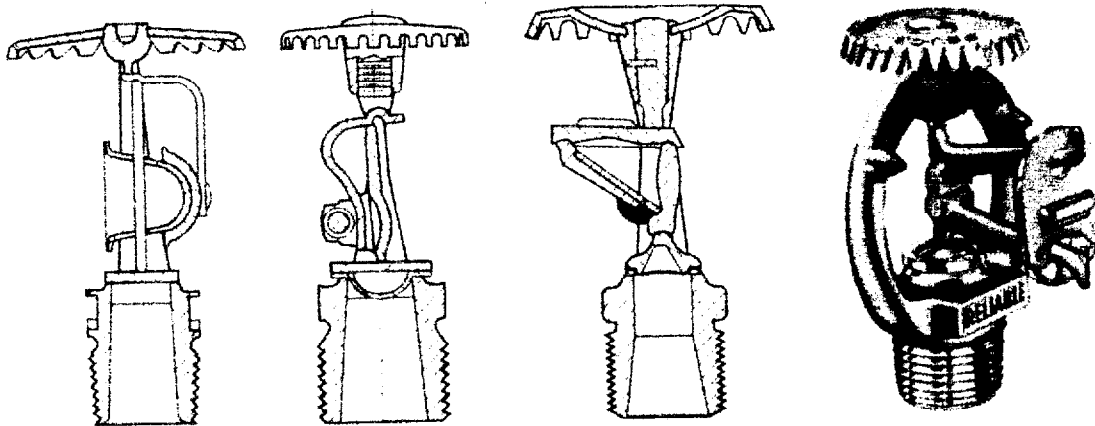


Figure 1. Different types of ceiling-mounted fire sprinklers

The time delay between the onset of the fire and the activation of the sprinkler depends upon several parameters, such as the placement of the sprinkler with respect to the fire, the dimensions of the enclosed space, the energy generated by the combustion and the “sensitivity” of the sprinkler. The latter depends on the size and composition of the metal link. Other conditions being equal, the sensitivity of a sprinkler is inversely proportional to the time required for the link to melt. Therefore, sprinklers are commonly rated according to their Response Time Index (RTI), which characterizes the rapidity of the sprinkler’s response to a fire. Table 1 shows the RTI values for some commercially available sprinklers (Central Sprinkler Company).

Sprinkler Type	RTI [(ms)^{1/2}]
Sprinkler "A"	170
Sprinkler "GB"	100

Table 1. RTI for commercially available fire sprinklers

The delay time for the activation of a given sprinkler can be predicted by applying the lumped heat capacity model to the metal link and calculating the transient response to hot gas flowing over it. This approach is commonly followed to determine the placement of fire sprinkler arrays in buildings. According to the model's predictions, the first sprinkler to activate will be the one closest to the location of the fire. If the water released by the first (primary) sprinkler is not sufficient to extinguish the fire, this will grow and the hot gases will reach the surrounding (secondary) sprinklers. Still according to the RTI model, the secondary sprinklers will also activate, after a certain time delay, and release more water on the fire. Therefore, the model is used to optimize the spacing between the sprinklers, in order to maximize the chance of extinguishing the fire without using too much water (which would cause other types of damages to the property).

Recent experiments on warehouse fires revealed a behavior of the sprinklers which does not correspond to the predictions of the RTI model. The primary sprinkler does indeed activate as predicted, but the secondary ones only respond after a much longer delay than suggested by the model. In some cases, the sprinklers immediately surrounding the primary do not activate at all, whereas those farther away do. These observations can be justified by considering the presence of water droplets in the gas plume following the activation of the primary sprinkler. In fact, part of the spray droplets does not reach the ground but are entrained and carried away by the ascending plume. Most of these droplets evaporate inside the plume, but a fraction of them travels far enough to reach the secondary sprinklers and impact on their surface. The subsequent evaporation of the droplets from the link surface produces a cooling effect, which delays the heating of the metal link.

The objective of this work is to provide a revised model for the sprinkler thermal response, which includes the evaporative cooling effect of the water droplets. An experimental apparatus is also built in order to validate the new model and provide quantitative values for the empirical constants that will be introduced. The model will be tested under a broad range of the governing parameters, which include the water droplets volumetric fraction and the gas stream temperature and velocity.

The following chapters describe the theoretical framework for the new model, the setup of the experimental facility and instrumentation, the experimental procedure and the results of the campaign.

2. THEORETICAL FRAMEWORK

2.1. Response Time Index (RTI) Model

The metal link of a ceiling-mounted fire sprinkler can be schematized as a cylinder placed vertically a few centimeters below the ceiling surface, as shown in Figure 2. The small dimensions of these components (about 6-10 mm in diameter and 20 mm long) and their relatively high thermal conductivity warrant the applicability of the lumped heat capacity method. Therefore, the energy balance for the link can be written as:

$$\rho_s V_s c_s \frac{dT_s}{dt} = q_{\text{conv}} + q_{\text{cond}} + q_{\text{rad}} \quad (1)$$

where the subscript 's' refers to the sprinkler link and q_{conv} , q_{cond} , q_{rad} are respectively the convective, conductive and radiative heat transfer components indicated in Figure 2.

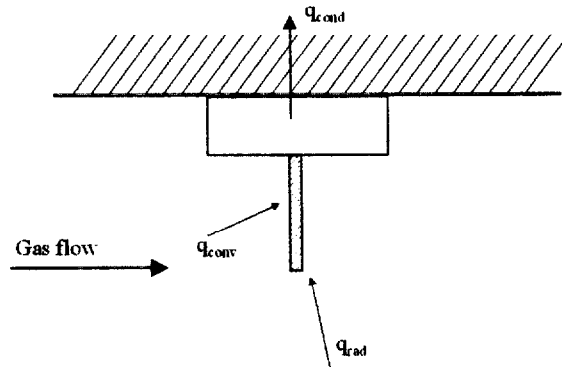


Figure 2. Heat transfer between hot gas and fire sprinkler

During the initial stages, the size of the fire is typically small, so the radiative heat transfer component can be neglected. The effect of conductive term can be properly quantified as described by Heskestad and Bill (1998). However the conductive term is typically negligible with respect to the convective part, since most commercial sprinklers are insulated from the rest of the unit (SFPE Handbook, 1995). Therefore, equation (1) reduces to:

$$\rho_s V_s c_s \frac{dT_s}{dt} = q_{\text{conv}} = h A_s (T_g - T_s) \quad (2)$$

where the subscript 'g' refers to the hot gas and h is the convective heat transfer coefficient.

Considering the link to be a cylinder of diameter D and length L , and introducing the Nusselt number ($Nu = h D / k_g$) into equation (2), the following is obtained:

$$\frac{dT_s}{dt} = \frac{4 k_g \alpha_s Nu}{\pi k_s D^2} (T_g - T_s) \quad (3)$$

The fluid mechanic interaction of the gas flow with the sprinkler link can be modeled as the cylinder in cross-flow problem. For this configuration, the correlation for the convective heat transfer presents a dependence of the Nusselt number on the Reynolds and Prandtl numbers as follows (Zakauskas, 1985):

$$Nu = C_1 Re^{0.5} Pr^{0.4} \quad (4)$$

The Reynolds and Prandtl numbers are defined, respectively, as:

$$Re = \frac{U D}{\nu_g} \quad (5)$$

where U is the free-stream gas velocity, and:

$$Pr = \frac{\nu_g}{\alpha_g} \quad (6)$$

The constant C_1 in equation (4) is equal to 0.52 for a cylinder in cross-flow. Because of the different boundary conditions between the actual problem and the cylinder in cross-flow (in particular, the far-field velocity profile), it is chosen to leave the numerical value of this constant unspecified. Experimental data will be used to determine the value of the constants that will appear in the final model equation.

Substituting equations (4, 5, 6) into (3) gives the following:

$$\frac{dT_s}{dt} = \left[C_2 \frac{k_g \alpha_s}{k_s \alpha_g} \nu_g^{0.5} Pr^{-0.6} D^{-3/2} \right] \sqrt{U} (T_g - T_s) \quad (7)$$

where $C_2 = (4 / \pi) C_1$. The term between square brackets is a function of the link geometry and of the thermophysical properties of link and fluid. For a given sprinkler, this term can be considered a constant over a wide range of temperatures. Its inverse is known as the Response Time Index (RTI) of the sprinkler link:

$$RTI = C_3 \frac{k_s \alpha_g}{k_g \alpha_s} \nu_g^{-0.5} Pr^{0.6} D^{3/2} \quad (8)$$

Introducing the above expression for RTI, the transient energy balance for the thermal link becomes:

$$\frac{dT_s}{dt} = \frac{\sqrt{U} (T_g - T_s)}{RTI} \quad (9)$$

which can be integrated with the initial condition $T_s(t=0) = T_{s,0}$ to give:

$$T_g - T_s(t) = (T_g - T_{s,0}) \exp \left[-\frac{\sqrt{U}}{RTI} t \right] \quad (10)$$

The Response Time Index has units of $[(m\ s)^{1/2}]$ and is indicative of the thermal inertia of the metal link. A sprinkler with a higher RTI will respond more slowly to the presence of hot gases, which causes a longer delay between the onset of the fire and the activation of the sprinkler. On the other hand, a very small RTI may cause the sprinkler to be activated by heat sources other than a fire. This is also undesirable, because of the damages that the water spray would cause to the property.

The time required for the activation of a ceiling-mounted fire sprinkler is calculated on the basis of equation (9), coupled with the ceiling-jet model which describes the spreading of the hot gases under the ceiling (Alpert 1975). The same model can be extended to the case of an array of sprinklers, in which case it provides the means to determine the optimum spacing between the sprinklers (SFPE Handbook, 1998).

However, recent experiments on fires in a warehouse revealed discrepancies between the predictions of the RTI model and the actual behavior of the different sprinklers. The model proved accurate in the simulation of the primary sprinkler (the one closest to the fire), but it could not accurately predict the response of the secondary sprinklers. These sprinklers, in fact, were observed to activate only after a much longer time than expected and, in some cases, they did not activate at all. The explanation for the deficiency of the RTI model is discussed in the next section, together with the derivation of a new theory that improves its predictive capabilities.

2.2. Evaporative Cooling

The RTI model described in the previous section does not consider the water that is sprayed on the fire plume when the primary sprinkler is activated. Previous studies (Alpert 1984) showed that part of the spray droplets does not reach the ground, but is entrained and carried away by the ascending plume. Therefore, the gas stream contains water droplets, and their presence must be taken into account. Indeed, the droplets even though progressively evaporate as they travel with the hot gas flow, part of them “survive” long enough to reach the surrounding fire sprinklers. When this happens, some droplets impact and deposit on the surface of the metal link; subsequently, the droplets evaporate by absorbing heat from the metal. This has a cooling effect on the link, which counteracts the heating process due to the hot gas flow. The net result is that the link takes a longer time to reach the melting point. If the evaporative effect is strong, it is even possible for the sprinkler to “fail”, that is, the link never melts so the spray does not actuate. If this scenario is considered, the previously described phenomenology of the warehouse fire experiments can be explained: before the actuation of the primary sprinkler, there is no water in the gas flow, therefore the RTI model is applicable. After water is sprayed on the fire, water droplets are carried with the gas stream and impact on the surrounding sprinklers, delaying their activation because of their evaporative cooling effect.

A revised model for the thermal response of a fire sprinkler link is proposed here, to overcome the deficiencies of the previous approach. As schematized in Figure 3, the new model includes an additional term (q_{evap}) in the energy balance for the thermal link (equation 2), to account for the evaporative cooling effect:

$$\rho_s V_s c_s \frac{dT_s}{dt} = q_{\text{conv}} - q_{\text{evap}} \quad (11)$$

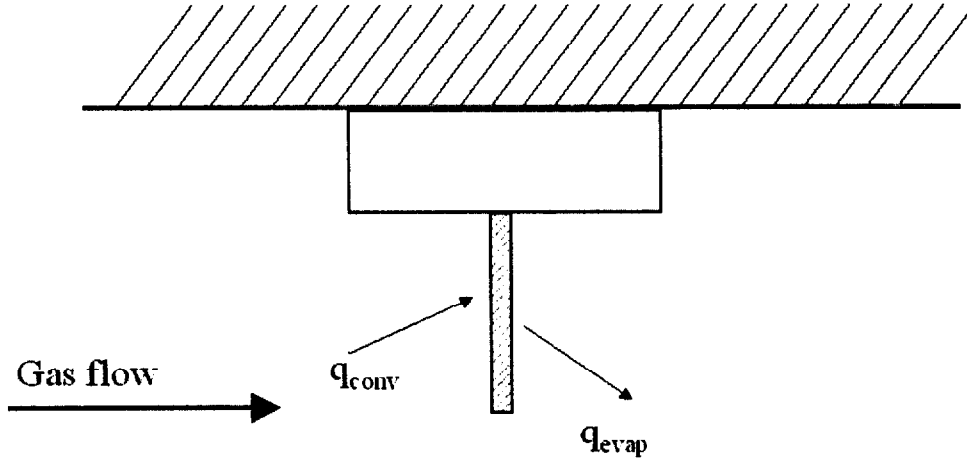


Figure 3. Diagram for the evaporative cooling model

The convective heat transfer term in equation (11) is treated just like in the RTI model. The evaporative cooling term is proportional to the mass flow rate of water droplets that deposit on the link surface. The following assumptions are made:

- The droplets in the gas stream are at saturated liquid conditions, therefore, the evaporative cooling per unit mass of water is equal to the latent heat of vaporization, Λ ;
- The droplet mass flux, G , is constant and uniform throughout the gas stream.

With these assumptions, the evaporative cooling term can be expressed as:

$$q_{\text{evap}} = \xi G A_s \Lambda \quad (12)$$

where ξ is the droplet collection efficiency of the sprinkler surface. The droplet collection efficiency takes into account the effect of the gas flow velocity on the droplets as they approach the sprinkler. The following section discusses the derivation of an expression for the droplet collection efficiency, ξ .

2.2.1. Droplet Collection Efficiency

The cylinder in cross-flow problem is used to model the fluid mechanic interaction of the link with the hot gas. The flow away from the cylinder has uniform velocity U , which is assumed to be aligned with the x -axis as shown in Figure 4. The potential flow theory is applied in order to obtain an approximate solution for the gas velocity field around the cylinder (Panton 1984):

$$\frac{u(x,y)}{U} = 1 - \frac{R^2(x^2 - y^2)}{(x^2 + y^2)^2} \quad (13)$$

$$\frac{v(x,y)}{U} = -\frac{2R^2xy}{(x^2 + y^2)^2} \quad (14)$$

where R is the radius of the sprinkler link. An example of the streamlines for the potential flow (13, 14) is shown in Figure 4.

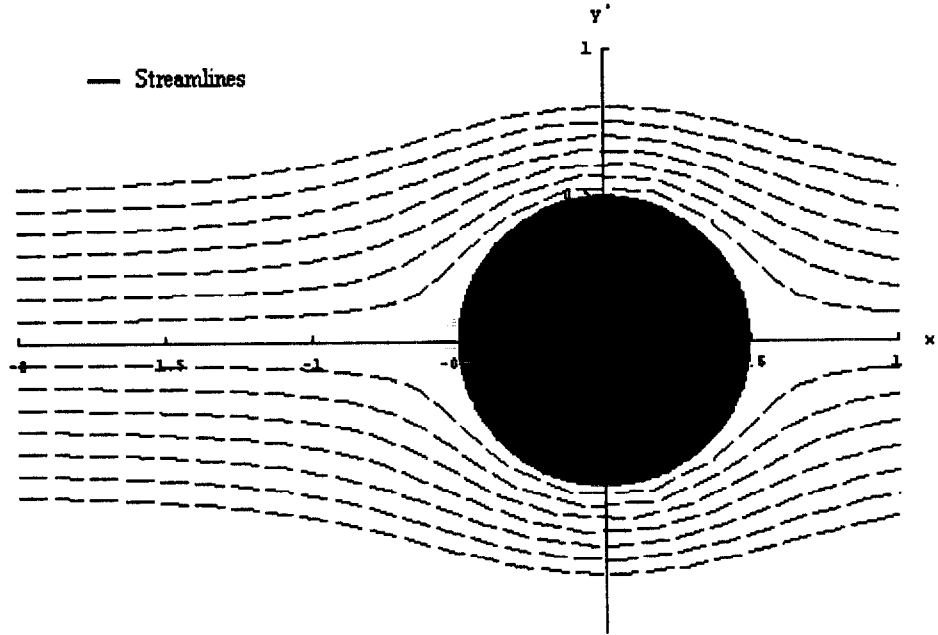


Figure 4. Potential flow solution for the gas around the sprinkler link

The behavior of the water droplets in the gas plume can be determined from the theory of dispersed flows (Crowe *et al.* 1998). For the typical water fraction obtained from fire sprinklers (about 10^{-6}), the average droplet spacing in the gas plume is very large (about 80 times the droplets diameter). Therefore, the droplet-droplet interactions are negligible and individual droplets can be treated as isolated.

Changes in the gas streamlines, such as those occurring near the sprinkler link, also affect the entrained droplets. However, the droplets present a certain inertia to these changes, which plays a fundamental role in determining their trajectory and, in particular, whether they impact the solid surface or not. In general, larger droplets respond rather

slowly, which makes them more likely to deposit on the link surface, while smaller droplets respond faster and, consequently, are more likely to escape the impact.

The collection efficiency provides a measure of the fraction of droplets that cannot avoid the cylindrical obstacle and deposit on its surface. To determine ξ we need to solve the equation of motion for a particle in a gas flow. Under the Stokes flow approximation, this becomes (Panton 1984):

$$m_d \frac{d\vec{v}_d}{dt} = 3\pi \mu D_d (\vec{v}_g - \vec{v}_d) \quad (15)$$

where the subscript 'd' indicates the droplet and 'g' the gas phase. Equation (15) can be non-dimensionalized by introducing the following quantities:

$$\vec{v}^* = \frac{\vec{v}}{U} \quad (16a)$$

$$\vec{x}^* = \frac{\vec{x}}{D_s} \quad (16b)$$

$$t^* = t \frac{D_s}{U} \quad (16c)$$

where D_s is the diameter of the sprinkler link and U is the free-stream velocity of the ceiling-jet. Therefore:

$$\frac{d\vec{v}_d^*}{dt} = \frac{9}{\left[\text{Re} \frac{D_d \rho_d}{D_s \rho_g} \right]} (\vec{v}_g^* - \vec{v}_d^*) \quad (17)$$

The quantity between square brackets represents the inertia of the droplet to changes in the flow field. Equation (17) can be solved numerically by using the potential flow solution for the gas velocity, v_g . This allows to determine the trajectories of individual droplets as a function of their initial position, y_i^* , in the free-stream region. An example of these trajectories is given in Figure 5.

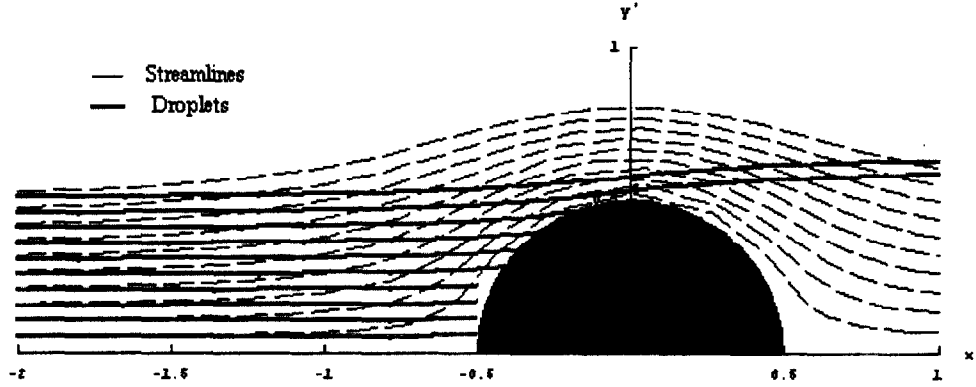


Figure 5. Trajectory of water droplets approaching the sprinkler link

From the solution of (17), for any given value of the inertia term it is possible to identify a critical distance, y_c^* , such that the droplets with $y_i^* \leq y_c^*$ impact the link surface, whereas those with $y_i^* > y_c^*$ flow around the obstacle. In the extreme case of droplets with infinite inertia, the changes in the gas flow field would have no effect on their trajectories. Therefore, they would continue traveling parallel to the x-axis, which means that all and only the droplets in the region $-1/2 < y < 1/2$ would deposit on the surface of the cylinder. The collection efficiency, ξ , is given by the ratio between the actual number of droplets depositing on the cylinder and those that would deposit if they had infinite inertia:

$$\xi = 2 y_c^* \quad (18)$$

The collection efficiency has been calculated over a wide range of values of the inertia term. The following curve has been found to best fit the results:

$$\xi(K) = \frac{K^{1.08}}{K^{1.08} + 8.80} - 0.04 \quad (19)$$

where $K = \text{Re}(D_d \rho_d) / (D_s \rho_g)$.

Figure 6 shows the fitted curve for the collection efficiency. For typical fire and sprinkler characteristics ($U=5$ m/s, $T_g=500$ K, $D_d=65\mu$), the value of K is centered around about 160. From the curve shown in Figure 6, the collection efficiency ξ is calculated to be in the order of 95%. Furthermore, the collection efficiency curve is near its asymptote in that region, which allows to approximate ξ as a constant. This assumption will be verified from the analysis of the experimental data.

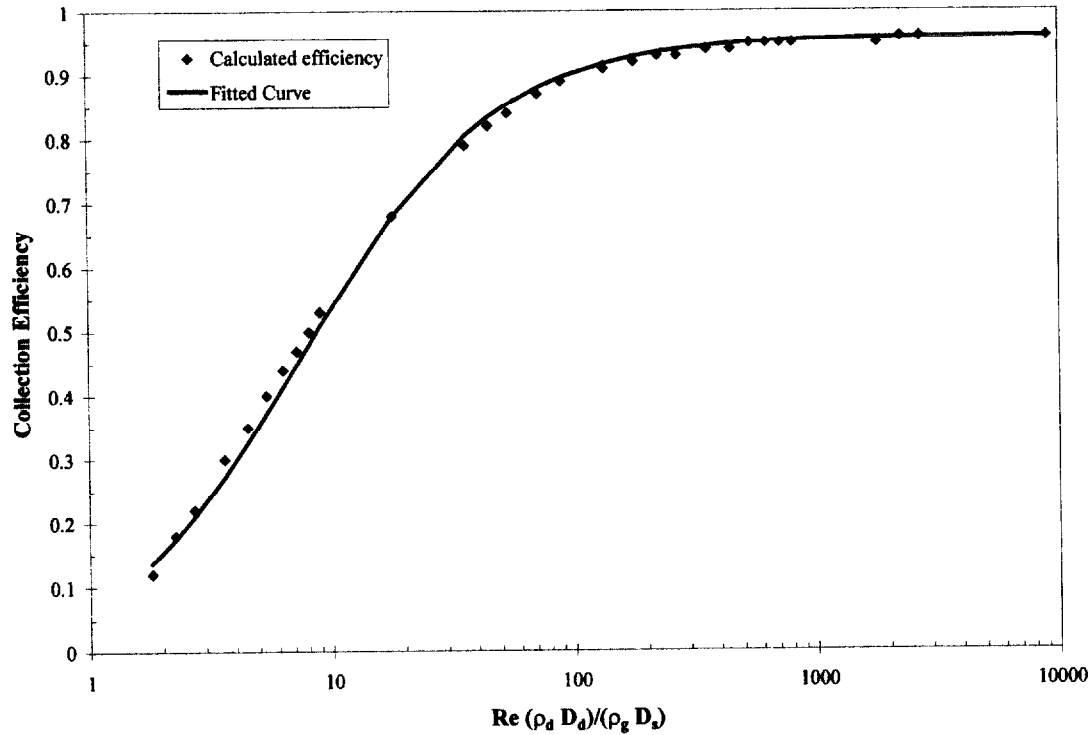


Figure 6. Collection efficiency as a function of the droplet inertia term

2.2.2. Modified Sprinkler Response Model

If the convective and evaporative heat transfer terms ((2), (12)) are introduced in the energy balance equation (11), the following is obtained:

$$\rho_s V_s c_s \frac{dT_s}{dt} = h A_s (T_g - T_s) - \xi G A_s \Lambda \quad (20)$$

The water mass flux, G , can be expressed in terms of the droplet velocity, U , and volumetric fraction, β , as follows:

$$G = \rho_d U \beta \quad (21)$$

The water volumetric fraction can be calculated as the ratio of the volumetric flow rates of water and hot gases through a given cross-section. However, because of the evaporation of the droplets in the gas stream, the value of β is largely dependent on the location under consideration, as well as on the gas temperature and water droplet size distribution. Therefore, local measurements of β are necessary in order to implement equation (21). Substituting equation (21) into (20) gives:

$$\frac{dT_s}{dt} = \frac{\sqrt{U}(T_g - T_s)}{RTI} - \frac{C U \beta}{RTI} \quad (22)$$

where RTI has the same expression as in (8) and C is given by:

$$C = C_4 \frac{e_d}{e_s} \frac{\xi \Lambda}{c_s D_s} RTI \quad (23)$$

Equation (22) represents the proposed new model for the thermal response of a sprinkler link in the presence of a flow of hot gas and water droplets. The experimental validation of the model, as well as the quantification of the constant C that appears in equation (22) are presented in following chapters.

3. FACILITY AND INSTRUMENTATION

The model presented in the previous chapter needs experimental validation. For this purpose, a new facility has been built in the Engineering Laboratory Building at the University of Maryland. The facility, known as the Evaporative Cooling Sensor Accuracy Test (ECSAT) is designed to allow the measurement of the thermal response of a simulated fire sprinkler link immersed in a hot gas flow. The characteristics of this system allow to perform accurate measurements of the link's behavior over a broad range of the main parameters, such as: gas temperature and velocity, water droplet volumetric fraction and size distribution. The following sections describe the setup of the experimental facility and the available instrumentation.

3.1. Facility Setup

Experimental facilities for the study of the sprinkler link thermal response typically consist of a closed-circuit duct in which a hot gas flow is established (UL199, 1995). Once the desired conditions are obtained, the sprinkler head is rapidly inserted into the gas flow, and the transient response is studied. This procedure is commonly known as a "plunge test"; the capability of creating steady-state gas flow conditions before inserting the link has the advantage of greatly simplifying the analysis of the data, which makes this the standard procedure for testing fire sprinkler performance.

For the present study, which involves a two-phase gas-droplet flow, the plunge-test approach is still applicable, although some modifications are necessary. The two-phase flow can still be adjusted until the desired conditions are obtained and a steady state is reached, before inserting the probe. However, the closed-circuit configuration cannot be maintained because of the presence of water droplets in the flow. In fact, the droplets sprayed into the hot gas rapidly evaporate, which causes the relative humidity of the gas mixture to increase. If the flow were recirculated, the continuous addition of water to the gas would alter the composition of the gas to the point where the droplet evaporation process would be affected. To maintain a low relative humidity in the gas stream, therefore, a once-through circuit is chosen as shown in Figure 7.

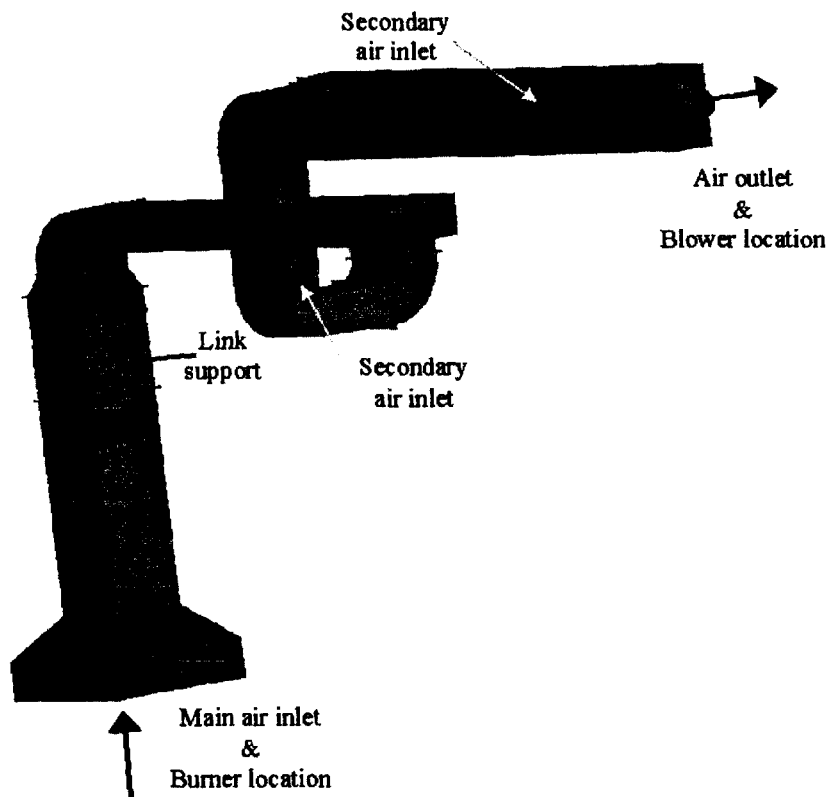


Figure 7. Layout of the facility

A blower placed near the outlet of the ductwork generates the gas flow inside the system. The air entering the is heated up by a natural gas burner, and then flows upward through a square duct section (60.96 cm x 60.96 cm). A honeycomb structure, about 20 cm thick and made of tightly packed steel wool, is placed in the initial portion of the duct. Its purpose is to force the gas stream to spread over the entire cross-section, as well as to obtain a more uniform temperature distribution. As the hot gas emerges from the honeycomb, it reaches the spray location. A finely atomized water spray is injected into the gas stream, simulating the effect of the activation of the primary sprinkler.

A square-edged circular orifice (25 cm diameter) is located about 49 cm downstream of the spray. The orifice represents an abrupt restriction of the cross-sectional area for the two-phase flow. The orifice induces a vena contracta in the flow, which is responsible for the near parallel streamline profile schematized in Figure 8.

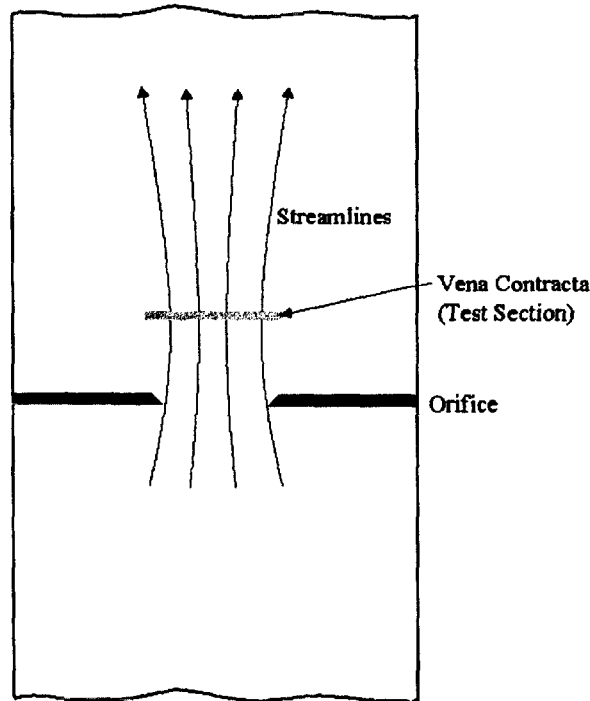


Figure 8. Flow field across the circular orifice

At the location of the vena contracta, which occurs about 0.9 diameters downstream of the orifice, the velocity field is parallel to the axis of the orifice (no radial velocity component). Because of this characteristic of the flow field, which simplifies the boundary conditions, the vena contracta is chosen as the test section for the plunge-test experiments. Figure 7 shows the location of the link support through which the simulated sprinkler link is inserted into the test section.

After the vena contracta, the flow spreads and returns to occupy the entire duct cross-section. About 1.5 m after the test section, the vertical duct is reduced to a rectangular cross section (30.48 cm x 60.96 cm) before turning to proceed horizontally. For the current set of experiments, the horizontal portion of the duct is simply utilized to cool down the hot gases before they reach the blower (which cannot operate above 70 °C). However, provisions have been made to allow the placement of additional instrumentation in this section, as required by future studies. The hot gas is cooled down by transferring heat to the duct walls as well as by mixing with the cold air drawn in through the secondary inlets indicated in Figure 7.

The entire duct is made of 1.6 mm-thick galvanized steel. To satisfy the safety regulations, which require the temperature of accessible surfaces to be below 50 °C, the portion of the ductwork located inside the laboratory is insulated with 5 cm thick ceramic fiber insulation and covered with a thin aluminum sheet. Due to space constraints inside the laboratory, the final section of the duct (after the C-shaped turn shown in Figure 7) is located above the laboratory ceiling. This part is left uninsulated, in order to accelerate the cooling of the hot gases and protect the blower from high-temperature damage.

The following sections describe the main components of the ECSAT facility, as well as the available instrumentation.

3.1.1. Blower

The gas flow in the duct is generated by a 1.5 horsepower blower (Dayton, model 4C119), shown in Figure 9. When installed in the ECSAT ductwork, the blower can establish a maximum flow rate of approximately 0.473 m³/s (1,000 cfm), which corresponds to a gas velocity of about 10.3 m/s in the vena contracta, at ambient temperature. Adjustable secondary air intakes are present at different locations along the duct, as shown in Figure 7. Varying the open area of these inlets provides control of the flow rate through the test section; the velocity in the vena contracta can be reduced to a minimum of about 3.0 m/s at ambient temperature.

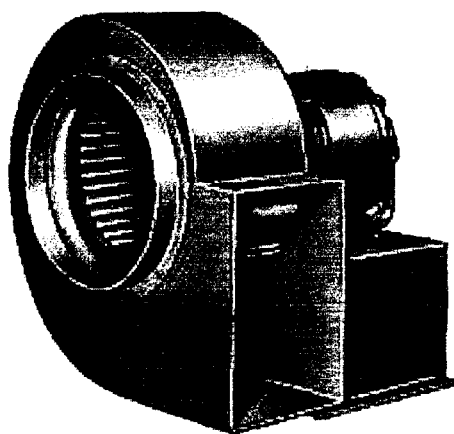


Figure 9. Dayton blower

The blower may be damaged if operating with gas temperatures in excess of 70°C. Therefore, the gas flow must be cooled down before it reaches the fan. As previously mentioned, the cooling is obtained by mixing the hot gas with the secondary air intakes. A temperature readout is available for the operator to monitor the gas temperature at the blower inlet. If the temperature approaches the safety limit, the operator can activate a set of three sprays that inject water into the final section of the duct, to provide additional cooling (the secondary air intakes cannot be modified during an experiment, because that

would also alter the flow rate through the test section). A safety temperature switch is also placed immediately upstream of the fan inlet. The switch cuts the power to the burner if the temperature exceeds the safety limit.

3.1.2. Gas Burner

The air entering the vertical section of the duct is heated up by a natural gas burner (Eclipse Combustion, model 200 "JIB-C2"), shown in Figure 10. The maximum power output is rated at 73.3 kW (250,000 Btu/hr). However, a setscrew placed along the gas inlet line can be used to reduce this value. Currently, the maximum power output for the burner is limited to about 44.0 kW (150,000 Btu/hr). Fine-tune adjustments of the burner power output are possible, during the setup phase of an experiment, by means of a remotely controlled gear motor which is connected to a butterfly valve placed on the gas line.

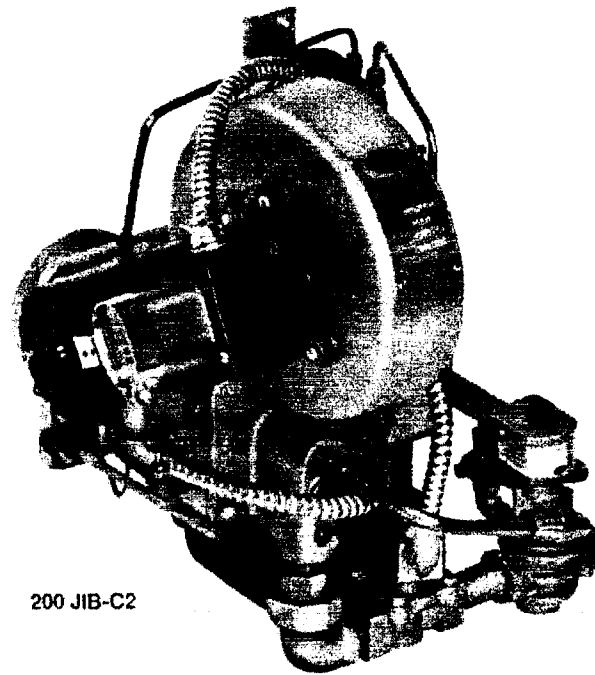


Figure 10. Natural gas burner

The natural gas is premixed with a forced air flow; the air/gas mixture is ignited by a pilot light. The gas flow to both the pilot light and the main combustion chamber is controlled by electrically activated solenoid valves. This allows the immediate shutdown of the combustion if the electrical circuit is opened, which can occur by intervention of the operator or automatically. The operator can control the burner from the control area,

along with the rest of the equipment and instrumentation: a switch powers the electrical circuit and another one controls the gear motor. Two temperature-activated safety switches are also connected in series with the main power switch: one is placed immediately upstream of the blower, to protect it from overheating; the other one is located in the hooded portion of the duct, to turn the burner off in case the air flow is unexpectedly interrupted. Figure 11 shows a schematic of the wiring of the gas burner controls.

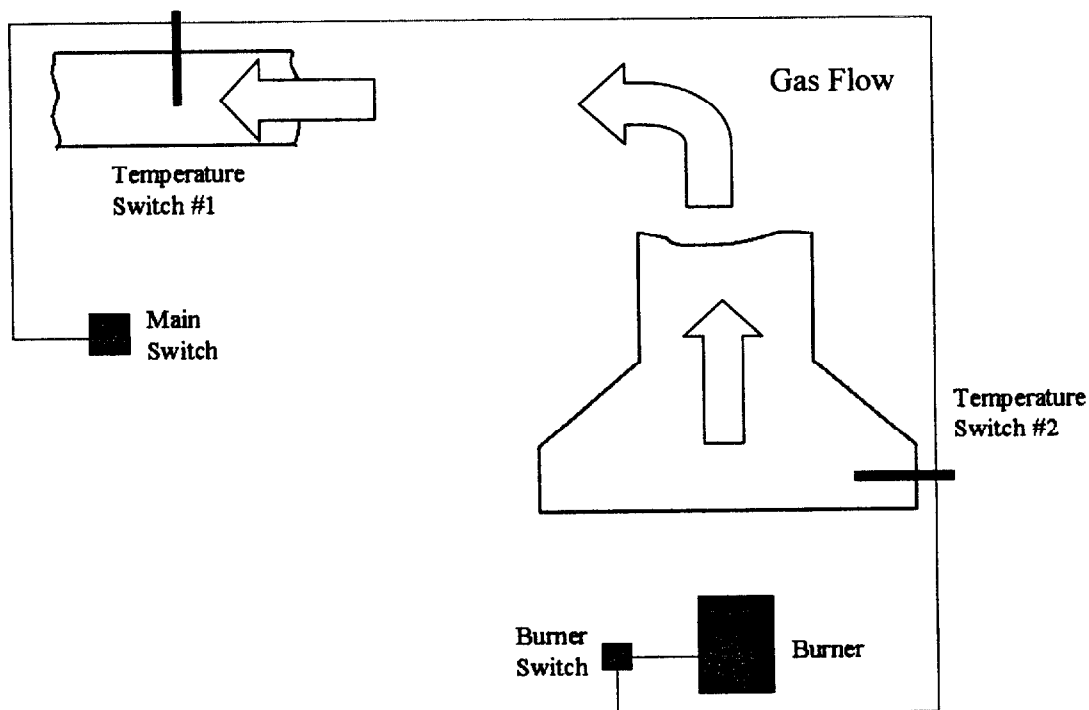


Figure 11. Gas burner control diagram

3.1.3. Water Spray Nozzles

Five spray nozzles are placed about 24 cm downstream of the steel wool honeycomb. When one or more of the nozzles are active, water droplets are released into the hot gas stream, which carries them towards the orifice as shown in Figure 12. The water flow is supplied by a variable-flow gear pump (Cole-Parmer, model GX-74011) which can deliver a maximum flow rate of 0.01 liters/second. The five nozzles are

independently controlled by ball valves, so that different spray flow rates can be obtained.

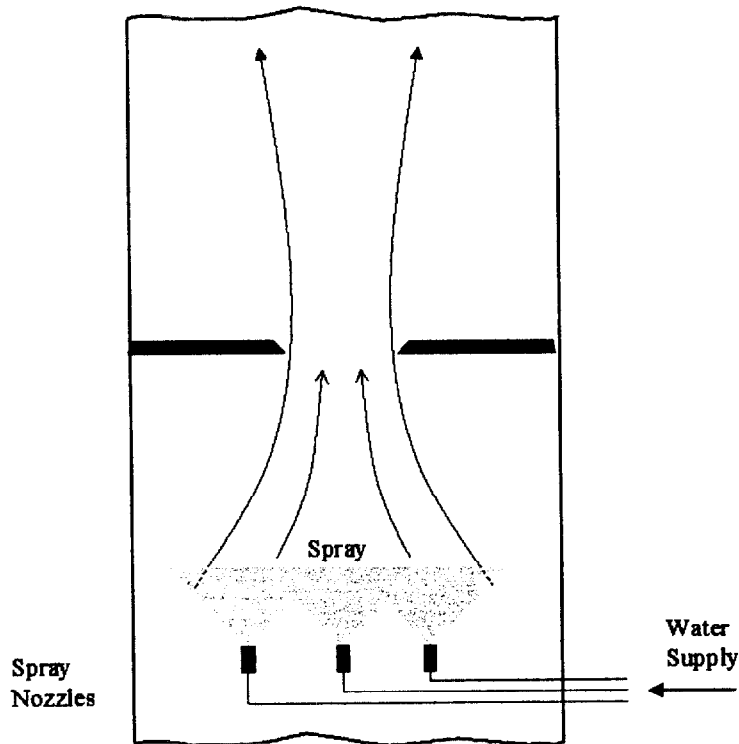


Figure 12. Water spray setup

Currently, only one nozzle is used at a time. Two different spray nozzle sizes are available (BETE Fog Nozzle, models PJ8 and PJ10), which allows to test the sprinkler response under different water flow rate and droplet size distribution. A PJ8 nozzle is shown in Figure 13. Table 2 reports some of the characteristics of the two nozzles at the nominal operating pressure of 482 kPa (70 psig); more detailed information can be found in Appendix.

	Flow Rate (l/s)	Sauter Mean Diameter (μm)	Volume Median Diameter (μm)
PJ8	$9.45 \cdot 10^{-4}$	50.0	65.0
PJ10	$1.42 \cdot 10^{-3}$	63.0	82.0

Table 2. Performance characteristics of PJ8 and PJ10 nozzles (@ 482 kPa)

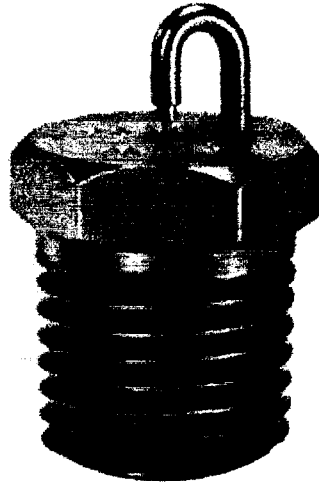


Figure 13. PJ8 spray nozzle

3.1.4. Test Section and Simulated Sprinkler Link

The test section is located in the vena contracta of the orifice, where the gas velocity is maximum and parallel to the axis of the aperture. This choice provides the cleanest possible boundary conditions for the study of the sprinkler link response to the gas-droplet flow.

As shown in Figure 14, the simulated link penetrates horizontally to the center of the test section. So far, two different links have been prepared for testing in the ECSAT facility. They both consist of aluminum cylinders, 2 cm long and with diameters, respectively, of 6.4 and 10 mm. The links are placed on a rigid ceramic insulator (61 cm long), in order to minimize the conductive heat losses to the support. Two type-K thermocouples are placed into the aluminum cylinder to measure its temperature during the plunge tests. The Biot number of the link is, in both cases, in the order of 10^{-4} . Therefore, the link can be modeled as a lumped heat capacity, consistently with the assumptions of the theoretical model presented in Chapter 2.

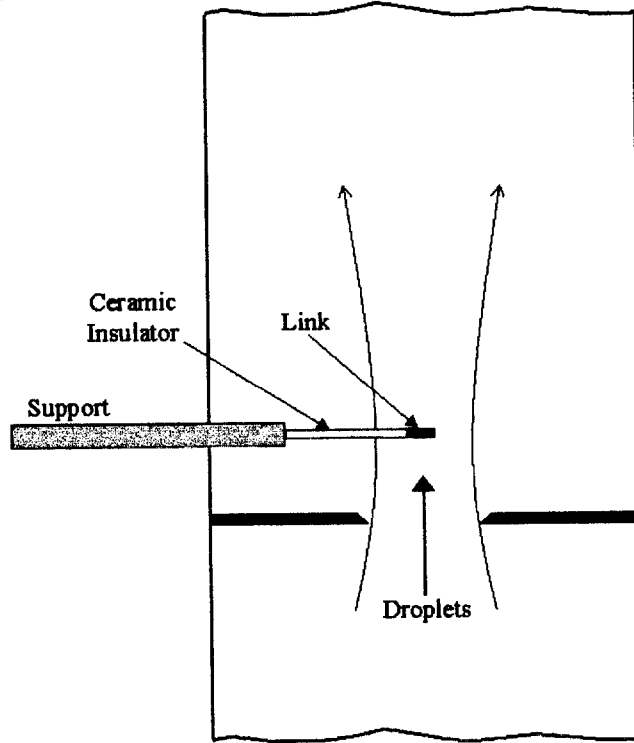


Figure 14. Diagram of the test section.

3.2. Instrumentation Setup

Several quantities need to be determined experimentally in order to validate the sprinkler link response model and quantify the constants that appear in the formulation (19), namely:

- Gas temperature, T_g
- Gas velocity, U
- Sprinkler link temperature, T_s
- Water volumetric fraction, β

The temperature measurements are obtained from several thermocouples, placed along the flow path and inside the link. The water volumetric fraction and the gas velocity, instead, are obtained by optical measurements. The details of the instrumentation setup and measurement techniques are explained in the following sections.

3.2.1. Temperature Measurements

A total of 13 type-K thermocouples (TCs) are inserted in the proximity of the test section. As previously mentioned, the simulated link cylinder carries two TCs, which measure the temperature response after the link has been inserted into the gas flow. Five more TCs are placed about 5 cm above the honeycomb (one at the center of the duct, the other 4 close to the walls), to ensure that the temperature of the hot air emerging from the steel wool is indeed uniform. The remaining 6 TCs are placed along the axis of the orifice, downstream of the test section. These probes are supported by a metal rake and are spaced about 15 cm apart from each other, as shown in Figure 15. The temperature measurements obtained from these probes allow to measure the cooling of the gas flow along the duct. This information is also used to infer at what distance from the test section all the water droplets have evaporated.

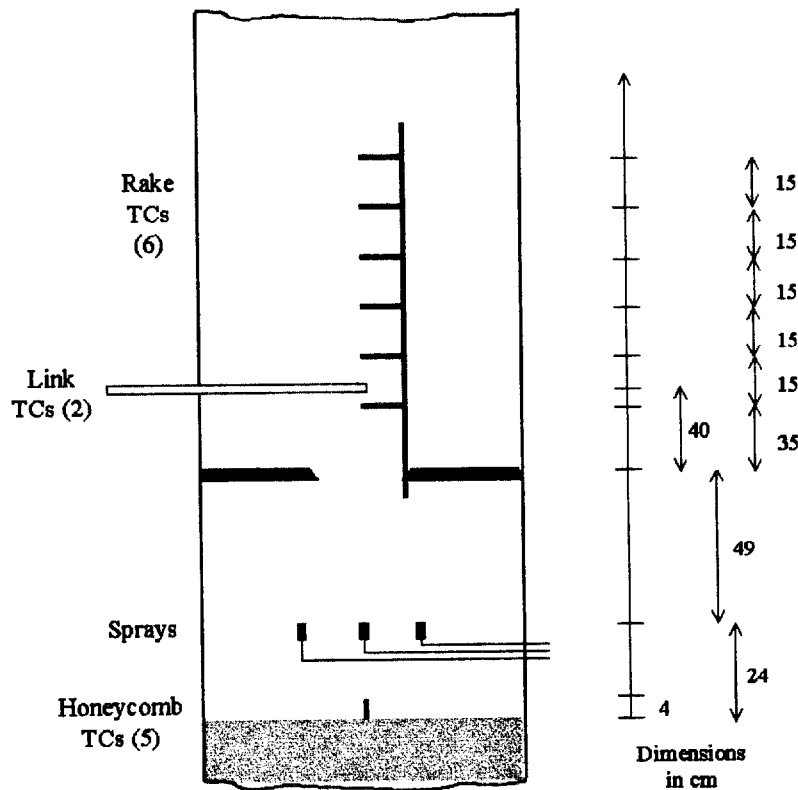


Figure 15. Thermocouple location

Only up to 8 thermocouples can be sampled simultaneously, at a frequency of 100 Hz, by the current data acquisition (A/D) board by Omega. Therefore, all thermocouples mount quick-disconnect junctions, which allow a rapid switch of the probes being sampled. Typically, the 5 TCs near the honeycomb are scanned only during the setup phase of the experiments, when the gas flow conditions are being adjusted to meet the test requirements. Subsequently, when an uniform gas temperature has been obtained,

this information becomes redundant; therefore, four of these five probes are disconnected and replaced with those placed on the vertical rake.

3.2.2. Optical measurements

The velocity of the gas stream and the volumetric fraction of the water droplets are measured with an optical technique. A 600 mW multiline Argon-Ion laser (Spectra-Physics model 175-F01) is used to generate a laser beam, which is then spread by a cylindrical lens to form a thin vertical sheet (about 3 mm thick and 4 cm high). The laser sheet enters the duct through a window opening in the duct wall and traverses the test section along the centerline, as shown in Figure 16.

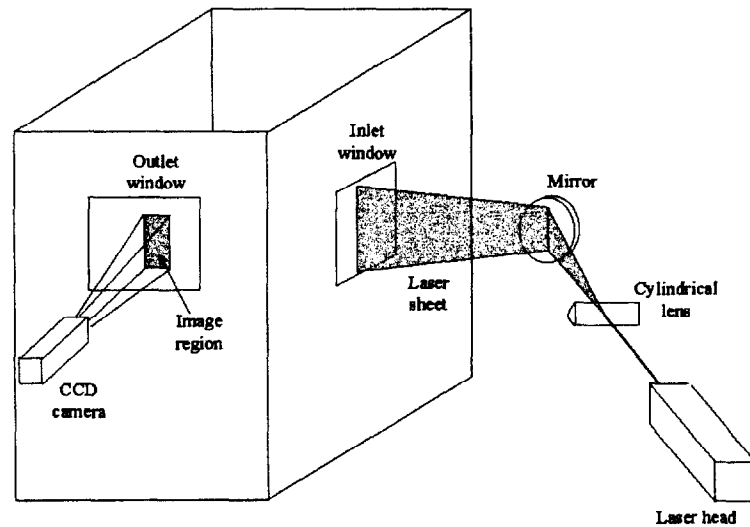


Figure 16. Optical setup for velocity and liquid fraction measurements

The laser sheet is used to illuminate the water droplets in the gas flow. The light scattered by the illuminated droplets is then captured by a couple-charged device (CCD) camera focused on the lighted region. A Cohu camera (series 4910) is used for this purpose, equipped with a 200-mm manual focus Canon lens. The camera collects the light scattered by the droplets that travel through this region while the shutter is open. Because of the characteristics of the flow in the vena contracta, the droplets flow vertically, which means that the droplets entering the laser-sheet volume from the bottom face are likely to leave it through the top face. Therefore, the droplets are continuously illuminated while in the laser sheet, and their path is captured on the CCD snapshot as a streak. The software that controls the operation of the CCD (Image-Pro Plus) saves the snapshots taken by the camera as bitmap images, as shown in Figure 17.

These images can be processed by the same software to obtain the length and number of the streaks. The length-measuring tool is calibrated to give the physical length of each droplet trace; the velocity of the droplet can be calculated by dividing the length of the trace by the exposure time of the image (i.e., the camera “shutter speed”). The characteristics and placement of the camera allow focusing on a region which measures 13 mm in the direction of the flow and 10 mm across. The CCD has a resolution of 640 by 480 pixels (the camera is placed on its side, so that the 640 pixels are aligned with the direction of the flow), which allows to resolve droplets that have a minimum diameter of about 25 μm . The shutter speed can be varied from 1 to 1/4000 seconds, which allows to optimize the streak lengths for different velocities to minimize the measurement error.

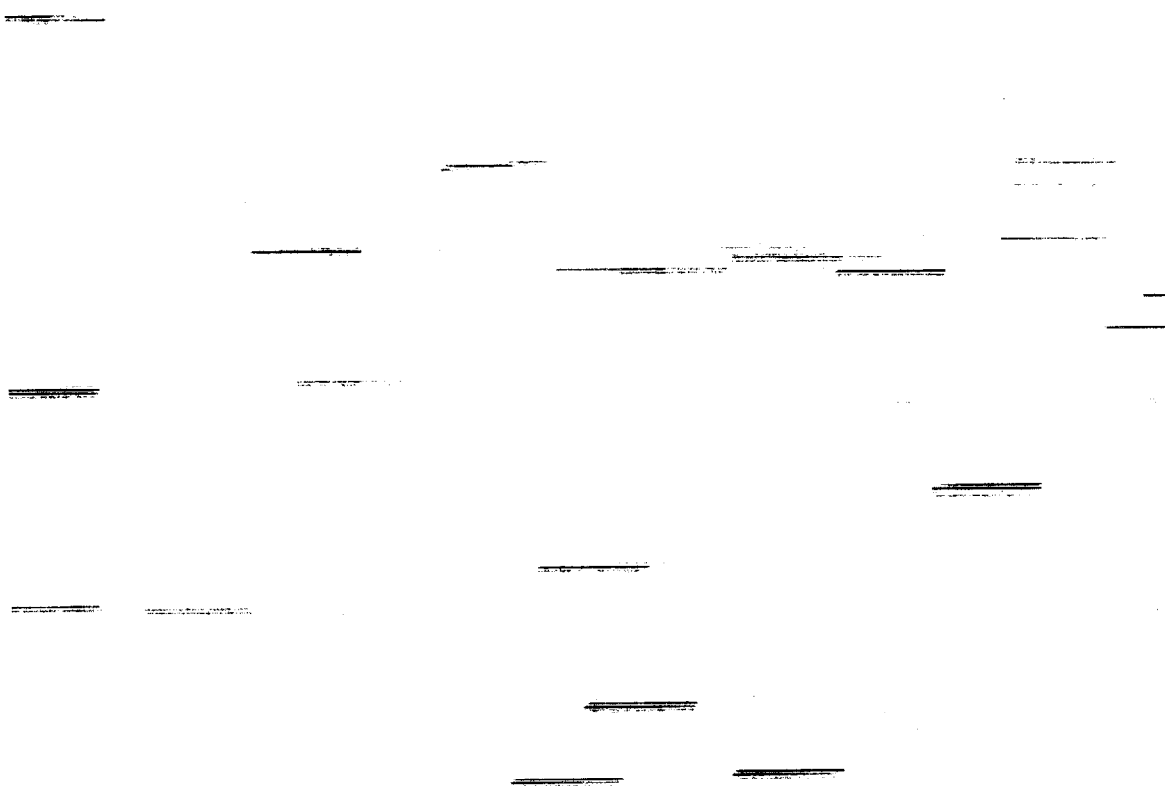


Figure 17. Snapshot of the water droplets in the gas stream

4. EXPERIMENTS

The proposed model for the thermal response of a sprinkler link immersed in a two-phase flow of hot gas and water droplets is represented by equation (22):

$$\frac{dT_s}{dt} = \frac{\sqrt{U} (T_g - T_s)}{RTI} - C U \beta \quad (22)$$

This equation indicates how the rate of change of the link temperature is determined by the balance of two counteracting effects: the convective heat transferred from the hot gas to the link, and the cooling effect due to the evaporation of the water droplets from the link surface. The gas and sprinkler temperatures, as well as the gas velocity and the water volumetric fraction can be directly obtained from experimental measurements. However, this leaves two quantities (RTI and C) to be determined.

The value of C cannot be determined from a single test, but must be derived from the general behavior of the probe subject to a wide range of boundary conditions. In fact, equation (23) shows that C depends on the thermophysical and geometric properties of the link as well as on the thermophysical properties of the gas-droplet flow. Therefore, equation (22) cannot be used directly to obtain information on both the unknowns. The following procedure has been developed to allow the quantification C and RTI from the plunge-test simulations conducted at the facility.

4.1. Reformulation of the Problem

The following non-dimensional temperature can be defined:

$$\theta = \frac{T_g - T_s}{T_g - T_{s,0}} \quad (24)$$

where $T_{s,0}$ is the initial temperature of the sprinkler link, before being inserted inside the duct. Therefore, the initial condition for θ is:

$$\theta(t=0) = 1 \quad (25)$$

If a dry gas stream is considered ($\beta = 0$), equation (22) reduces to the original RTI model (9), which can be written as:

$$\frac{dT_s^{\text{DRY}}}{dt} = \frac{\sqrt{U}}{\text{RTI}} (T_g - T_s^{\text{DRY}}) \quad (26)$$

where the superscript 'DRY' has been added to characterize the flow conditions under which the sprinkler temperature is measured. Introducing the non-dimensional temperature θ , this becomes:

$$\frac{d\theta^{\text{DRY}}}{dt} = -\frac{\sqrt{U}}{\text{RTI}} \theta^{\text{DRY}} \quad (27)$$

which can be solved with the initial condition (25) to give:

$$\theta^{\text{DRY}}(t) = \text{Exp}\left[-\frac{\sqrt{U}}{\text{RTI}} t\right] \quad (28)$$

All quantities in this equation, except RTI, can be directly measured during a single dry-gas plunge test. Therefore, the Response Time Index can be inferred from the experimental data.

Introducing the non-dimensional temperature into the model equation for a wet gas (22) and solving with the same initial condition (25) gives:

$$\theta^{\text{WET}}(t) = \frac{C \sqrt{U} \beta}{T_g - T_{s,0}} + \left(1 - \frac{C \sqrt{U} \beta}{T_g - T_{s,0}} \right) \text{Exp} \left[-\frac{\sqrt{U}}{RTI} t \right] \quad (29)$$

where the superscript 'WET' indicates that water droplets are now present in the gas stream. Combining the expressions (25, 28 and 29), assuming the same gas flow velocity and temperature for the two cases, the following is obtained:

$$\frac{\theta^{\text{DRY}} - \theta^{\text{WET}}}{\theta^{\text{DRY}} - 1} = \frac{T_s^{\text{DRY}} - T_s^{\text{WET}}}{T_s^{\text{DRY}} - T_{s,0}} = \frac{C \sqrt{U} \beta}{T_g - T_{s,0}} \quad (30)$$

Taking a closer look at the term in the central portion of this equation, it can be noted that the numerator is the difference between the link temperature during a dry and a wet gas plunge test: it indicates the cooling effect due to the presence of the water droplets evaporating on the link surface. The temperatures must be taken at the same time from the plunging of the link into the gas flow. The denominator, instead, represents the heating of the link during the dry plunge.

According to the assumptions of the model, the right hand side of (30) is a constant; this means that the ratio of the evaporative cooling effect to the heating of the dry link must also be a constant during the experiment. The experimental results will allow to determine whether this assumption is correct. Solving for C from equation (30) gives:

$$C = \frac{T_s^{\text{DRY}} - T_s^{\text{WET}}}{T_s^{\text{DRY}} - T_{s,0}} \frac{T_g - T_{s,0}}{\sqrt{U} \beta} = \text{RHS} \quad (31)$$

where the quantity on the right hand side is indicated with RHS for simplicity of notation.

All the terms in RHS can be determined experimentally. The parameters U, β and $T_g - T_{s,0}$ can be controlled and set as boundary conditions for each experiment. According to the assumptions of the proposed model, tests conducted on a given sprinkler link should result in similar values of C over a wide range of variation of the boundary conditions. The initial part of the experimental campaign is aimed at verifying the validity of such statement, as described in the following sections.

4.2. Experimental Procedure

The procedure followed during each test can be subdivided into three parts:

1. **System Set-Up.** The apparatus is started and adjustments are made to the gas burner power and to the air intake louvers, until the specified gas temperature and velocity are obtained. The system is then allowed to reach steady state.
2. **Wet test.** The water sprays are activated, which creates a two-phase flow of hot gas and water droplets in the test section. The water flow rate and droplet size distribution can be adjusted by varying the type of the spray, the number of active

sprays and the pump power. Some fine-tuning adjustment of the gas velocity and temperature is usually required after the activation of the sprays, in order to restore the desired test conditions. While the two-phase flow reaches the steady-state, the sprinkler link is maintained at the initial temperature $T_{s,0} = 300$ K. Once the system conditions are stabilized, gas velocity and water volumetric fraction are measured with the optical techniques described in Chapter 3. Subsequently, the recording of the thermocouple measurements is started and the sprinkler link is inserted into the test section. The plunge test ends when the link temperature reaches a plateau. At this point, the link is extracted and returned to its initial temperature, $T_{s,0}$. The plunge-test procedure is repeated 3 times, with the same boundary conditions, in order to establish the repeatability of the results.

3. **Dry test.** After the completion of the 3 wet tests, the water sprays are turned off and the system is allowed to reach a new steady state under single-phase gas flow conditions. In order to have test conditions (in particular, the gas temperature) comparable with the wet case, the initial link temperature must be adjusted by an amount ΔT , so that $T_{s,0}^{\text{DRY}} = T_{s,0}^{\text{WET}} + \Delta T$. The procedure followed to determine the value of ΔT , which must be evaluated on a case-by-case basis, will be described later. Once the desired steady-state conditions are obtained, a plunge test is conducted similarly to the wet case. The temperatures are again recorded until the link reaches a plateau, then the system is returned to the initial conditions. Three runs are performed in the dry case, as well. However, because of the uncertainty associated with the determination of ΔT during the course of the experiments, the 3 tests are conducted with a slightly different initial link temperature (respectively: $T_{s,0}^{\text{DRY}}$, $T_{s,0}^{\text{DRY}} + 2$, $T_{s,0}^{\text{DRY}} - 2$). During the processing of the data, the ‘correct’ initial link temperature is calculated with more accuracy, which allows to determine which of the three dry tests can be compared with the wet runs.

4.3. Test Matrix

In order to validate the proposed model, a series of experiments need to be conducted over a wide range of boundary conditions. As mentioned earlier, the ECSAT facility allows the control of 3 parameters: the gas velocity U , the water droplet volumetric fraction β , and the gas temperature T_g (more precisely, the term that appears in (31) is the difference between the gas and the initial link temperatures, $T_g - T_{s,0}$).

Under the current configuration, a rather limited range of variation of the three parameters is allowed. The limiting constraint is given by the need to conduct wet and dry experiments under the same conditions, so that the transient link temperature profiles can be combined into (31). As will be explained later, in order to satisfy this requirement it is necessary for the water droplets to be present in measurable quantity at the test section location and to be completely evaporated before reaching the end of the thermocouple rake (see Figure 15). This constrains the water volumetric fraction within a rather narrow range (about $4\text{-}8 \cdot 10^{-6}$) and also imposes a correlation between the gas velocity and temperature during each test. For example, if the gas temperature is lowered the droplets evaporate more slowly, therefore a longer residence time in the duct (that is,

a lower gas velocity) is necessary in order for all the droplets to evaporate before they reach the end of the rake.

The gas velocity is determined by the blower characteristics and the configuration of the secondary air inlets, and is therefore bounded between approximately 3 and 10 m/s. Because of the above mentioned constraint on the water droplets, the gas temperature can only be varied between about 360 and 500 K.

The second part of this project will include additional instrumentation along the discharge duct. This will allow the operation of the facility under a much wider range of boundary conditions.

Table 3 lists the experiments conducted with the current test configuration. Note that two different spray nozzles are utilized (PJ8 and PJ10). The water volumetric fraction in the two cases is comparable, but the water droplet size distribution is quite different, with the mean droplet diameter varying from 65 μm for the PJ8 nozzle to 80 μm for the PJ10.

test name	T_{gas} (K)	u (m/s)	$\beta \cdot 10^6$	nozzle
02-16-1	485	7.7	4.9	PJ8
02-16-2	387	5.3	5.4	"
02-17-1	486	7.4	6.2	"
02-17-2	378	4.5	9.4	"
02-18	436	6.1	3.8	"
02-19	440	5.8	4.6	"
02-22	494	7.4	5.2	"
02-23	440	5.8	7.6	"
02-24	480	6.1	2.6	"
02-25-1	377	3.2	8.1	"
02-25-2	362	4.5	5.9	"
02-26	360	3.5	8.2	"
03-01-1	404	3.9	6.1	"
03-01-2	424	3.9	5.6	"
03-02	442	4.8	5.4	"
03-03	413	4.0	7.9	"
03-04	442	7.1	3.8	"
04-01	468	7.9	8.2	PJ10
04-02	443	5.8	7.1	"
04-05	397	6.4	8.1	"
04-12	406	3.2	7.8	"
04-12	442	3.6	7.2	"
04-14	385	3.6	5.7	"
04-15	386	4.6	3.9	"
04-16	430	5.8	3.7	"
04-19-1	381	4.1	4.4	"
04-19-2	437	5.3	5.6	"

Table 3. Test matrix for the experimental campaign.

The test nomenclature follows the notation **mm-dd(-nt)**, where

- **mm-dd** is the date (month and day) in which the test is executed
- **nt** is the sequential order of the test, in case more than one set is executed on the same day

As discussed in the previous chapter, each test generates a substantial amount of data of different types:

- gas velocity measurements, as well as water droplet counts, are obtained from CCD camera pictures
- temperature measurements are obtained from thermocouples placed in the sprinkler link and other locations around the test section

The images taken during the wet tests to measure U and β are named as **mm-dd(-nt)-ni-''#''p**, where:

- **mm-dd(-nt)** identify the test
- **ni** is the sequential image number for each run (typically, 20 images are taken for each plunge test)
- **p** is the plunge test number (each test is repeated 3 times)

The temperature measurements are stored in Microsoft Excel files, named according to **mm-dd(-nt)-elab**.

4.4. Data Analysis

The purpose of the experimental campaign is to validate the proposed model (31) and its assumptions, providing at the same time quantitative values for the constants there introduced: RTI and C .

The following sections describe the procedure followed to obtain answers to these questions from the data collected during the experiments.

4.4.1. Measure of the Response Time Index

The Response Time Index (RTI) remains defined as in the original sprinkler response model. Therefore, its value can be obtained by fitting equation (10) to the experimental data from a dry test. Figure 18 shows the fitted vs. experimental curves for one such case.

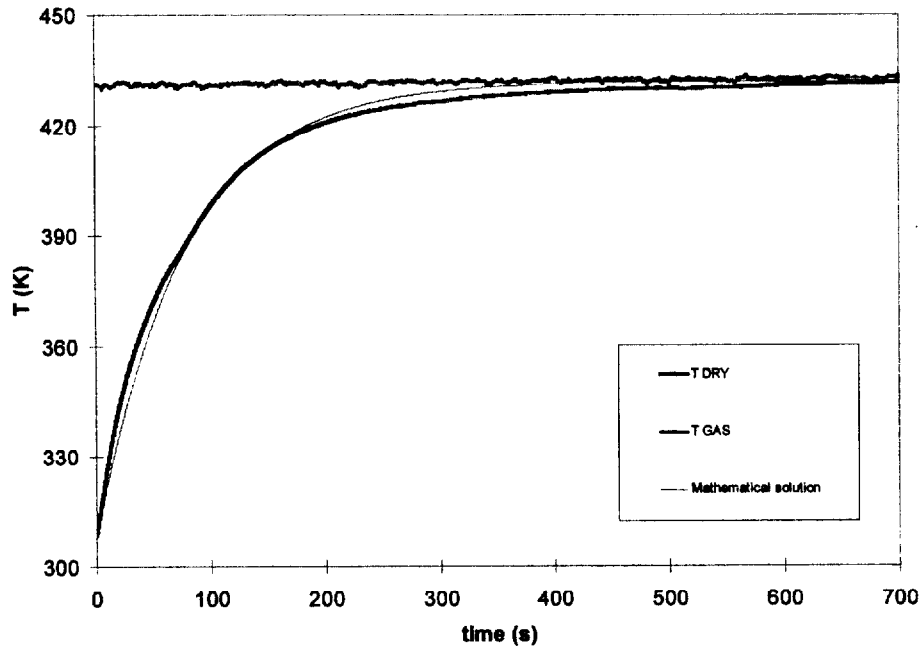


Figure 18. Measure of RTI from a dry test

Two different simulated sprinkler links have been used for this campaign. The RTI for the smaller link (a 2 cm long aluminum cylinder with a 6.4 mm diameter) is calculated to be 138 ± 34 , whereas the larger link (a 2 cm long aluminum cylinder with a 10 mm diameter) has an RTI of 201 ± 29 . Figure 19 summarizes the values of RTI calculated for the smaller link during the experimental campaign.

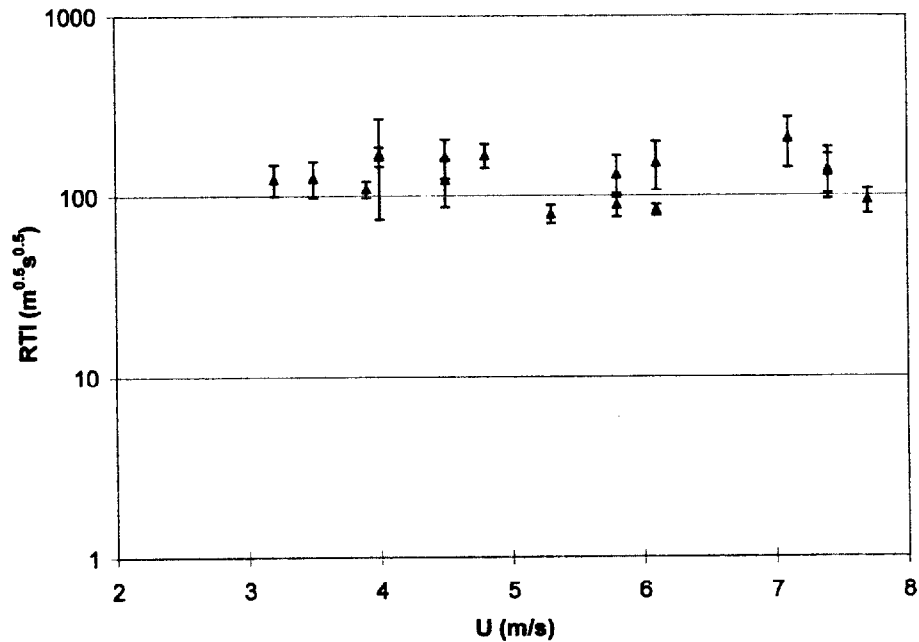


Figure 19. RTI values for different tests

The value of C can be calculated from (31), since all terms in RHS can be determined experimentally. Before C can be calculated, however, some more details on the measurement of U , β and T_g need to be discussed.

4.4.2. Gas Velocity Measurement

The gas velocity is measured from the images of the two-phase flow through the test section. As the water droplets cross the test section, carried by the gas flow, they are illuminated by a laser sheet oriented along the direction of the flow. A CCD camera is focused on a portion of the illuminated region and records the streaks formed by the droplets scattering the laser light, as shown in Figure 20.

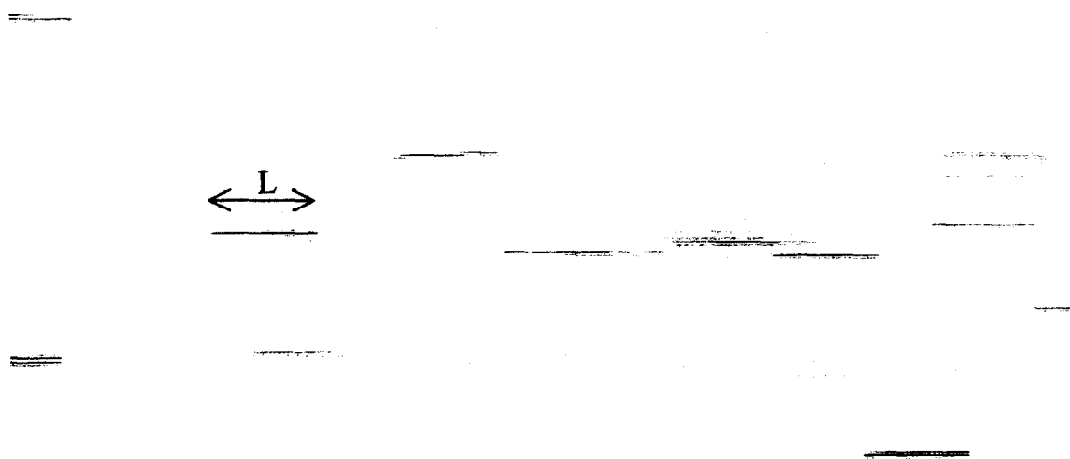


Figure 20. Picture of the droplets crossing the test section (negative)

An initial calibration of the real image size allows to determine the actual length L of each observed streak; dividing this by the exposure time ϵ gives the velocity of the water droplet, $U = L / \epsilon$. If it is assumed that the droplets move with the same velocity of the gas flow, then the previous calculation determines the velocity of the gas. Given the particular characteristics of flow in the vena contracta, this assumption is retained reasonable. About 30 streaks are measured for each test, in order to determine the gas velocity with some statistical significance.

4.4.3. Water Volumetric Fraction Measurement

The water volumetric fraction β can also be determined from the images of the droplet streaks. Indeed, β is defined as the ratio of the volumetric flow rate of water droplets over the volumetric flow rate of the gas, through a given cross section A :

$$\beta = \frac{\dot{V}_d}{\dot{V}_g} \quad (32)$$

The gas volumetric flow rate is equal to the product $V_g = A * U$. The droplets flow rate, instead, is given by the sum of the volume of each droplet that crosses A in a given amount of time Δt :

$$\dot{V}_d = \frac{\sum_i \frac{\pi}{6} D_i^3}{\Delta t} \quad (33)$$

In principle, therefore, the droplets crossing the target of the CCD camera over the exposure time ϵ could be counted and their diameters measured, thus allowing to calculate β from (32). However, some complications arise when this calculation is attempted:

- The droplet diameter cannot be resolved with sufficient accuracy from the available images (the resolution is about 25 μm), so (33) cannot be used.
- The images are taken at the test section, which is located about 65 cm above the spray nozzle location. The evaporation of the droplets in the hot gas flow causes a reduction in the size and number of droplets that reach the test section, and this reduction is dependent upon the gas temperature and velocity.

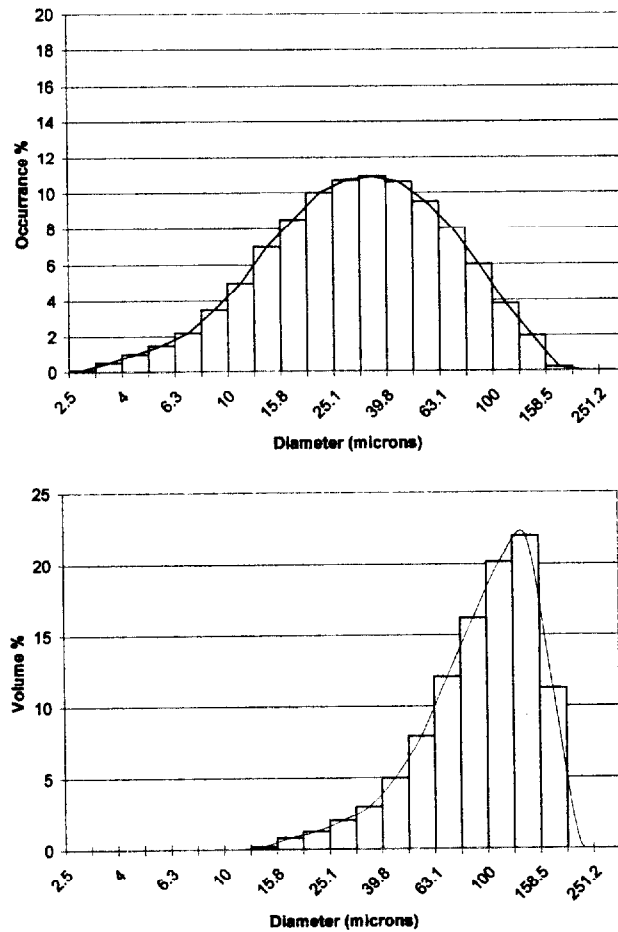


Figure 21. Droplet Size Distribution for the PJ8 Nozzle

The first obstacle is overcome thanks to the particular droplet size distribution of both available spray nozzles, which is shown in Figure 21 for the PJ8 nozzle and in Figure 22 for the PJ10 nozzle). It is reasonable to assume that the evaporation process for all droplets is proportional to their surface area. Under these circumstances, over a given time interval each droplet would lose by evaporation a “shell” of equal thickness. The minimum image resolution is 25 μm , which means that no droplets with a diameter less than 25 μm can be observed. However, Figures 21 and 22 show that, for both nozzle sizes, the contribution of these droplets to the spray volume (and, hence, to β) is negligible. Therefore, the image resolution does not introduce a relevant bias to the calculations.

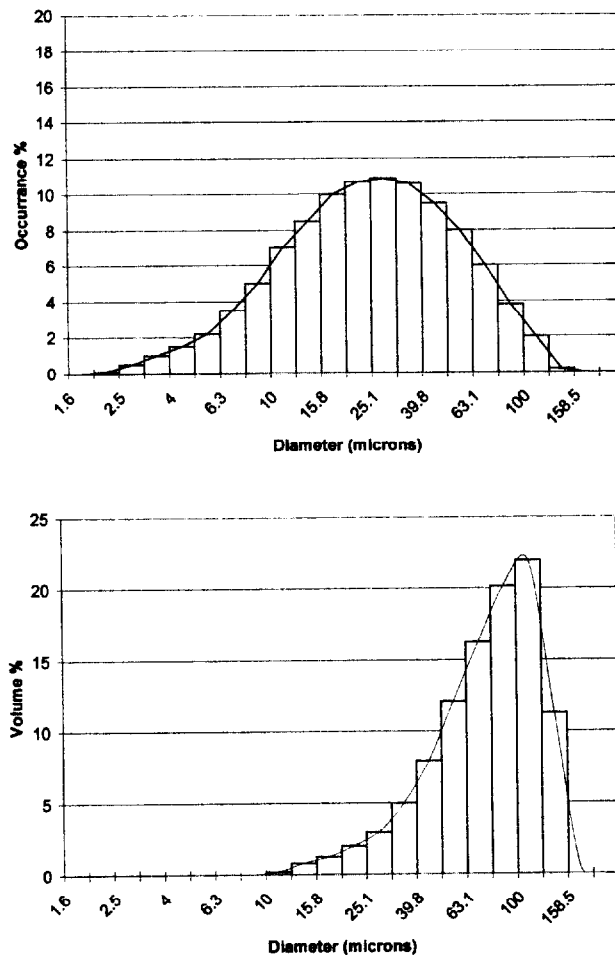


Figure 22. Droplet Size Distribution for the PJ10 Nozzle

Therefore, the residual water volume and droplets number can be calculated at different times during the evaporation process. Figure 23 shows that the average normalized droplet volume (and, hence, diameter) remains approximately constant. This result is very useful because it removes the uncertainty associated with the determination of the droplet diameter from the experimental data. Instead, it can simply be assumed that the droplets have a constant average diameter D , equal to the value provided by the manufacturer ($65 \mu\text{m}$ for the PJ8 and $80 \mu\text{m}$ for the PJ10, respectively). Therefore, (33) can be simplified as:

$$\dot{V}_d = \frac{n \frac{\pi}{6} D^3}{\epsilon} \quad (34)$$

and β can be calculated from:

$$\beta = \frac{n \frac{\pi}{6} D^3}{U A \epsilon} \quad (35)$$

where A is the area lighted by the laser.

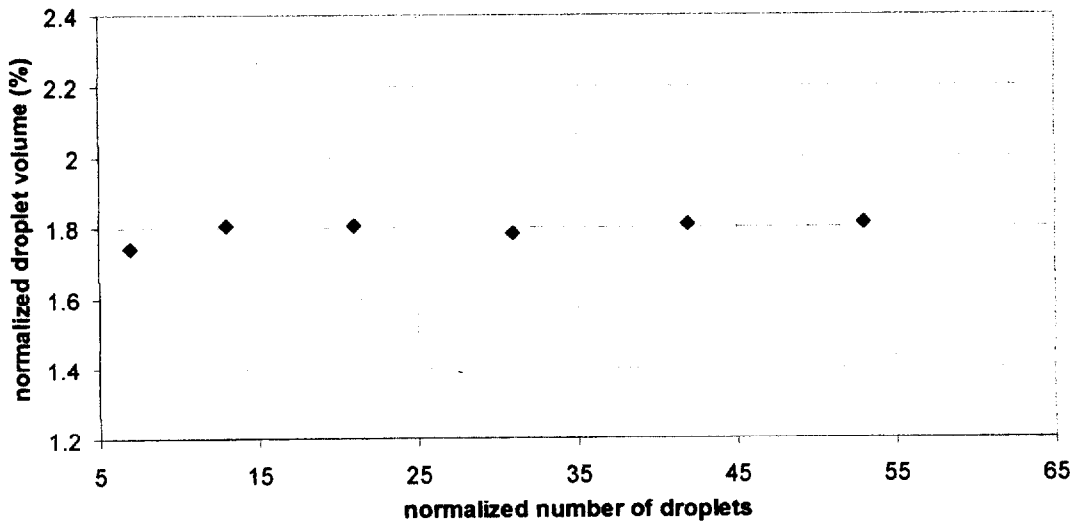


Figure 23. Normalized droplet volume versus the number of droplets

The second problem is due to the evaporation of the droplets between the spray nozzle location and the test section, where they are observed. In order to measure the actual β , a set of “cold” tests are performed: the spray is injected in a gas flow at ambient temperature, so that no evaporation occurs and a number of droplets n_0 is counted at the test section. flow. The flow rate released by the spray nozzles is independent of the velocity of the gas stream into which the water droplets are released. Therefore, the total number of droplets that cross a given cross-section of the streamtubes is expected to be constant. However, the number of droplets that are observed to cross the target region of the CCD camera increases linearly with the gas velocity U , as shown in Figure 24. Recalling that this region is only a small portion of the vena contracta, this result

indicates that the distribution of the water droplets in the stream is not uniform but tends to concentrate near the axis of the duct as the gas velocity increases. Figure 25 shows the portion of the test section in which the droplets are concentrated.

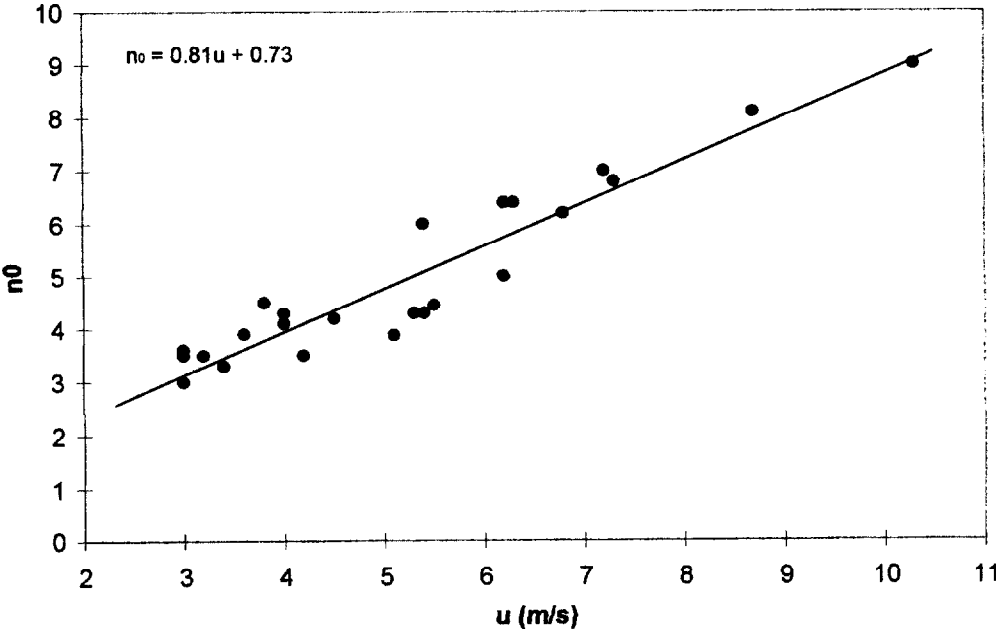


Figure 24. Variation of n_0 with the gas velocity

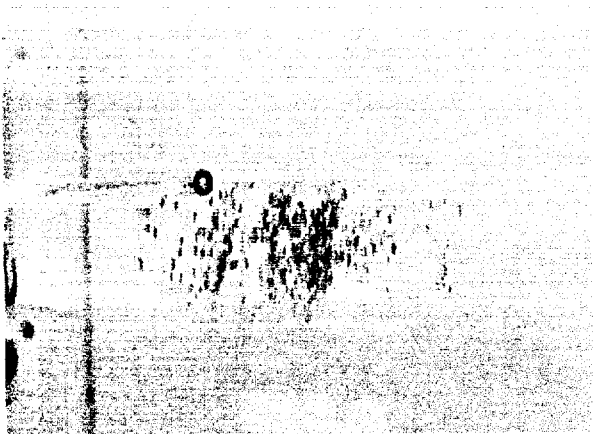


Figure 25. Water spray distribution through the test section

4.4.4. Gas Temperature Measurement

In order for the results from wet and dry tests to be comparable, the difference between the gas and the initial link temperatures must be the same in the two cases. Measuring T_g in the dry case is trivial, as it is directly obtained from the thermocouples located around the test section. The task is more difficult in the wet case, as the temperature measurements are affected by the random deposition of water droplets on the probes.

The obstacle may be overcome if the test conditions are such that the droplets completely evaporate before reaching the end of the TC rake, as previously mentioned. If this happens, the temperature profile assumes the inverted parabolic shape shown in Figure 26 (squares): the apparent temperature increase along the initial part of the rake is due to the decreasing number of droplets that reach farther locations; once all the water has evaporated, the temperature begins to decrease along the rake as the flow is cooled down by losses to the ambient. Only in this region, therefore, these readings do represent the actual gas temperature.

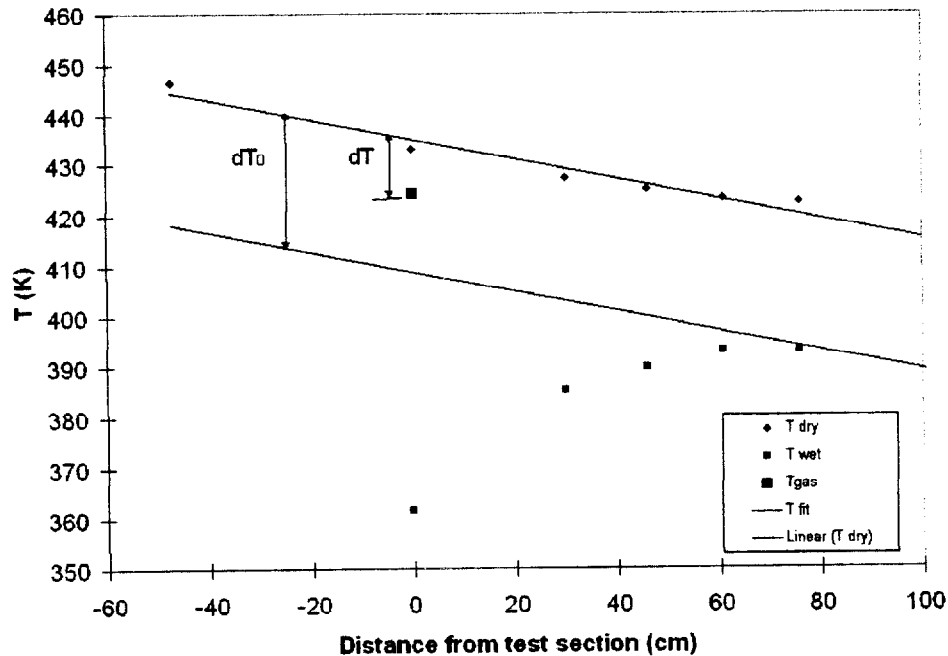


Figure 26. Temperatures profile along the duct, in dry and in wet conditions.

The value of T_g that is of interest for the data analysis is the one at the test section location; however, because of the presence of water droplets, this value cannot be directly obtained from the thermocouple reading as in the dry case. Figure 26 shows graphically how T_g can be determined. The diamond-shaped dots indicate the temperature measurements along the rake during the dry test and the thick line represents the linear fit

through those values (i.e., it provides the cooling curve along the rake in the dry case). The thin line is constructed by assuming that the gas temperature in the wet case follows the same cooling trend as in the dry case. Knowing that the last rake thermocouple is not affected by water droplet and, therefore, measures the true gas temperature, a new line (thin line in the figure) can be drawn, parallel to the dry case and passing through the last diamond dot. The distance between the two lines, ΔT_0 , represents the asymptotic difference between the gas temperature in the dry and wet cases once all the water has evaporated.

If the temperature difference between the gas temperature at the test section in the dry case, T^{DRY} , and in the wet case, T_g , is indicated with $\Delta T = T^{\text{DRY}} - T_g$, we can say that $0 \leq \Delta T \leq \Delta T_0$ depending on the amount of evaporation that has occurred between the spray location and the test section. Assuming the cooling due to water evaporation to be a linear function of the amount of water evaporated, we can write:

$$\frac{\Delta T}{\Delta T_0} = \frac{\beta_0 - \beta}{\beta_0} \quad (36)$$

where β_0 is the water volumetric fraction measured during a “cold” test (without evaporation).

Recalling (35) it is easily observed that:

$$\frac{\beta}{\beta_0} = \frac{n}{n_0} \quad (37)$$

from which it follows that T_g can be calculated from:

$$\frac{T^{\text{DRY}} - T_g}{\Delta T_0} = 1 - \frac{n}{n_0} \quad (38)$$

The value of T_g so calculated is indicated in Figure 26 with a large square dot. It can be noted that, in general, the gas temperature during the wet and dry runs is not exactly the same. However, it must be observed that T_g appears in (31) only as the difference $T_g - T_{s,0}$. Therefore, the two cases can still be compared provided the initial link temperature is adjusted to make that term identical.

4.4.5. Calculation of C

Once β , U and T_g have been obtained, the evaporative cooling constant can be calculated from:

$$C = \frac{T_s^{\text{DRY}} - T_s^{\text{WET}}}{T_s^{\text{DRY}} - T_{s,0}} \frac{T_g - T_{s,0}}{\sqrt{U} \beta} \quad (31)$$

The first fraction on the right hand side of (31) is obtained by comparing the transient link temperature traces during wet and dry tests run under the same boundary conditions. An example of these traces is shown in Figure 27, where significant evaporative cooling

effect observed during the wet test results in a large temperature difference with respect to the dry case.

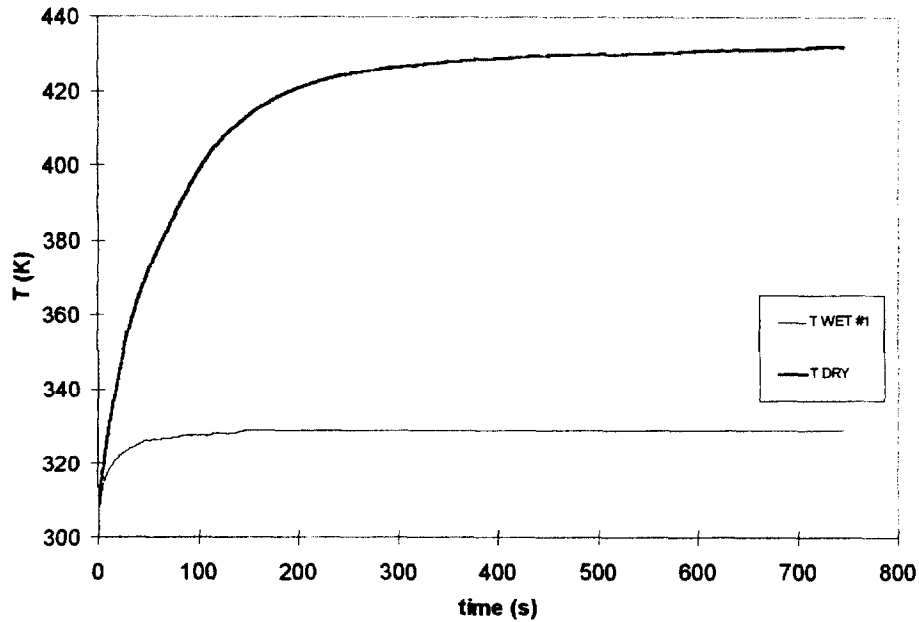


Figure 27. Transient link temperature during wet and dry tests

Figure 28 summarizes the values of C calculated from the different tests conducted during the experimental campaign. It can be noticed that the values are contained over a rather narrow interval, which indicates that C can indeed be considered a constant as assumed in the derivation of the sprinkler thermal response model. From Figure 28 the value of C is estimated at $5.8 \cdot 10^6$ $[\text{K} (\text{s m})^{1/2}]$.

This result also validates the assumption made on the collection efficiency ξ being constant. Indeed, from equation (23), in order for C to be nearly constant over a wide range of gas velocity and droplet diameter, ξ must also be approximately constant.

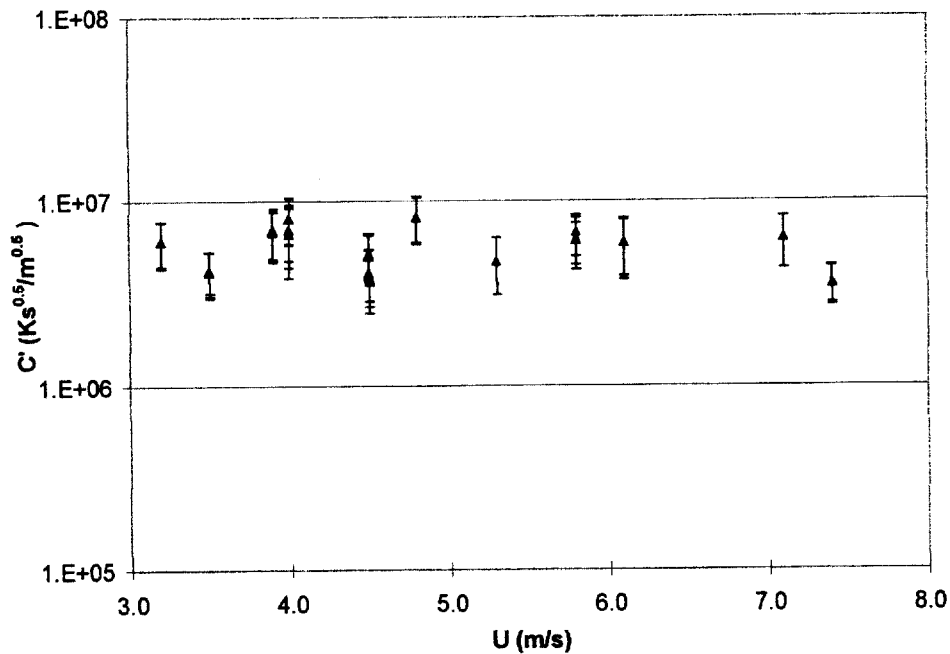


Figure 28. Values of C for the different tests

4.5. Determination of the delay time

Once C and RTI are calculated, the model for the thermal response of a sprinkler link can be implemented in the design stage of sprinkler arrays. Equation (28) can be used to calculate the transient heating of the sprinkler under dry gas conditions, and equation (30) can provide the same type of information for a sprinkler immersed in a two-phase flow. The two curves can be compared to determine the time delay with which the sprinkler activates under 'wet' conditions as opposed to 'dry' ones. From Figure 29, the time delay is the difference between t_w and t_D , these being the instants in which the link reaches the activation temperature, in wet and in dry conditions respectively.

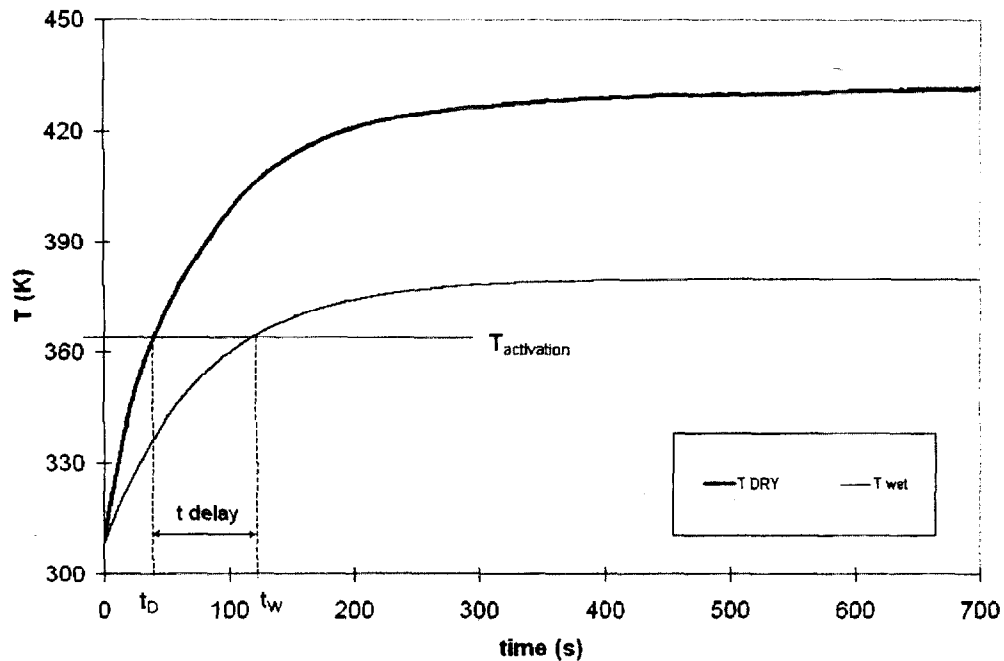


Figure 29. Time delay

5. CONCLUSIONS

This report presents the derivation of an improved model for the prediction of the transient thermal response of a ceiling-mounted fire detection sprinkler link in the event of a fire. The model expands the range of applicability of the current approach to include the presence of minute water droplets being carried by the hot gas plume. This situation has been observed experimentally in situations where a fire develops in an enclosed space equipped with an array of sprinklers: the activation of the first sprinkler releases a fine water spray, part of which is entrained by the rising plume and affects the operation of the surrounding devices.

A new test facility has been built in order to verify the proposed model, as well as to investigate, in a controlled environment, the effect of the water droplets on different sprinkler links. The experimental results indicate that the model is able to describe the transient response of a sprinkler link immersed in a two-phase flow of hot gas and water droplets, and the assumptions made in deriving such model have been verified. Compatibility with the current sprinkler response model, in the absence of water droplets in the stream, has also been verified. Finally, numerical values have been obtained for the constants introduced with the proposed model. Future enhancements of the instrumentation capabilities will allow to broaden the range of conditions that can be tested.

6. REFERENCES

1. Heskestad G., Bill R.G., 'Quantification of thermal responsiveness of automatic sprinkler including conduction effects'. *Fire Safety Journal*, Vol.14 (1988) 113-125.
2. Society of Fire Protection Engineers. *Fire Protection Handbook* 2nd Edition (1995).
3. Alpert, Ronald L., 'Calculated interaction of sprays with large scale buoyant flows'. *Journal of Heat Transfer*, 1984, Vol.106, pp. 310-317.
4. Crowe, Clayton, Sommerfeld, Martin, Tsuji, Yutaka, 'Multiphase flow with droplets and particles', CRC Press, 1998, ISBN 0-8493-9469-4.
5. Alpert, Ronald L., 'Turbulent ceiling-jet induced by large-scale fires', *Combustion Science and Technology*, 1975, Vol.11, pp. 197-213.
6. Panton, Ronald L., 'Incompressible flow'. John Wiley&Sons, 1984. ISBN 0-471-89765-5
7. Zakauskas A. and Ziugzda J., 'Heat transfer of a cylinder in crossflow'. Hemisphere Publishing Corporation, 1985.
8. Standard for automatic sprinklers for fire protection service, UL199, 8th edition, June 26, 1995.
9. Central Sprinkler Company, Private Communications.

7. APPENDIX: Standardized Test Reports

2/16/99

Task:

One PJ8 spray nozzle water injection
middle air velocity (5.3 m/s)
low air temperature ($T_{\text{gas}} = 387 \text{ K}$).

Objectives:

Calculate the response time index (RTI) of the probe and the parameter RHS.

Procedure:

The test consists of two parts:

- 1) Steady-state conditions with water spray on. Plunge test of the probe, with initial temperature $T_0=300 \text{ K}$. Gas velocity and number of water droplets are measured in the test section.
- 2) Steady-state conditions with water spray off. Plunge test of the probe, with initial temperature $T_0=310 \text{ K}$ and its transient heating is measured until it reaches steady-state.

	units	Wet conditions	Dry conditions
T_0	K	300	310
T before sprays	K	400	404
T rake #1	K	311	394
T rake #3	K	329	392
T rake #4	K	345	391
T rake #5	K	352	389
T rake #6	K	359	389

Table 1. Temperature at the seven recorded locations.

ΔT_0	K	25
u_{average}	m/s	5.3
n_{average}		1.7
n_0 [from $n_0(u)$ curve and 20 samples]		2
D	m	$65 \cdot 10^{-6}$
ϵ	s	1/4000
A	m^2	$3 \cdot 10^{-5}$
β		$5.4 \cdot 10^{-6}$
T_{gas}	K	387
T_{s0} dry	K	310
T_{s0} wet	K	300
RTI		80 ± 9
		hot/wet cond.#1
RHS		16.3 ± 0.10
$\frac{T^{\text{DRY}} - T}{T^{\text{DRY}} - T_0}$		0.79 ± 0.08

Table 2. Test parameters.

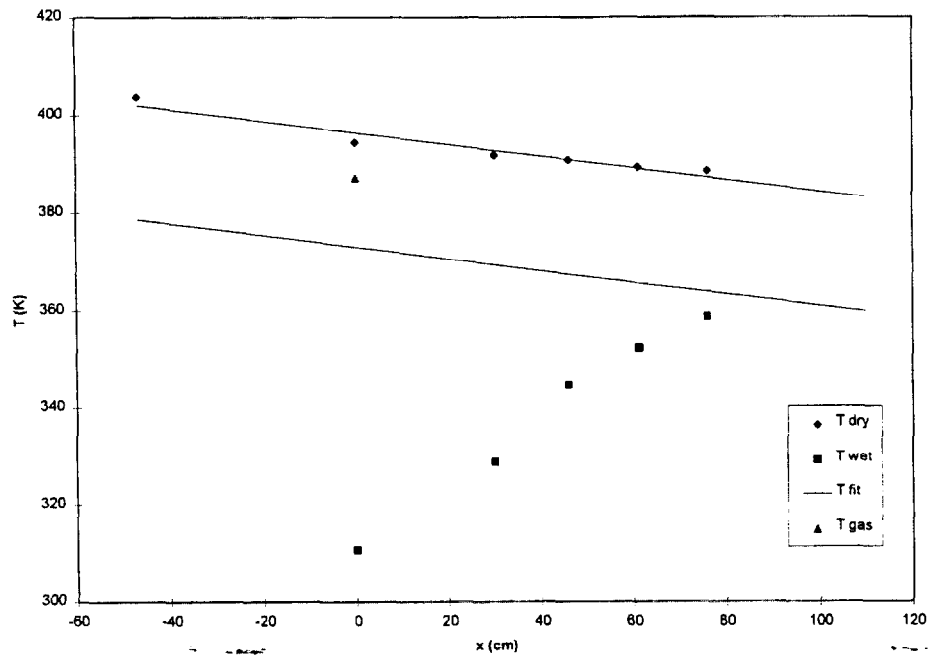


Figure 1. Steady-state temperatures along the duct.

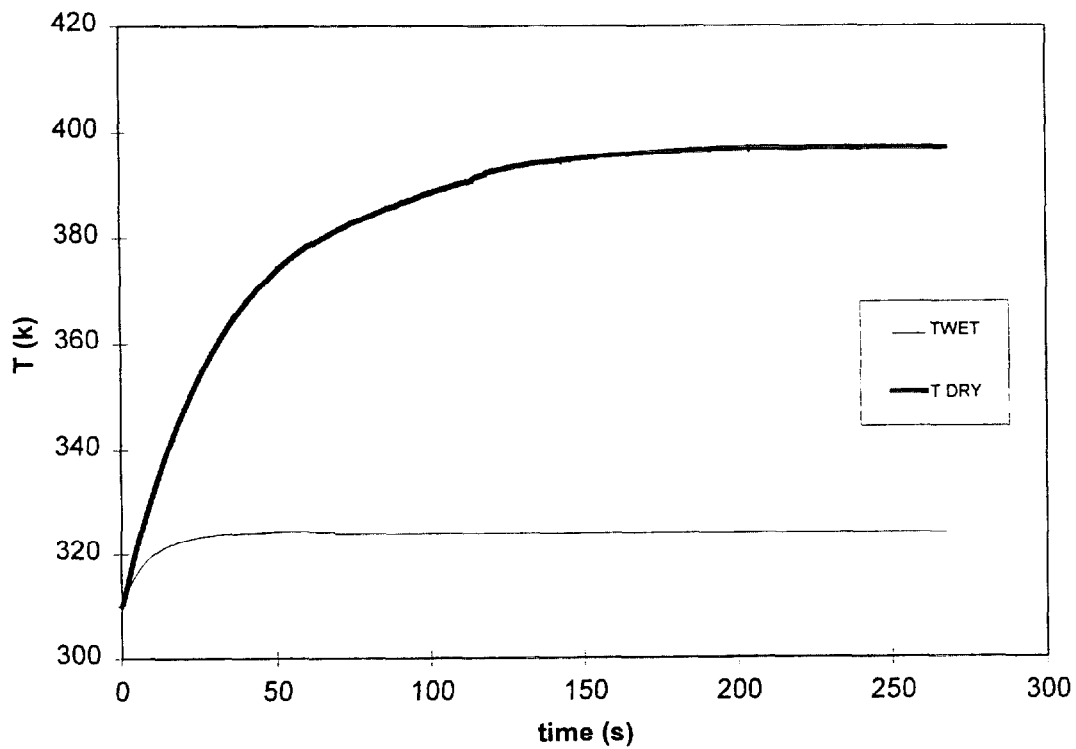


Figure 2. Transient probe temperature profiles during plunge tests.

2/17/99

Task: One PJ8 spray nozzle water injection
middle air velocity (4.5 m/s)
low air temperature ($T_{\text{gas}} = 378 \text{ K}$).

Objectives: Calculate the response time index (RTI) of the probe and the parameter RHS.

Procedure: The test consists of two parts:

- 1) Steady-state conditions with water spray on. Plunge test of the probe, with initial temperature $T_0 = 300 \text{ K}$. Gas velocity and number of water droplets are measured in the test section. The procedure is repeated three times to verify repeatability.
- 2) Steady-state conditions with water spray off. Plunge test of the probe, with initial temperature $T_0 = 312 \text{ K}$ and its transient heating is measured until it reaches steady-state.

	units	Wet conditions	Dry conditions
T_0	K	300	312
T before sprays	K	391	395
T rake #1	K	309	388
T rake #3	K	335	384
T rake #4	K	344	383
T rake #5	K	348	381
T rake #6	K	351	380

Table 1. Temperature at the seven recorded locations.

ΔT_0	K	27		
run #1 u	m/s	4.5		
run #2 u	m/s	4.6		
run #3 u	m/s	4.5		
$u_{\text{average}} \pm \sigma_{n-1}$	m/s	4.5 ± 0.1		
run #1 n (20 samples)		2.4 ± 1.2		
run #2 n (20 samples)		2.1 ± 0.6		
run #3 n (20 samples)		2.1 ± 1.5		
$n_{\text{average}} \pm \sigma_{n-1}$		2.2 ± 1.1		
n_0 [from 20 samples]		7		
D	m	$65 \cdot 10^{-6}$		
ϵ	s	1/2000		
A	m ²	$3 \cdot 10^{-5}$		
β		$(5.1 \pm 2.6) \cdot 10^{-6}$		
T_{gas}	K	378		
T_{s0} dry	K	312		
T_{s0} wet	K	300		
RTI		124 ± 37		
		hot/wet cond.#1	hot/wet cond.#2	hot/wet cond.#3
RHS		15.77 ± 0.09	15.79 ± 0.08	15.80 ± 0.08
$\frac{T^{\text{DRY}} - T}{T^{\text{DRY}} - T_0}$		0.83 ± 0.07	0.84 ± 0.07	0.85 ± 0.07

Table 2. Test parameters.

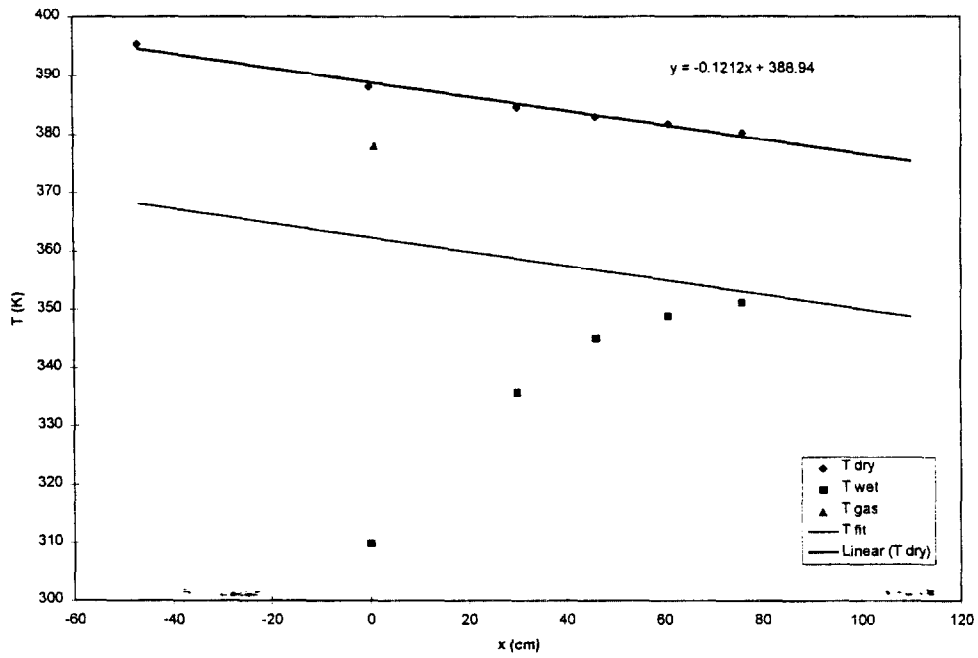


Figure 1. Steady-state temperatures along the duct.

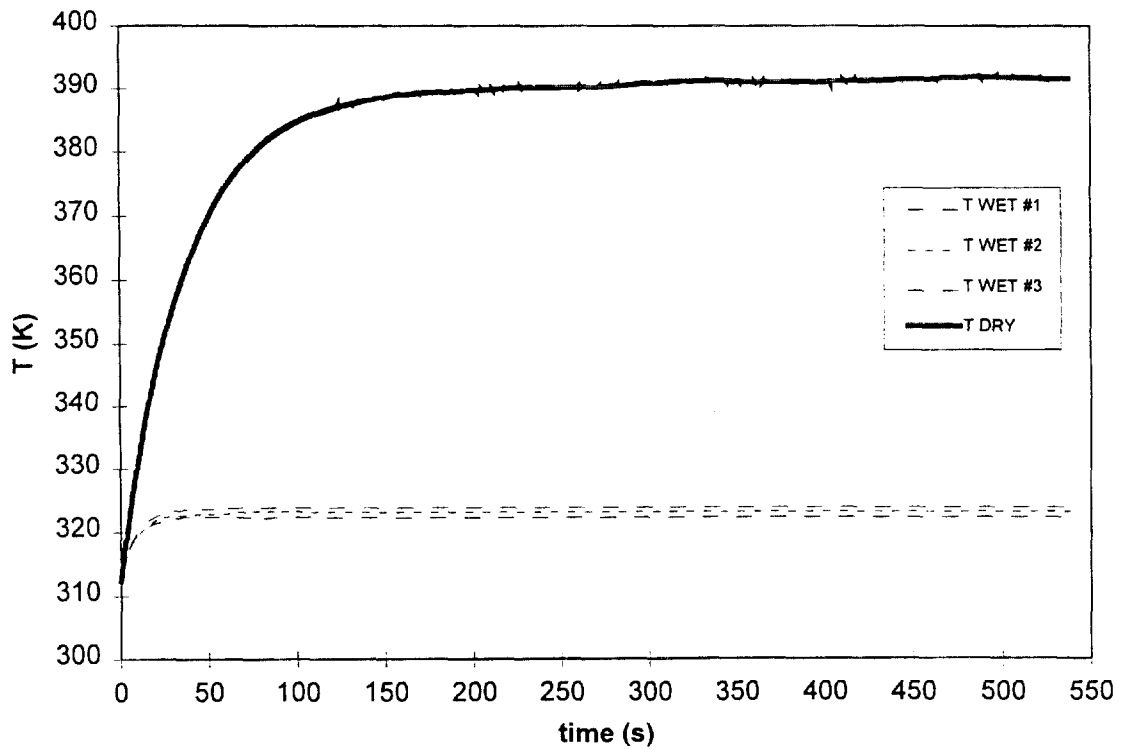


Figure 2. Transient probe temperature profiles during plunge tests.

2/18/99

Task:

One PJ8 spray nozzle water injection
high air velocity (6.1 m/s)
middle air temperature ($T_{\text{gas}} = 436 \text{ K}$).

Objectives:

Calculate the response time index (RTI) of the probe and the parameter RHS.

Procedure:

The test consists of two parts:

1) Steady-state conditions with water spray on. Plunge test of the probe, with initial temperature $T_0=300 \text{ K}$. Gas velocity and number of water droplets are measured in the test section. The procedure is repeated three times to verify repeatability.

2) Steady-state conditions with water spray off. Plunge test of the probe, with initial temperature $T_0=307 \text{ K}$ and its transient heating is measured until it reaches steady-state. The procedure is repeated three times to verify repeatability.

(the initial probe temperature is varied by $\pm 2 \text{ K}$ in the second and third runs, respectively).

	units	Wet conditions	Dry conditions
T_0	K	300	307
T before sprays	K	451	452
T rake #1	K	373	441
T rake #3	K	398	438
T rake #4	K	404	436
T rake #5	K	408	434
T rake #6	K	410	431

Table 1. Temperature at the seven recorded locations.

ΔT_0	K	20		
run #1 u	m/s	6.3		
run #2 u	m/s	5.7		
run #3 u	m/s	6.4		
$u_{\text{average}} \pm \sigma_{n-1}$	m/s	6.1 ± 0.3		
run #1 n (20 samples)		2.4 ± 0.5		
run #2 n (20 samples)		1.8 ± 0.5		
run #3 n (20 samples)		2		
$n_{\text{average}} \pm \sigma_{n-1}$		2.1 ± 0.3		
n_0 [from $n_0(u)$ curve]		2.7		
D	m	$65 \cdot 10^{-6}$		
ϵ	s	1/4000		
A	m^2	$3 \cdot 10^{-5}$		
β		$(6.3 \pm 1.2) \cdot 10^{-6}$		
T_{gas}	K	436		
T_{s0} dry	K	307		
T_{s0} wet	K	300		
RTI		84 ± 6		
		hot/wet cond.#1	hot/wet cond.#2	hot/wet cond.#3
RHS		16.47 ± 0.15	16.50 ± 0.12	16.52 ± 0.12
$\frac{T^{\text{DRY}} - T}{T^{\text{DRY}} - T_0}$		0.67 ± 0.08	0.69 ± 0.07	0.70 ± 0.07

Table 2. Test parameters.

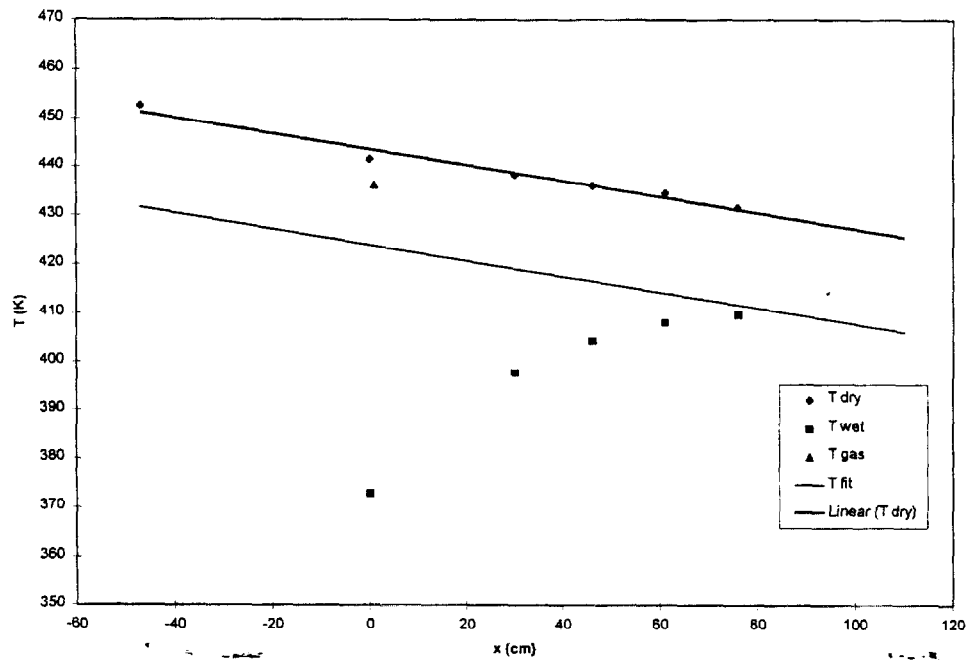


Figure 1. Steady-state temperatures along the duct.

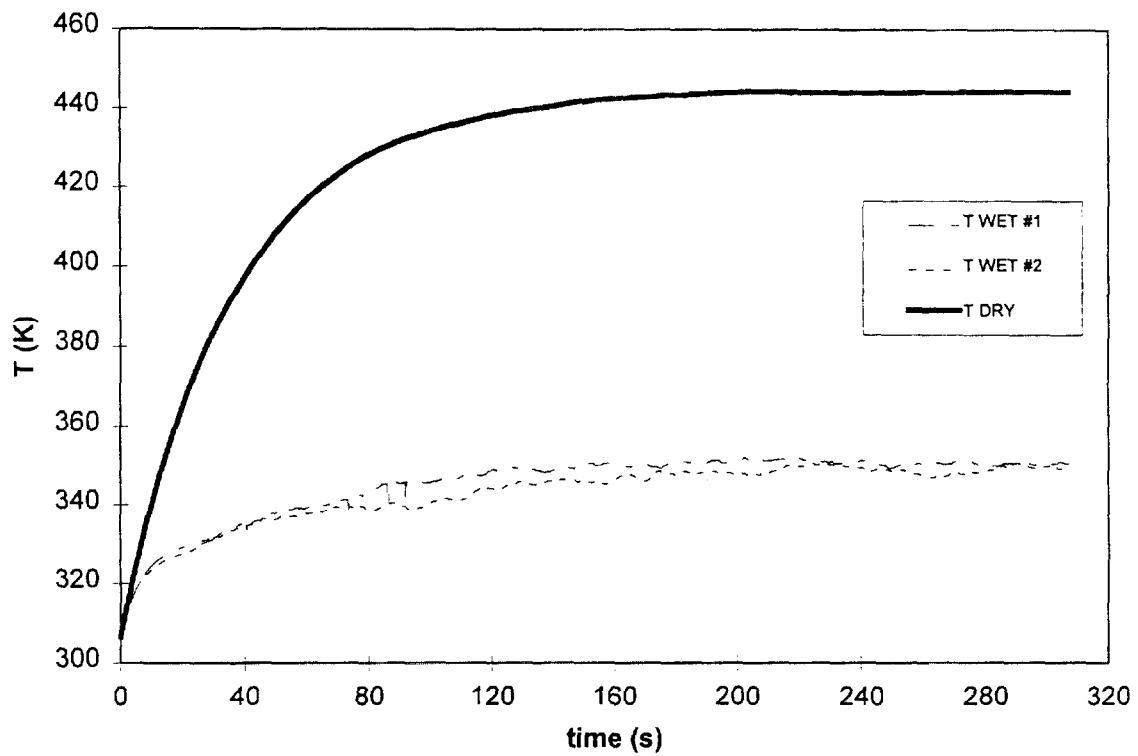


Figure 2. Transient probe temperature profiles during plunge tests.

2/19/99

Task:

One PJ8 spray nozzle water injection
middle air velocity (5.8 m/s)
middle air temperature ($T_{\text{gas}} = 440 \text{ K}$).

Objectives:

Calculate the response time index (RTI) of the probe and the parameter RHS.

Procedure:

The test consists of two parts:

1) Steady-state conditions with water spray on. Plunge test of the probe, with initial temperature $T_0=300 \text{ K}$. Gas velocity and number of water droplets are measured in the test section. The procedure is repeated three times to verify repeatability.

2) Steady-state conditions with water spray off. Plunge test of the probe, with initial temperature $T_0=308 \text{ K}$ and its transient heating is measured until it reaches steady-state.

The procedure is repeated three times to verify repeatability.

(the initial probe temperature is varied by $\pm 2 \text{ K}$ in the second and third runs, respectively).

	units	Wet conditions	Dry conditions
T_0	K	300	308
T before sprays	K	455	461
T rake #1	K	394	449
T rake #3	K	409	445
T rake #4	K	414	443
T rake #5	K	416	442
T rake #6	K	417	439

Table 1. Temperature at the seven recorded locations.

ΔT_0	K	20		
run #1 u	m/s	6.0		
run #2 u	m/s	5.6		
run #3 u	m/s	5.7		
$u_{\text{average}} \pm \sigma_{n-1}$	m/s	5.8 ± 0.2		
run #1 n (20 samples)		1.5		
run #2 n (20 samples)		1.7		
run #3 n (20 samples)		1.1		
$n_{\text{average}} \pm \sigma_{n-1}$		1.4 ± 0.3		
n_0 [from $n_0(u)$ curve]		2.6		
D	m	$65 \cdot 10^{-6}$		
ϵ	s	1/4000		
A	m^2	$3 \cdot 10^{-5}$		
β		$(4.6 \pm 1.1) \cdot 10^{-6}$		
T_{gas}	K	440		
T_{s0} dry	K	308		
T_{s0} wet	K	300		
RTI		90 ± 13		
		hot/wet cond.#1	hot/wet cond.#2	hot/wet cond.#3
RHS		16.88 ± 0.10	16.83 ± 0.08	16.82 ± 0.08
$\frac{T^{\text{DRY}} - T}{T^{\text{DRY}} - T_0}$		0.70 ± 0.08	0.66 ± 0.06	0.55 ± 0.06

Table 2. Test parameters.

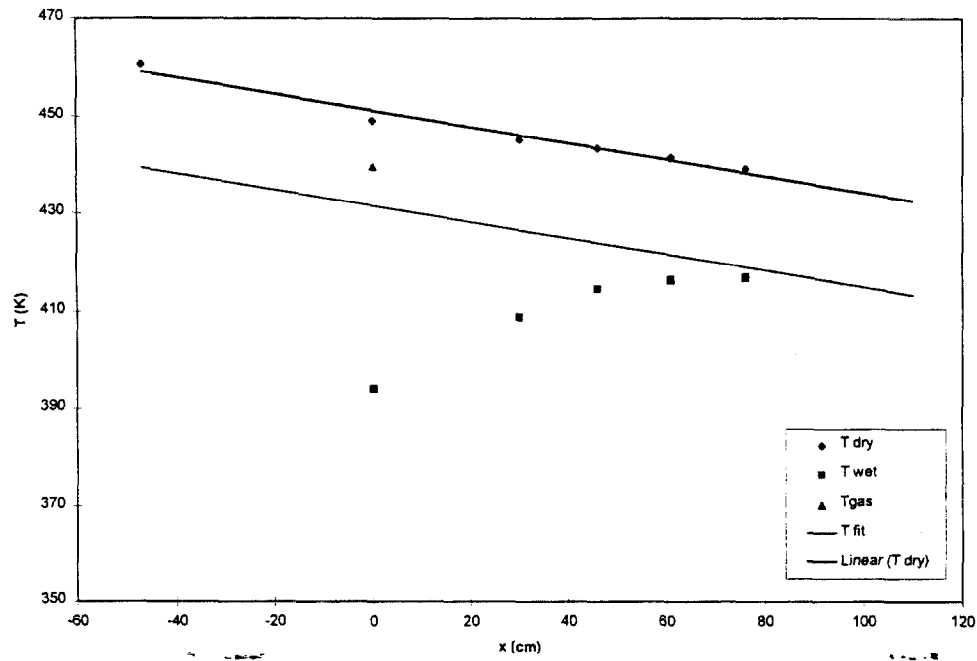


Figure 1. Steady-state temperatures along the duct.

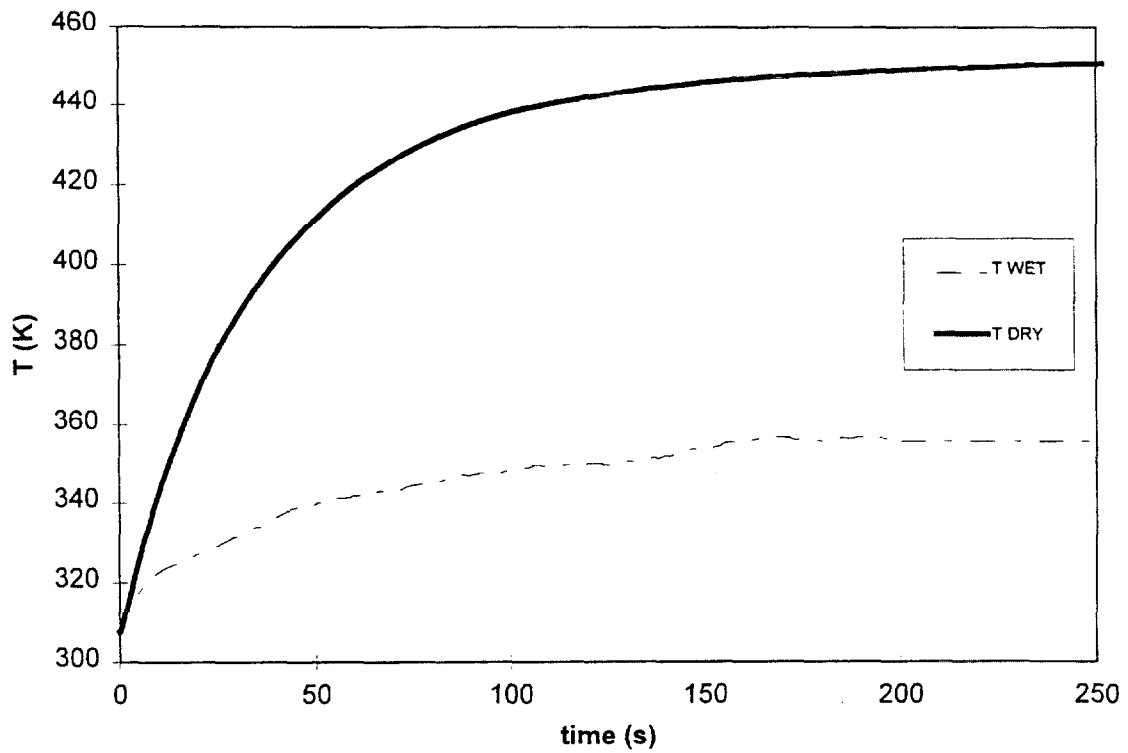


Figure 2. Transient probe temperature profiles during plunge tests.

2/22/99

Task: One PJ8 spray nozzle water injection
high air velocity (7.4 m/s)
high air temperature ($T_{\text{gas}} = 494 \text{ K}$).

Objectives: Calculate the response time index (RTI) of the probe and the parameter RHS.

Procedure: The test consist of two parts:

- 1) Steady-state conditions with water spray on. Plunge test of the probe, with initial temperature $T_0=300 \text{ K}$. Gas velocity and number of water droplets are measured in the test section. The procedure is repeated three times to verify repeatability.
- 2) Steady-state conditions with water spray off. Plunge test of the probe, with initial temperature $T_0=307 \text{ K}$ and its transient heating is measured until it reaches steady-state. The procedure is repeated three times to verify repeatability.
(the initial probe temperature is varied by $\pm 2 \text{ K}$ in the second and third runs, respectively).

	units	Wet conditions	Dry conditions
T_0	K	300	307
T before sprays	K	512	516
T rake #1	K	445	500
T rake #3	K	460	493
T rake #4	K	464	490
T rake #5	K	464	487
T rake #6	K	464	484

Table 1. Temperature at the seven recorded locations.

ΔT_0	K	18		
run #1 u	m/s	7.8		
run #2 u	m/s	7.0		
run #3 u	m/s	7.4		
$u_{\text{average}} \pm \sigma_{n-1}$	m/s	7.4 ± 0.4		
run #1 n (20 samples)		2.5		
run #2 n (20 samples)		2.6		
run #3 n (20 samples)		1.4		
$n_{\text{average}} \pm \sigma_{n-1}$		2.2 ± 0.7		
n_0 [from $n_0(u)$ curve]		3.2		
D	m	$65 \cdot 10^{-6}$		
ϵ	s	1/4000		
A	m ²	$3 \cdot 10^{-5}$		
β		$(5.2 \pm 1.9) \cdot 10^{-6}$		
T_{gas}	K	494		
T_{s0} dry	K	307		
T_{s0} wet	K	300		
RTI		137 ± 34		
		hot/wet cond.#1	hot/wet cond.#2	hot/wet cond.#3
RHS		16.28 ± 0.04	16.37 ± 0.09	16.31 ± 0.02
$\frac{T^{\text{DRY}} - T}{T^{\text{DRY}} - T_0}$		0.31 ± 0.04	0.35 ± 0.05	0.32 ± 0.03

Table 2. Test parameters.

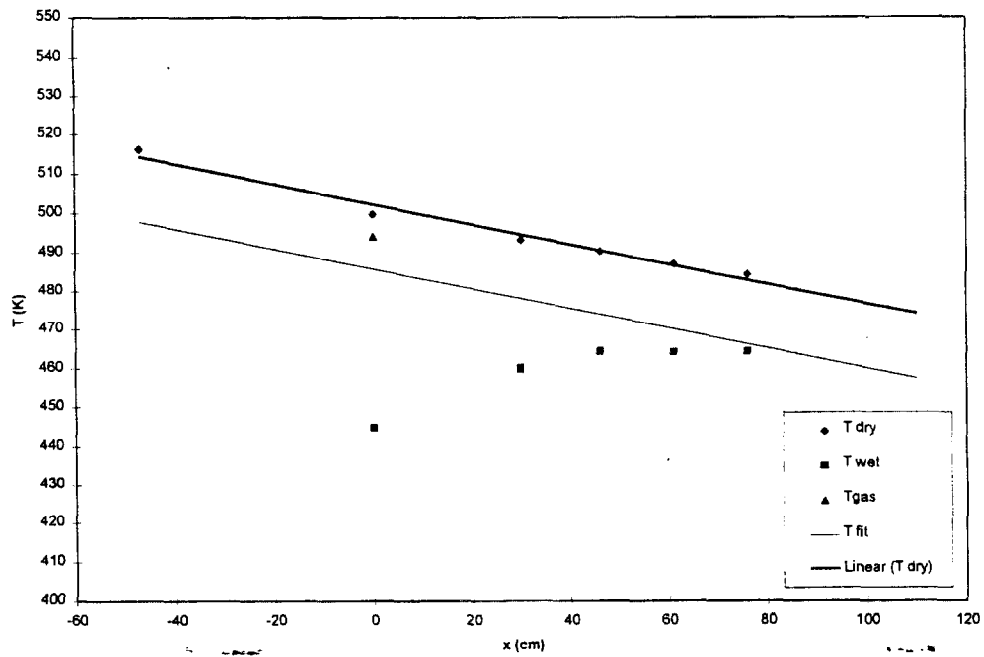


Figure 1. Steady-state temperatures along the duct.

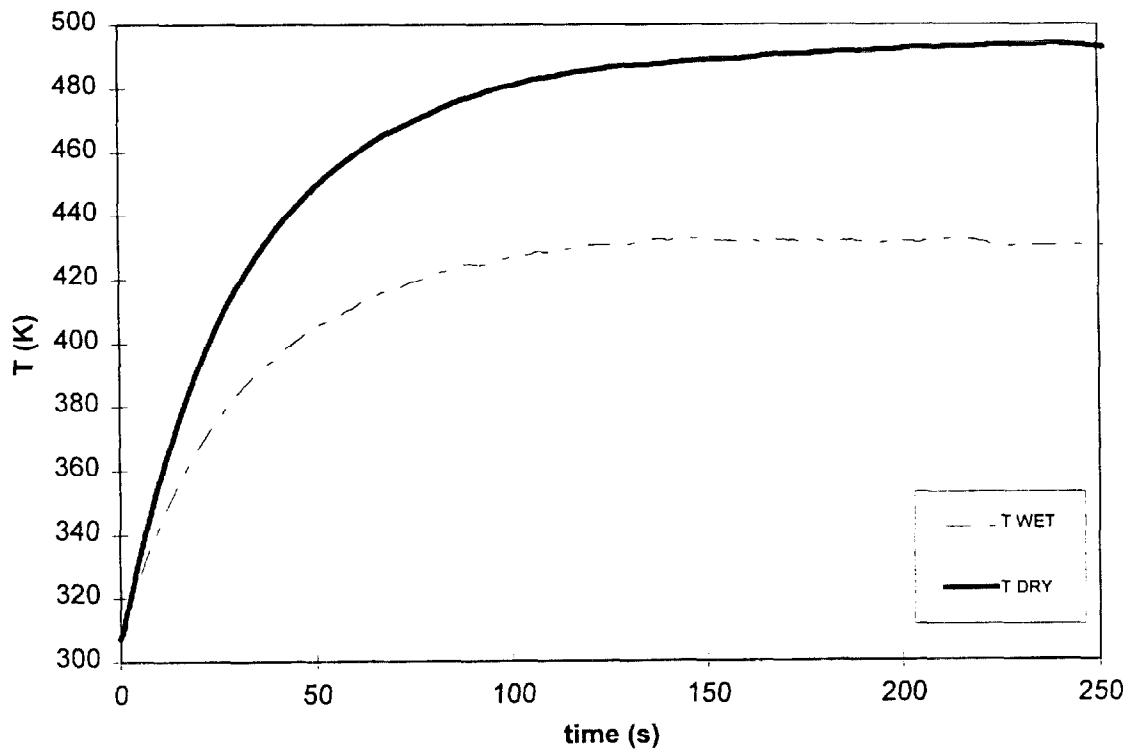


Figure 2. Transient probe temperature profiles during plunge tests.

2/23/99

Task: One PJ8 spray nozzle water injection
high air velocity (5.8 m/s)
middle air temperature ($T_{\text{gas}} = 440 \text{ K}$).

Objectives: Calculate the response time index (RTI) of the probe and the parameter RHS.

Procedure: The test consists of two parts:

- 1) Steady-state conditions with water spray on. Plunge test of the probe, with initial temperature $T_0=300 \text{ K}$. Gas velocity and number of water droplets are measured in the test section. The procedure is repeated three times to verify repeatability.
- 2) Steady-state conditions with water spray off. Plunge test of the probe, with initial temperature $T_0=310 \text{ K}$ and its transient heating is measured until it reaches steady-state. The procedure is repeated three times to verify repeatability.
(the initial probe temperature is varied by $\pm 2 \text{ K}$ in the second and third runs, respectively).

	units	Wet conditions	Dry conditions
T_0	K	300	310
T before sprays	K	459	464
T rake #1	K	378	451
T rake #3	K	406	447
T rake #4	K	412	445
T rake #5	K	415	443
T rake #6	K	416	440

Table 1. Temperature at the seven recorded locations.

ΔT_0	K	23		
run #1 u	m/s	5.9		
run #2 u	m/s	5.6		
run #3 u	m/s	5.9		
$u_{\text{average}} \pm \sigma_{n-1}$	m/s	5.8 ± 0.2		
run #1 n (20 samples)		2.5		
run #2 n (20 samples)		2.4		
run #3 n (20 samples)		2.2		
$n_{\text{average}} \pm \sigma_{n-1}$		2.4 ± 0.1		
n_0 [from 20 samples]		4.5		
D	m	$65 \cdot 10^{-6}$		
ε	s	1/4000		
A	m ²	$3 \cdot 10^{-5}$		
β		$(7.6 \pm 0.6) \cdot 10^{-6}$		
T_{gas}	K	440		
T_{s0} dry	K	310		
T_{s0} wet	K	300		
RTI		133 ± 35		
		hot/wet cond.#1	hot/wet cond.#2	hot/wet cond.#3
RHS		16.41 ± 0.05	16.46 ± 0.06	16.36 ± 0.05
$\frac{T^{\text{DRY}} - T}{T^{\text{DRY}} - T_0}$		0.72 ± 0.06	0.75 ± 0.07	0.68 ± 0.04

Table 2. Test parameters.

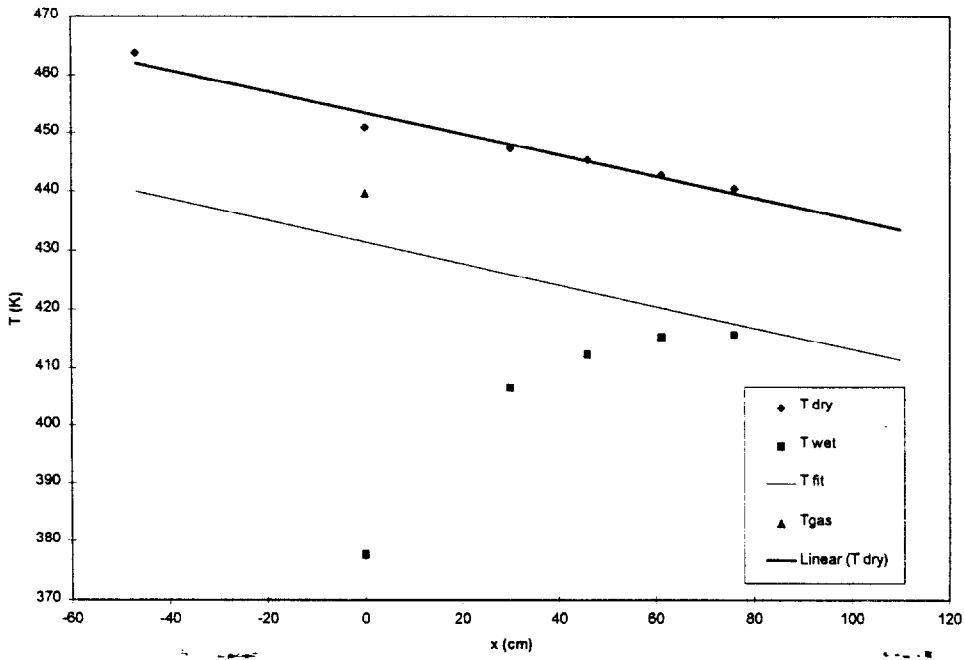


Figure 1. Steady-state temperatures along the duct.

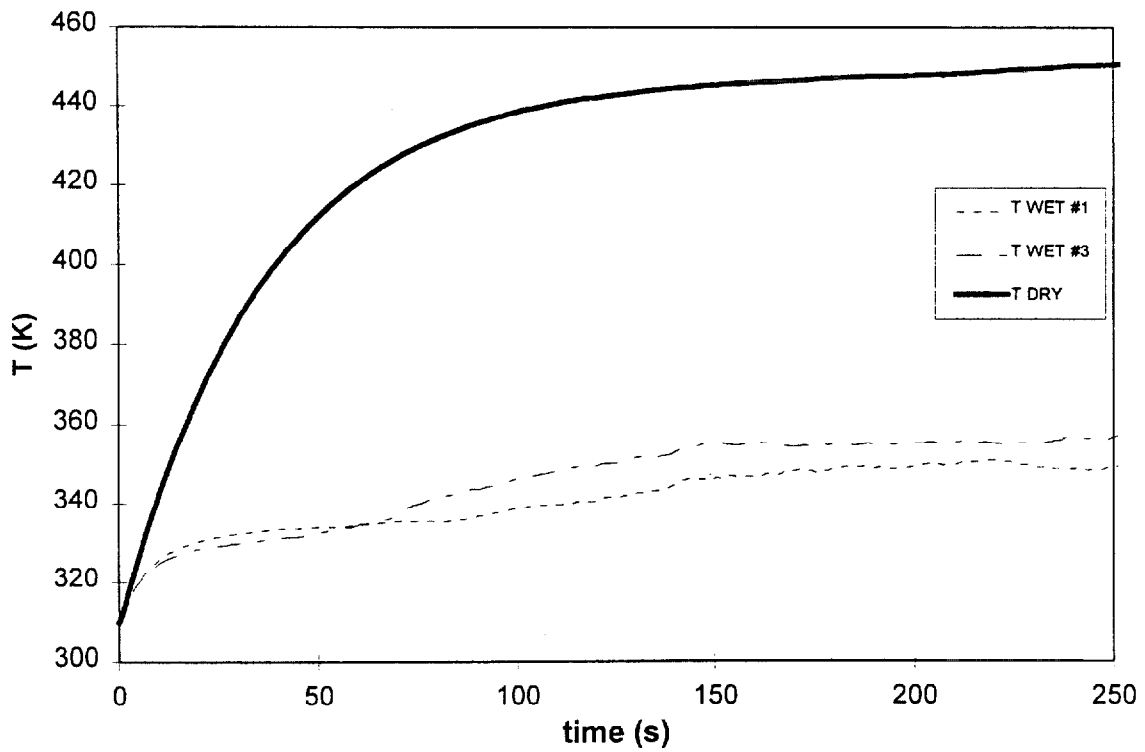


Figure 2. Transient probe temperature profiles during plunge tests.

2/25/99 test#1

Task: One PJ8 spray nozzle water injection
low air velocity (3.2 m/s)
low air temperature ($T_{\text{gas}} = 377 \text{ K}$).

Objectives: Calculate the response time index (RTI) of the probe and the parameter RHS.

Procedure: The test consists of two parts:

- 1) Steady-state conditions with water spray on. Plunge test of the probe, with initial temperature $T_0=300 \text{ K}$. Gas velocity and number of water droplets are measured in the test section. The procedure is repeated three times to verify repeatability.
- 2) Steady-state conditions with water spray off. Plunge test of the probe, with initial temperature $T_0=310 \text{ K}$ and its transient heating is measured until it reaches steady-state. The procedure is repeated three times to verify repeatability.
(the initial probe temperature is varied by $\pm 3 \text{ K}$ in the second and third runs, respectively).

	units	Wet conditions	Dry conditions
T_0	K	300	310
T before sprays	K	390	397
T rake #1	K	308	389
T rake #3	K	334	383
T rake #4	K	344	381
T rake #5	K	348	380
T rake #6	K	350	380

Table 1. Temperature at the seven recorded locations.

ΔT_0	K	25		
run #1 u	m/s	3.4		
run #2 u	m/s	2.8		
run #3 u	m/s	3.3		
$u_{\text{average}} \pm \sigma_{n-1}$	m/s	3.1 ± 0.3		
run #1 n (20 samples)		2.8		
run #2 n (20 samples)		1.9		
run #3 n (20 samples)		3.5		
$n_{\text{average}} \pm \sigma_{n-1}$		2.7 ± 0.8		
n_0 [from $n_0(u)$ curve]		3.7		
D	m	$65 \cdot 10^{-6}$		
ϵ	s	1/2000		
A	m ²	$3 \cdot 10^{-5}$		
β		$(8.1 \pm 3.2) \cdot 10^{-6}$		
T_{gas}	K	377		
T_{s0} dry	K	310		
T_{s0} wet	K	300		
RTI		125 ± 25		
		hot/wet cond.#1	hot/wet cond.#2	hot/wet cond.#3
RHS		15.95 ± 0.07	15.96 ± 0.06	15.96 ± 0.06
$\frac{T^{\text{DRY}} - T}{T^{\text{DRY}} - T_0}$		0.88 ± 0.06	0.89 ± 0.05	0.90 ± 0.05

Table 2. Test parameters.

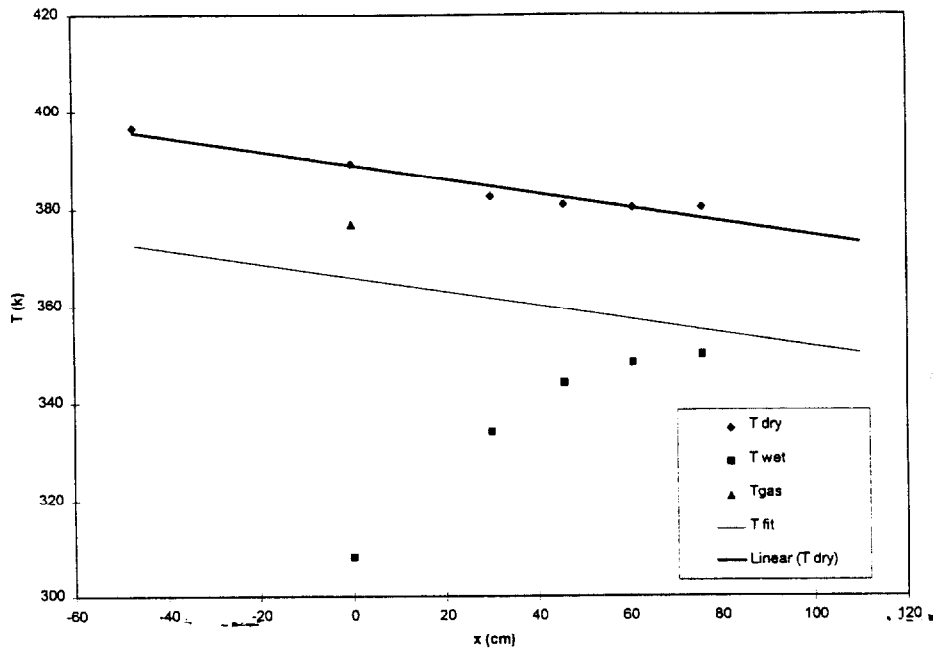


Figure 1. Steady-state temperatures along the duct.

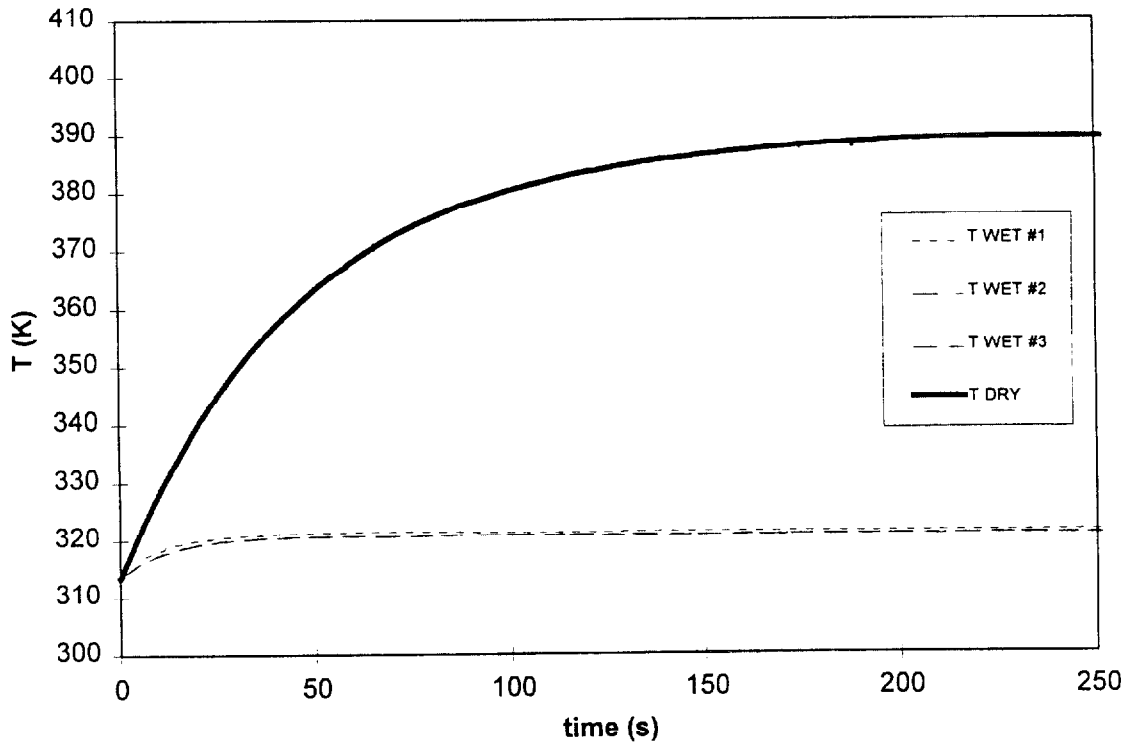


Figure 2. Transient probe temperature profiles during plunge tests.

2/25/99 test#2

Task:

One PJ8 spray nozzle water injection
middle air velocity (4.6 m/s)
low air temperature ($T_{\text{gas}} = 362 \text{ K}$).

Objectives:

Calculate the response time index (RTI) of the probe and the parameter RHS.

Procedure:

The test consists of two parts:

1) Steady-state conditions with water spray on. Plunge test of the probe, with initial temperature $T_0=300 \text{ K}$. Gas velocity and number of water droplets are measured in the test section. The procedure is repeated three times to verify repeatability.

2) Steady-state conditions with water spray off. Plunge test of the probe, with initial temperature $T_0=312 \text{ K}$ and its transient heating is measured until it reaches steady-state.

The procedure is repeated three times to verify repeatability.

(the initial probe temperature is varied by $\pm 4 \text{ K}$ in the second and third runs, respectively).

	units	Wet conditions	Dry conditions
T_0	K	300	308
T before sprays	K	372	373
T rake #1	K	306	370
T rake #3	K	313	368
T rake #4	K	327	367
T rake #5	K	336	365
T rake #6	K	341	365

Table 1. Temperature at the seven recorded locations.

ΔT_0	K	19		
run #1 u	m/s	4.7		
run #2 u	m/s	4.4		
run #3 u	m/s	4.5		
$u_{\text{average}} \pm \sigma_{n-1}$	m/s	4.6 ± 0.2		
run #1 n (20 samples)		3.0		
run #2 n (20 samples)		2.8		
run #3 n (20 samples)		2.6		
$n_{\text{average}} \pm \sigma_{n-1}$		2.8 ± 0.2		
n_0 [from $n_0(u)$ curve]		3.5		
D	m	$65 \cdot 10^{-6}$		
ε	s	1/2000		
A	m ²	$3 \cdot 10^{-5}$		
β		$(5.9 \pm 0.7) \cdot 10^{-6}$		
T_{gas}	K	362		
T_{s0} dry	K	308		
T_{s0} wet	K	300		
RTI		166 ± 40		
		hot/wet cond.#1	hot/wet cond.#2	hot/wet cond.#3
RHS		15.98 ± 0.16	16.01 ± 0.13	16.04 ± 0.10
$\frac{T^{\text{DRY}} - T}{T^{\text{DRY}} - T_0}$		0.83 ± 0.12	0.86 ± 0.10	0.88 ± 0.08

Table 2. Test parameters.

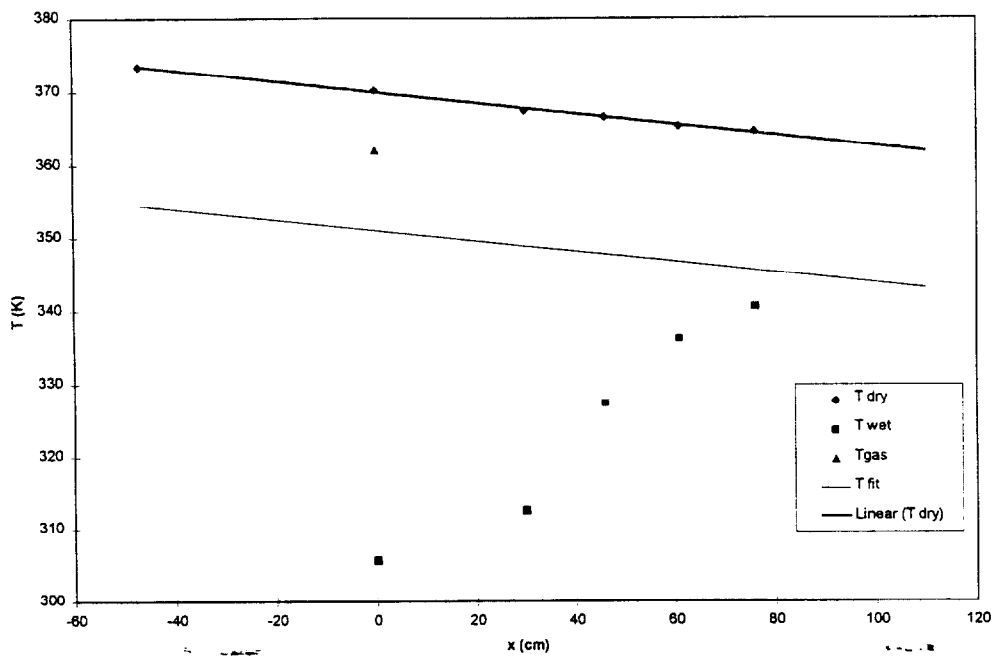


Figure 1. Steady-state temperatures along the duct.

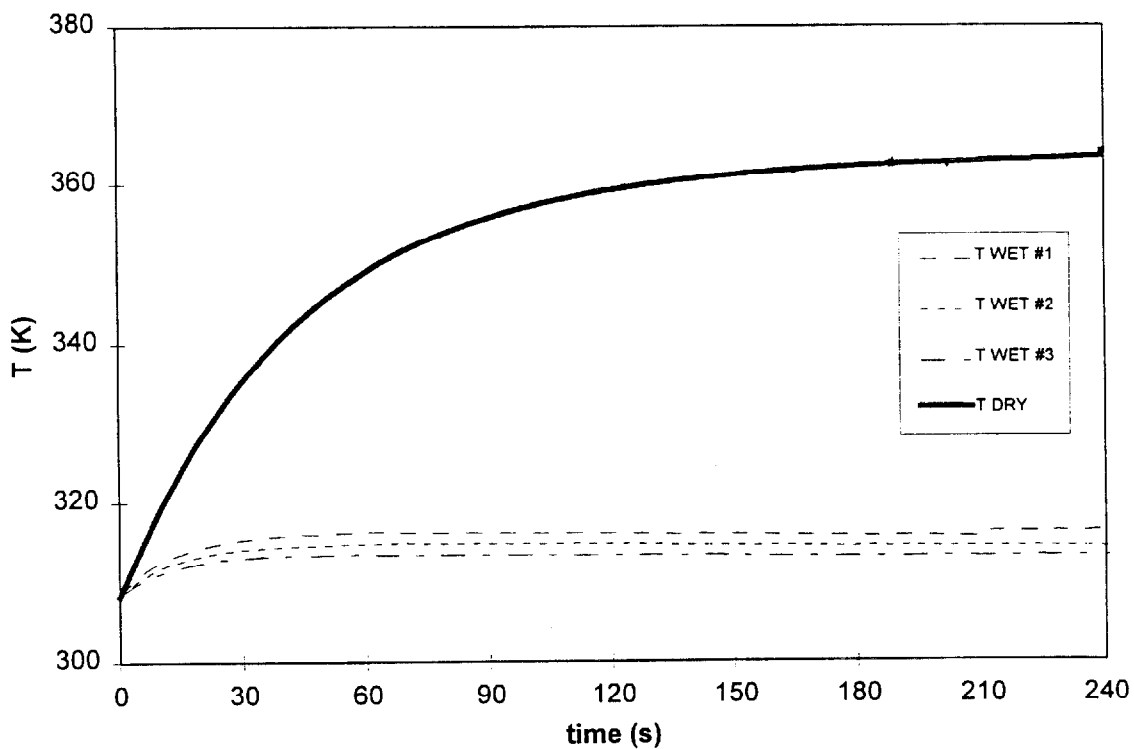


Figure 2. Transient probe temperature profiles during plunge tests.

2/26/99

Task: One PJ8 spray nozzle water injection
low air velocity (3.5 m/s)
low air temperature ($T_{\text{gas}} = 360 \text{ K}$).

Objectives: Calculate the response time index (RTI) of the probe and the parameter RHS.

Procedure: The test consists of two parts:

- 1) Steady-state conditions with water spray on. Plunge test of the probe, with initial temperature $T_0=300 \text{ K}$. Gas velocity and number of water droplets are measured in the test section. The procedure is repeated three times to verify repeatability.
- 2) Steady-state conditions with water spray off. Plunge test of the probe, with initial temperature $T_0=310 \text{ K}$ and its transient heating is measured until it reaches steady-state. The procedure is repeated three times to verify repeatability.
(the initial probe temperature is varied by $\pm 2 \text{ K}$ in the second and third runs, respectively).

	units	Wet conditions	Dry conditions
T_0	K	300	308
T before sprays	K	367	369
T rake #1	K	305	364
T rake #3	K	310	360
T rake #4	K	322	359
T rake #5	K	328	357
T rake #6	K	331	357

Table 1. Temperature at the seven recorded locations.

ΔT_0	K	22		
run #1 u	m/s	3.7		
run #2 u	m/s	3.4		
run #3 u	\bar{m}/s	3.5		
$u_{\text{average}} \pm \sigma_{n-1}$	m/s	3.5 ± 0.2		
run #1 n (20 samples)		4.0		
run #2 n (20 samples)		2.7		
run #3 n (20 samples)		2.9		
$n_{\text{average}} \pm \sigma_{n-1}$		3.2 ± 0.7		
n_0 [from $n_0(u)$ curve]		3.6		
D	m	$65 \cdot 10^{-6}$		
ϵ	s	1/2000		
A	m^2	$3 \cdot 10^{-5}$		
β		$(8.2 \pm 2.3) \cdot 10^{-6}$		
T_{gas}	K	360		
T_{s0} dry	K	308		
T_{s0} wet	K	300		
RTI		127 ± 29		
		hot/wet cond.#1	hot/wet cond.#2	hot/wet cond.#3
RHS		15.61 ± 0.07	15.63 ± 0.06	15.64 ± 0.05
$\frac{T^{\text{DRY}} - T}{T^{\text{DRY}} - T_0}$		0.90 ± 0.05	0.92 ± 0.04	0.94 ± 0.04

Table 2. Test parameters.

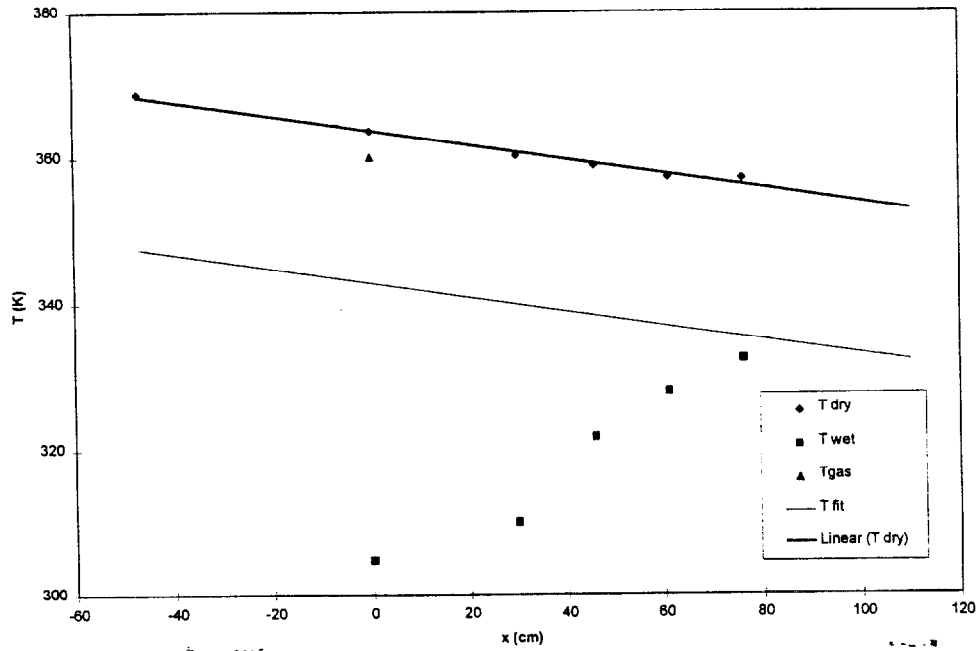


Figure 1. Steady-state temperatures along the duct.

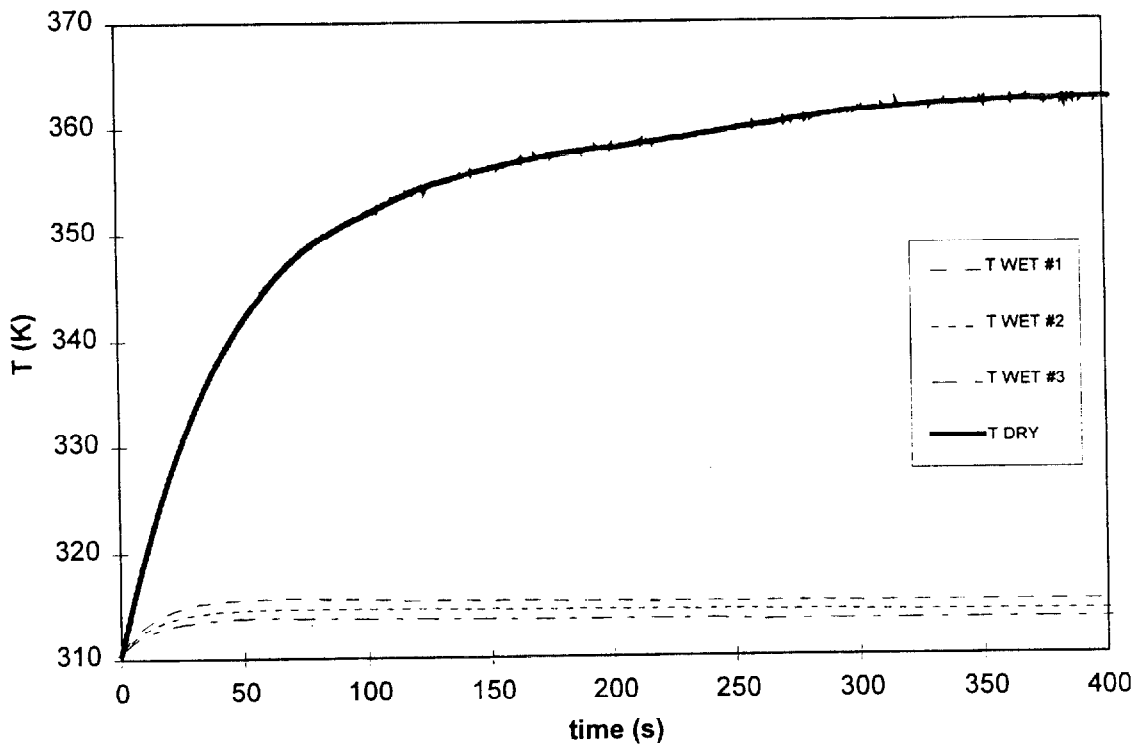


Figure 2. Transient probe temperature profiles during plunge tests.

3/1/99 test #1

Task:

One PJ8 spray nozzle water injection
low air velocity (3.9 m/s)
low air temperature ($T_{\text{gas}} = 404 \text{ K}$).

Objectives:

Calculate the response time index (RTI) of the probe and the parameter RHS.

Procedure:

The test consists of two parts:

1) Steady-state conditions with water spray on. Plunge test of the probe, with initial temperature $T_0=300 \text{ K}$. Gas velocity and number of water droplets are measured in the test section. The procedure is repeated three times to verify repeatability.

2) Steady-state conditions with water spray off. Plunge test of the probe, with initial temperature $T_0=310 \text{ K}$ and its transient heating is measured until it reaches steady-state. The procedure is repeated three times to verify repeatability.

(the initial probe temperature is varied by $\pm 2 \text{ K}$ in the second and third runs, respectively).

	units	Wet conditions	Dry conditions
T_0	K	300	310 ± 2
T before sprays	K	421	421
T rake #1	K	344	415
T rake #3	K	366	410
T rake #4	K	369	408
T rake #5	K	373	406
T rake #6	K	374	405

Table 1. Temperature at the seven recorded locations.

ΔT_0	K	29		
run #1 u	m/s	4		
run #2 u	m/s	3.7		
run #3 u	m/s	4		
$u_{\text{average}} \pm \sigma_{n-1}$	m/s	3.9 ± 0.2		
run #1 n (20 samples)		2.5		
run #2 n (20 samples)		2.6		
run #3 n (20 samples)		2.5		
$n_{\text{average}} \pm \sigma_{n-1}$		2.5 ± 0.1		
n_0 [from $n_0(u)$ curve]		4		
D	m	$65 \cdot 10^{-6}$		
ε	s	1/2000		
A	m ²	$3 \cdot 10^{-5}$		
β		$(6.1 \pm 0.2) \cdot 10^{-6}$		
T_{gas}	K	404		
T_{s0} dry	K	312		
T_{s0} wet	K	300		
RTI		110 ± 12		
		hot/wet cond.#1	hot/wet cond.#2	hot/wet cond.#3
RHS		16.43 ± 0.09	16.44 ± 0.10	16.45 ± 0.09
$\frac{T^{\text{DRY}} - T}{T^{\text{DRY}} - T_0}$		0.84 ± 0.02	0.84 ± 0.02	0.85 ± 0.02

Table 2. Test parameters.

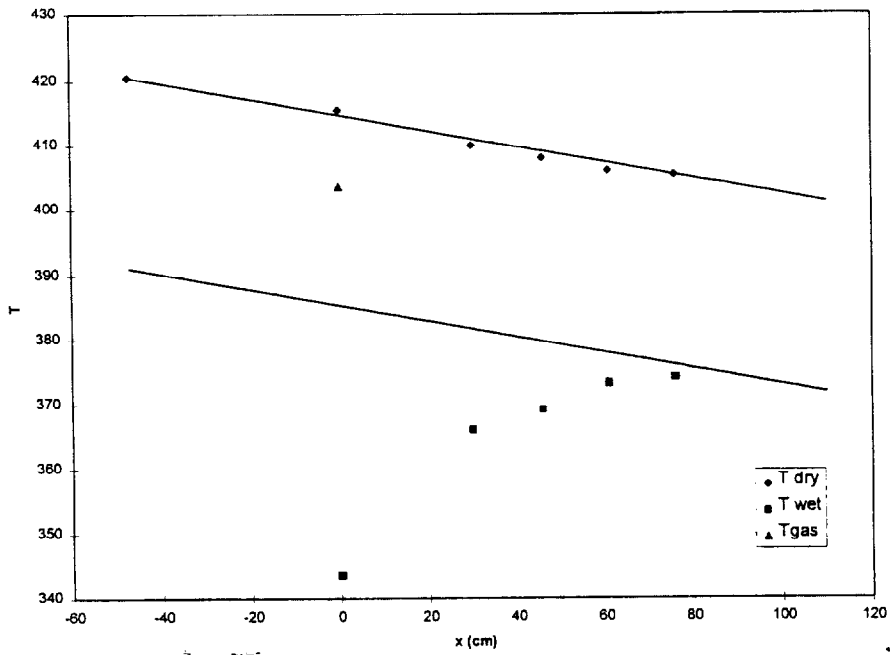


Figure 1. Steady-state temperatures along the duct.

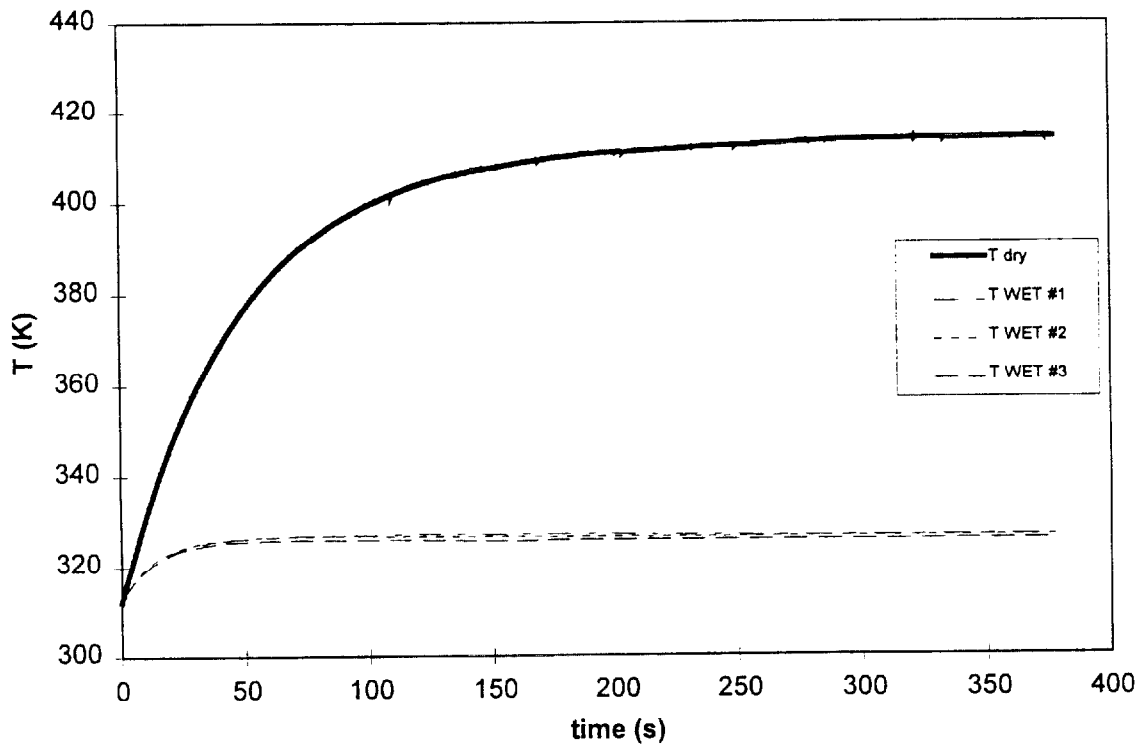


Figure 2. Transient probe temperature profiles during plunge tests.

3/1/99 test#2

Task: One PJ8 spray nozzle water injection
low air velocity (3.9 m/s)
middle air temperature ($T_{\text{gas}} = 424 \text{ K}$).

Objectives: Calculate the response time index (RTI) of the probe and the parameter RHS.

Procedure: The test consists of two parts:

- 1) Steady-state conditions with water spray on. Plunge test of the probe, with initial temperature $T_0 = 300 \text{ K}$. Gas velocity and number of water droplets are measured in the test section. The procedure is repeated three times to verify repeatability.
- 2) Steady-state conditions with water spray off. Plunge test of the probe, with initial temperature $T_0 = 308 \text{ K}$ and its transient heating is measured until it reaches steady-state. The procedure is repeated three times to verify repeatability.
(the initial probe temperature is varied by $\pm 2 \text{ K}$ in the second and third runs, respectively).

	units	Wet conditions	Dry conditions
T_0	K	300	308
T before sprays	K	443	447
T rake #1	K	362	433
T rake #3	K	385	427
T rake #4	K	390	425
T rake #5	K	393	423
T rake #6	K	393	423

Table 1. Temperature at the seven recorded locations.

ΔT_0	K	29		
run #1 u	m/s	3.8		
run #2 u	m/s	3.8		
run #3 u	m/s	4.3		
$u_{\text{average}} \pm \sigma_{n-1}$	m/s	3.9 ± 0.3		
run #1 n (20 samples)				
run #2 n (20 samples)		1.8		
run #3 n (20 samples)		2.8		
$n_{\text{average}} \pm \sigma_{n-1}$		2.3 ± 0.7		
n_0 [from 20 samples]		3.3		
D	m	$65 \cdot 10^{-6}$		
ϵ	s	1/2000		
A	m ²	$3 \cdot 10^{-5}$		
β		$(5.6 \pm 2.1) \cdot 10^{-6}$		
T_{gas}	K	424		
T_{s0} dry	K	308		
T_{s0} wet	K	300		
RTI		167 ± 20		
		hot/wet cond.#1	hot/wet cond.#2	hot/wet cond.#3
RHS		16.69 ± 0.07	16.72 ± 0.08	16.71 ± 0.08
$\frac{T^{\text{DRY}} - T}{T^{\text{DRY}} - T_0}$		0.81 ± 0.06	0.82 ± 0.06	0.81 ± 0.06

Table 2. Test parameters.

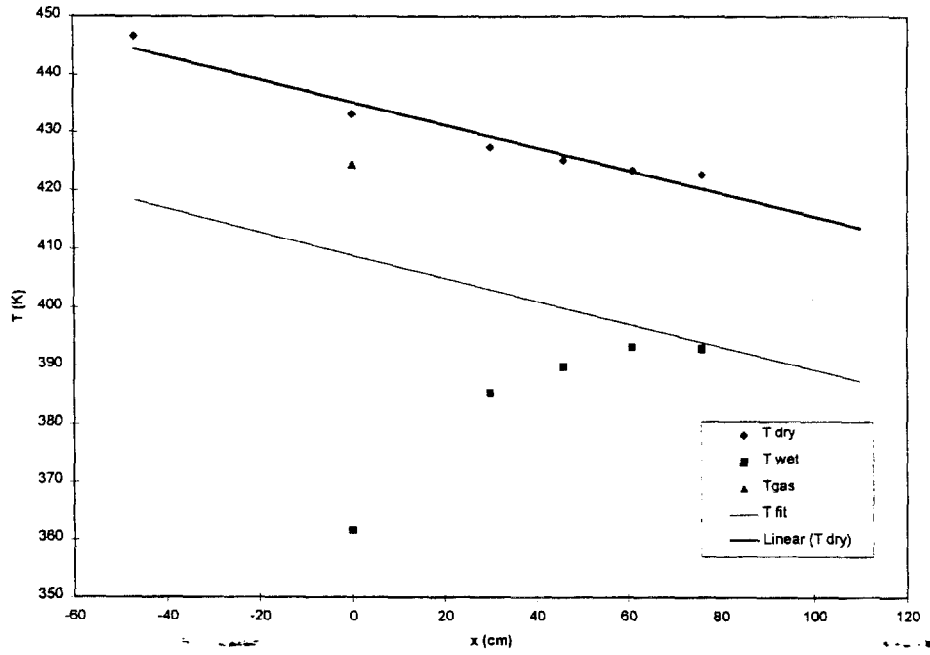


Figure 1. Steady-state temperatures along the duct.

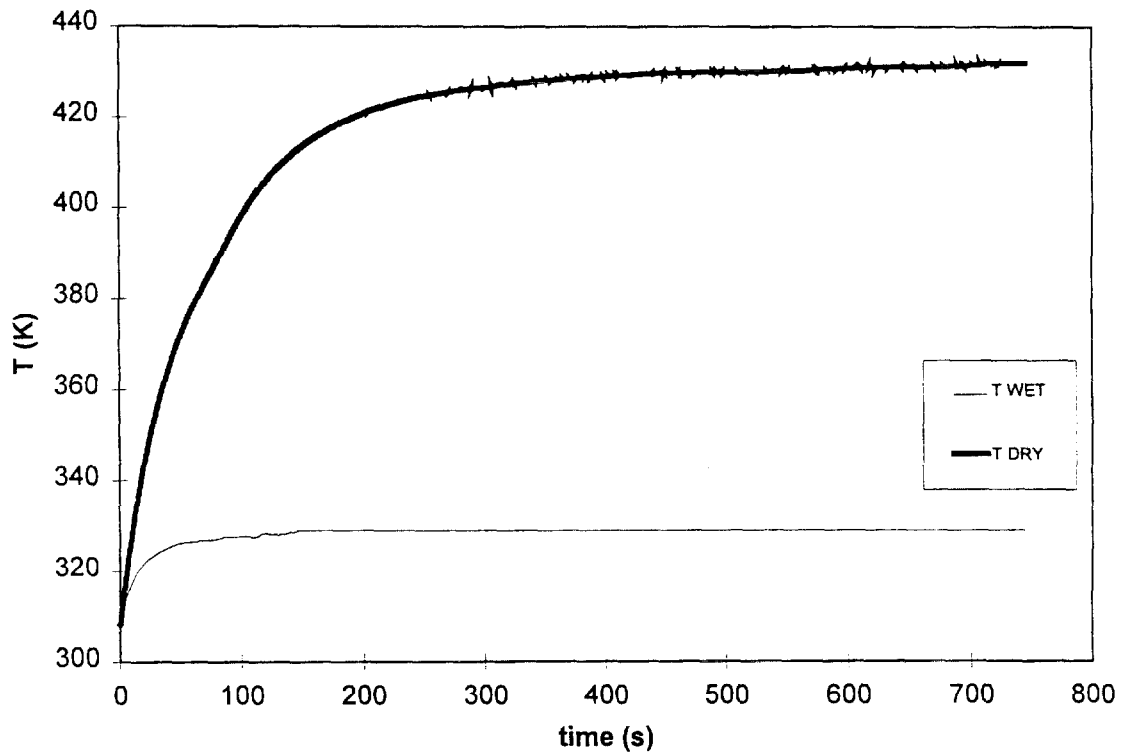


Figure 2. Transient probe temperature profiles during plunge tests.

3/2/99

Task:

One PJ8 spray nozzle water injection
middle air velocity (4.8 m/s)
middle air temperature ($T_{\text{gas}} = 442 \text{ K}$).

Objectives:

Calculate the response time index (RTI) of the probe and the parameter RHS.

Procedure:

The test consists of two parts:

1) Steady-state conditions with water spray on. Plunge test of the probe, with initial temperature $T_0=300 \text{ K}$. Gas velocity and number of water droplets are measured in the test section. The procedure is repeated three times to verify repeatability.

2) Steady-state conditions with water spray off. Plunge test of the probe, with initial temperature $T_0=311 \text{ K}$ and its transient heating is measured until it reaches steady-state.

The procedure is repeated three times to verify repeatability.

(the initial probe temperature is varied by $\pm 3 \text{ K}$ in the second and third runs, respectively).

	units	Wet conditions	Dry conditions
T_0	K	300	312
T before sprays	K	455	464
T rake #1	K	377	452
T rake #3	K	402	445
T rake #4	K	405	443
T rake #5	K	407	440
T rake #6	K	407	439

Table 1. Temperature at the seven recorded locations.

ΔT_0	K	29		
run #1 u	m/s	4.8		
run #2 u	m/s	4.8		
run #3 u	\bar{m}/s	4.8		
$u_{\text{average}} \pm \sigma_{n-1}$	m/s	4.8		
run #1 n (20 samples)		1.9		
run #2 n (20 samples)		2.9		
run #3 n (20 samples)		3.3		
$n_{\text{average}} \pm \sigma_{n-1}$		2.7 ± 0.7		
n_0 [from 20 samples]		4.1		
D	m	$65 \cdot 10^{-6}$		
ϵ	s	1/2000		
A	m^2	$3 \cdot 10^{-5}$		
β		$(5.4 \pm 1.4) \cdot 10^{-6}$		
T_{gas}	K	442		
T_{s0} dry	K	312		
T_{s0} wet	K	300		
RTI		169 ± 25		
		hot/wet cond.#1	hot/wet cond.#2	hot/wet cond.#3
RHS		16.85 ± 0.07	16.86 ± 0.08	16.87 ± 0.07
$\frac{T^{\text{DRY}} - T}{T^{\text{DRY}} - T_0}$		0.80 ± 0.06	0.82 ± 0.08	0.82 ± 0.07

Table 2. Test parameters.

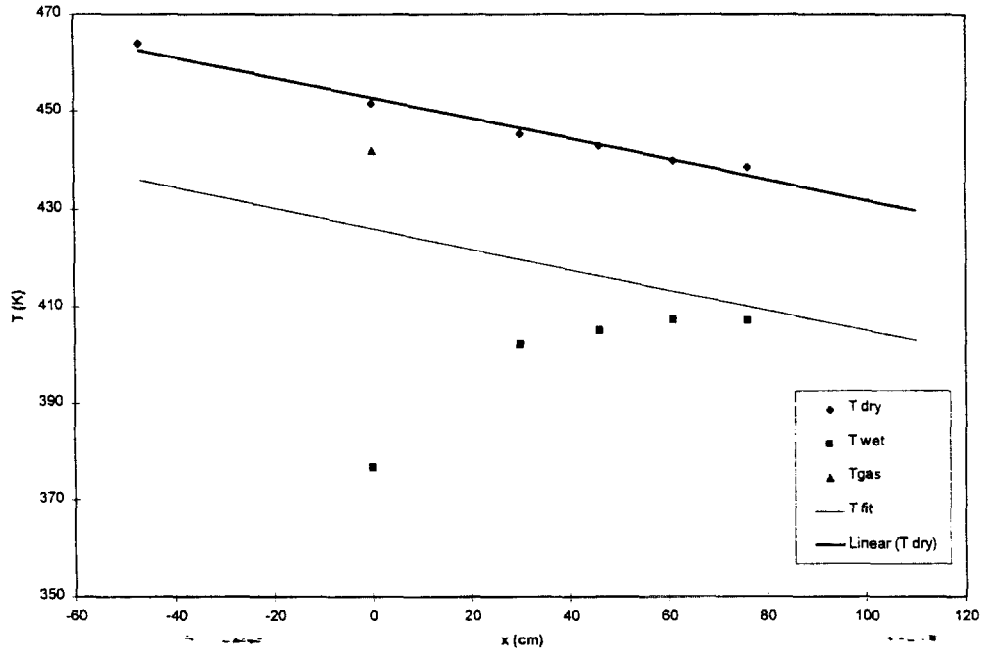


Figure 1. Steady-state temperatures along the duct.

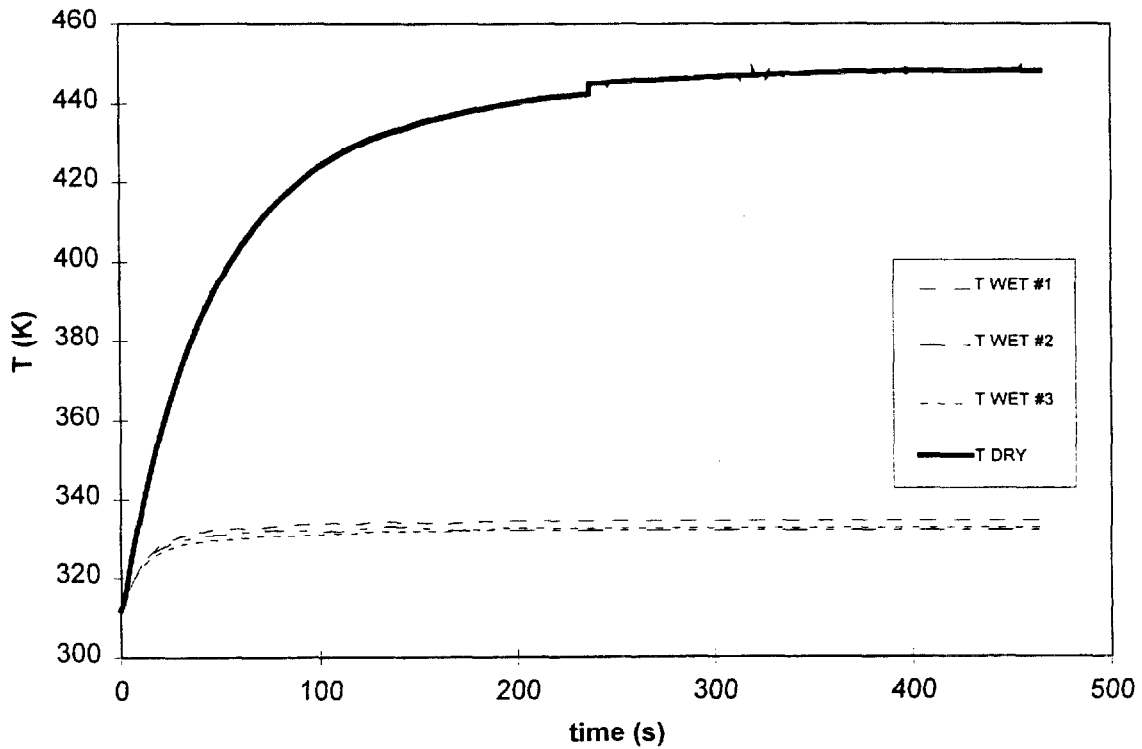


Figure 2. Transient probe temperature profiles during plunge tests.

3/3/99

Task:

One PJ8 spray nozzle water injection
middle air velocity (4 m/s)
middle air temperature ($T_{\text{gas}} = 413 \text{ K}$).

Objectives:

Calculate the response time index (RTI) of the probe and the parameter RHS.

Procedure:

The test consists of two parts:

1) Steady-state conditions with water spray on. Plunge test of the probe, with initial temperature $T_0=300 \text{ K}$. Gas velocity and number of water droplets are measured in the test section. The procedure is repeated three times to verify repeatability.

2) Steady-state conditions with water spray off. Plunge test of the probe, with initial temperature $T_0=313 \text{ K}$ and its transient heating is measured until it reaches steady-state.

The procedure is repeated three times to verify repeatability.

(the initial probe temperature is varied by $\pm 3 \text{ K}$ in the second and third runs, respectively).

	units	Wet conditions	Dry conditions
T_0	K	300	313
T before sprays	K	428	435
T rake #1	K	349	423
T rake #3	K	378	417
T rake #4	K	380	415
T rake #5	K	382	413
T rake #6	K	382	412

Table 1. Temperature at the seven recorded locations.

ΔT_0	K	29		
run #1 u	m/s	4.0		
run #2 u	m/s	4.3		
run #3 u	m/s	3.8		
$u_{\text{average}} \pm \sigma_{n-1}$	m/s	4.0 ± 0.3		
run #1 n (20 samples)		3.1		
run #2 n (20 samples)		3.6		
run #3 n (20 samples)		3.2		
$n_{\text{average}} \pm \sigma_{n-1}$		3.3 ± 0.3		
n_0 [from 20 samples]		3.9		
D	m	$65 \cdot 10^{-6}$		
ϵ	s	1/2000		
A	m ²	$3 \cdot 10^{-5}$		
β		$(7.9 \pm 1.3) \cdot 10^{-6}$		
T_{gas}	K	417		
T_{s0} dry	K	313		
T_{s0} wet	K	300		
RTI		172 ± 97		
		hot/wet cond.#1	hot/wet cond.#2	hot/wet cond.#3
RHS		16.17 ± 0.19	16.21 ± 0.11	16.21 ± 0.15
$\frac{T^{\text{DRY}} - T}{T^{\text{DRY}} - T_0}$		0.83 ± 0.08	0.84 ± 0.06	0.85 ± 0.07

Table 2. Test parameters.

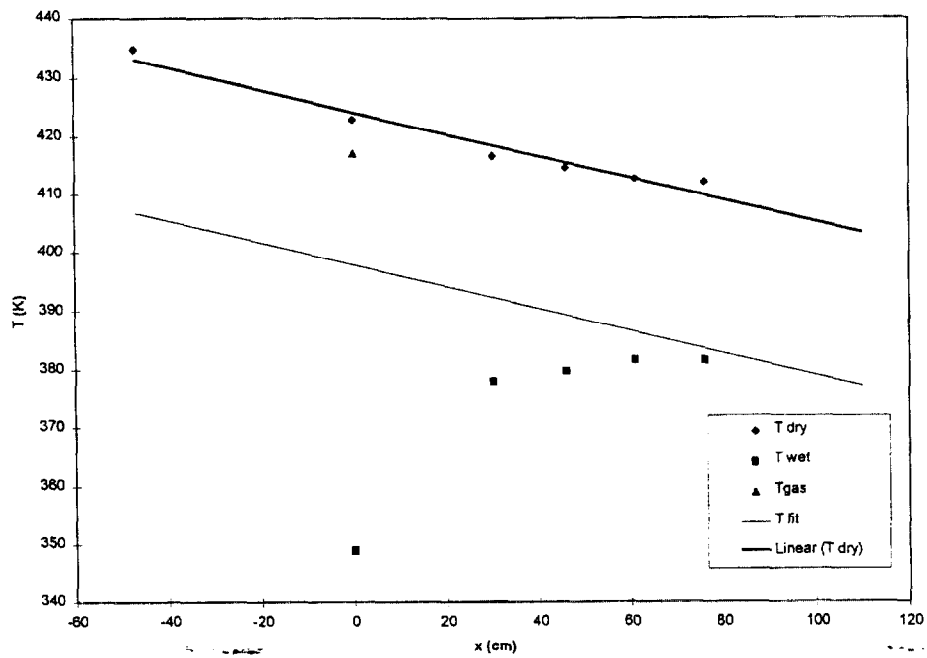


Figure 1. Steady-state temperatures along the duct.

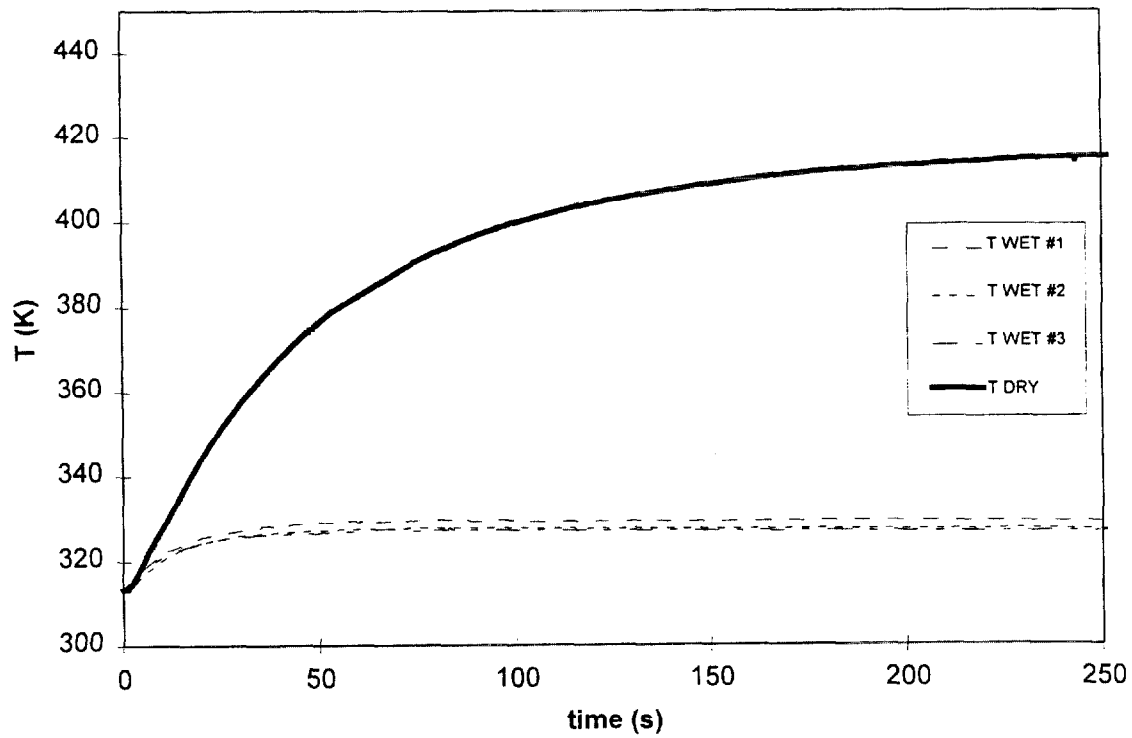


Figure 2. Transient probe temperature profiles during plunge tests.

3/4/99

Task:

One PJ8 spray nozzle water injection
high air velocity (7.1 m/s)
middle air temperature ($T_{\text{gas}} = 442 \text{ K}$).

Objectives:

Calculate the response time index (RTI) of the probe and the parameter RHS.

Procedure:

The test consists of two parts:

1) Steady-state conditions with water spray on. Plunge test of the probe, with initial temperature $T_0=300 \text{ K}$. Gas velocity and number of water droplets are measured in the test section. The procedure is repeated three times to verify repeatability.

2) Steady-state conditions with water spray off. Plunge test of the probe, with initial temperature $T_0=308 \text{ K}$ and its transient heating is measured until it reaches steady-state. The procedure is repeated three times to verify repeatability.

(the initial probe temperature is varied by $\pm 2 \text{ K}$ in the second and third runs, respectively).

	units	Wet conditions	Dry conditions
T_0	K	300	308
T before sprays	K	460	460
T rake #1	K	386	451
T rake #3	K	411	447
T rake #4	K	416	444
T rake #5	K	454	443
T rake #6	K	421	440

Table 1. Temperature at the seven recorded locations.

ΔT_0	K	16		
run #1 u	m/s	7.4		
run #2 u	m/s	6.8		
run #3 u	m/s	7.0		
$u_{\text{average}} \pm \sigma_{n-1}$	m/s	7.1 ± 0.3		
run #1 n (20 samples)		2.3		
run #2 n (20 samples)		2.9		
run #3 n (20 samples)		2.9		
$n_{\text{average}} \pm \sigma_{n-1}$		2.8 ± 0.3		
n_0 [from $n_0(u)$ curve]		6.1		
D	m	$65 \cdot 10^{-6}$		
ϵ	s	1/2000		
A	m^2	$3 \cdot 10^{-5}$		
β		$(3.8 \pm 0.6) \cdot 10^{-6}$		
T_{gas}	K	442		
T_{s0} dry	K	308		
T_{s0} wet	K	300		
RTI		209 ± 65		
		hot/wet cond.#1	hot/wet cond.#2	hot/wet cond.#3
RHS		17.16 ± 0.10	17.24 ± 0.07	17.13 ± 0.09
$\frac{T^{\text{DRY}} - T}{T^{\text{DRY}} - T_0}$		0.73 ± 0.03	0.82 ± 0.02	0.70 ± 0.01

Table 2. Test parameters.

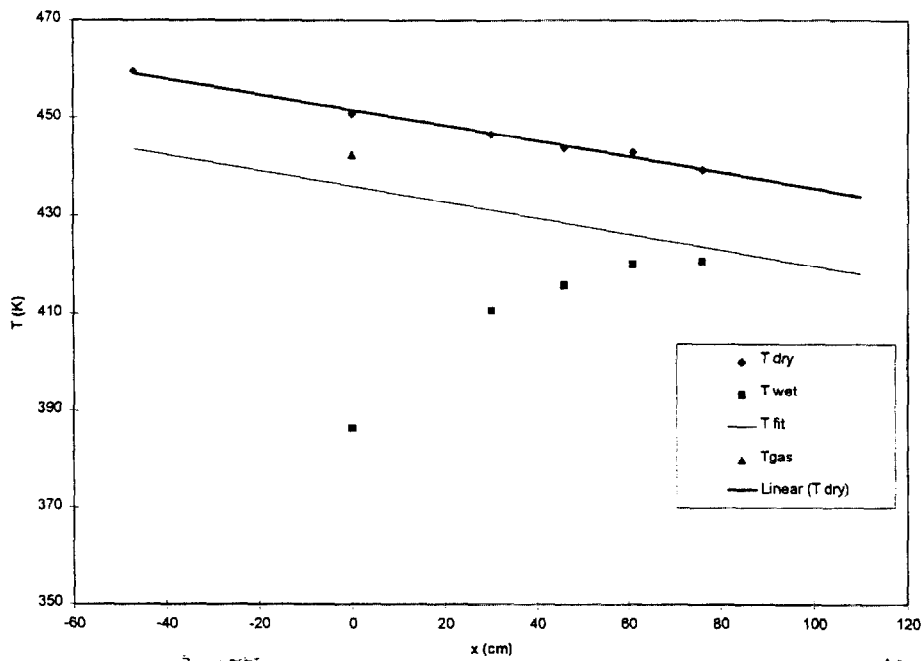


Figure 1. Steady-state temperatures along the duct.

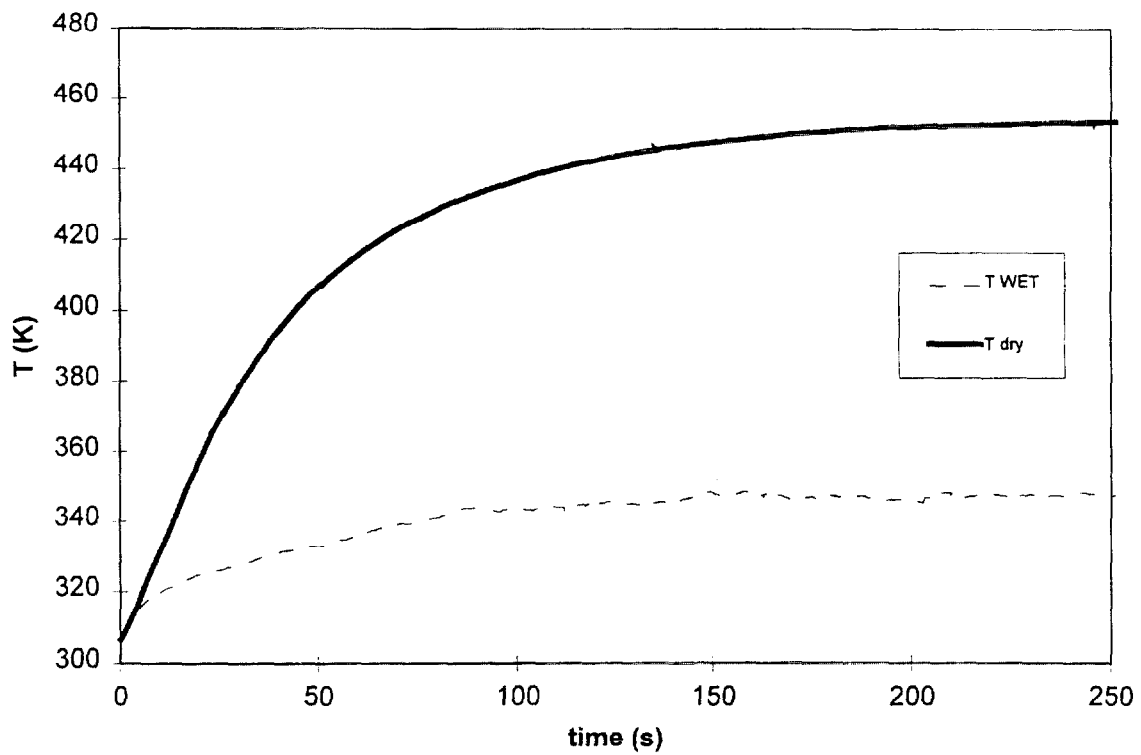


Figure 2. Transient probe temperature profiles during plunge tests.

4/2/99

Task:

One PJ10 spray nozzle water injection
high air velocity (5.8 m/s)
high air temperature ($T_{\text{gas}} = 432 \text{ K}$).

Objectives:

Calculate the response time index (RTI) of the probe and the parameter RHS.

Procedure:

The test consists of two parts:

- 1) Steady-state conditions with water spray on. Plunge test of the probe, with initial temperature $T_0=300 \text{ K}$. Gas velocity and number of water droplets are measured in the test section. The procedure is repeated three times to verify repeatability.
- 2) Steady-state conditions with water spray off. Plunge test of the probe, with initial temperature $T_0=309 \text{ K}$ and its transient heating is measured until it reaches steady-state.

	units	Wet conditions	Dry conditions
T_0	K	300	309
T before sprays	K	454	454
T rake #1	K	357	442
T rake #3	K	402	440
T rake #4	K	409	438
T rake #5	K	413	436
T rake #6	K	413	434

Table 1. Temperature at the seven recorded locations.

ΔT_0	K	18		
run #1 u	m/s	5.9 ± 0.1		
run #2 u	m/s	5.8 ± 0.1		
run #3 u	\bar{m}/s	5.8 ± 0.1		
$u_{\text{average}} \pm \sigma_{n-1}$	m/s	5.8 ± 0.1		
run #1 n (20 samples)		2.5 ± 1.8		
run #2 n (20 samples)		2.5 ± 2.5		
run #3 n (20 samples)		1.9 ± 1.7		
$n_{\text{average}} \pm \sigma_{n-1}$		2.3 ± 2.0		
n_0 [from $n_0(u)$ curve]		5.4		
D	m	$80 \cdot 10^{-6}$		
ϵ	s	1/2000		
A	m^2	$3 \cdot 10^{-5}$		
β		$(7.1 \pm 6.2) \cdot 10^{-6}$		
T_{gas}	K	432		
T_{s0} dry	K	309		
T_{s0} wet	K	300		
RTI		130 ± 16		
		hot/wet cond.#1	hot/wet cond.#2	hot/wet cond.#3
RHS		N/A	16.2 ± 0.1	N/A
$\frac{T^{\text{DRY}} - T}{T^{\text{DRY}} - T_0}$		N/A	0.57 ± 0.01	N/A

Table 2. Test parameters.

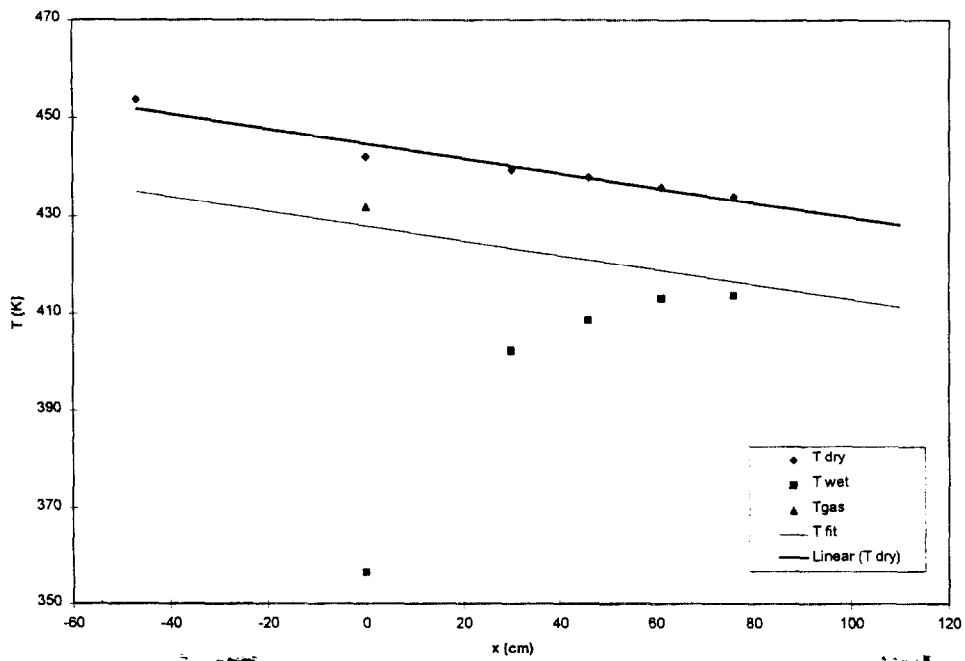


Figure 1. Steady-state temperatures along the duct.

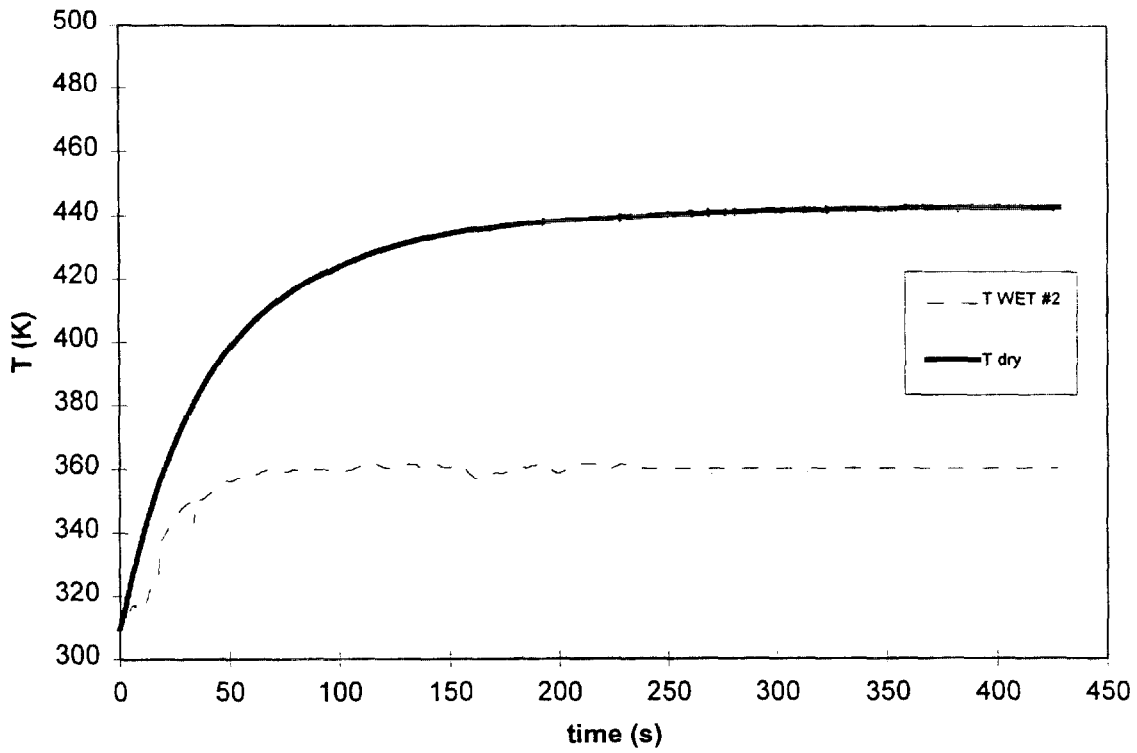


Figure 2. Transient probe temperature profiles during plunge tests.

4/5/99

Task:

One PJ10 spray nozzle water injection
high air velocity (6.4 m/s)
high air temperature ($T_{\text{gas}} = 388 \text{ K}$).

Objectives:

Calculate the response time index (RTI) of the probe and the parameter RHS.

Procedure:

The test consists of two parts:

- 1) Steady-state conditions with water spray on. Plunge test of the probe, with initial temperature $T_0=300 \text{ K}$. Gas velocity and number of water droplets are measured in the test section. The procedure is repeated three times to verify repeatability.
- 2) Steady-state conditions with water spray off. Plunge test of the probe, with initial temperature $T_0=313 \text{ K}$ and its transient heating is measured until it reaches steady-state.

	units	Wet conditions	Dry conditions
T_0	K	300	309
T before sprays	K	403	405
T rake #1	K	314	396
T rake #3	K	335	394
T rake #4	K	357	394
T rake #5	K	369	392
T rake #6	K	373	392

Table 1. Temperature at the seven recorded locations.

ΔT_0	K	17		
run #1 u	m/s	6.6 ± 0.1		
run #2 u	m/s	6.4 ± 0.1		
run #3 u	m/s	6.2 ± 0.1		
$u_{\text{average}} \pm \sigma_{n-1}$	m/s	6.4 ± 0.1		
run #1 n (20 samples)		3.5 ± 2.1		
run #2 n (20 samples)		2.5 ± 2.3		
run #3 n (20 samples)		2.9 ± 2.9		
$n_{\text{average}} \pm \sigma_{n-1}$		2.9 ± 2.4		
n_0 [from $n_0(u)$ curve]		5.9		
D	m	$80 \cdot 10^{-6}$		
ϵ	s	1/2000		
A	m^2	$3 \cdot 10^{-5}$		
β		$(8.1 \pm 6.7) \cdot 10^{-6}$		
T_{gas}	K	388		
T_{s0} dry	K	313		
T_{s0} wet	K	300		
RTI		119 ± 11		
		hot/wet cond.#1	hot/wet cond.#2	hot/wet cond.#3
RHS		16.2 ± 0.1	16.2 ± 0.1	16.2 ± 0.1
$\frac{T^{\text{DRY}} - T}{T^{\text{DRY}} - T_0}$		0.80 ± 0.03	0.78 ± 0.02	0.81 ± 0.02

Table 2. Test parameters.

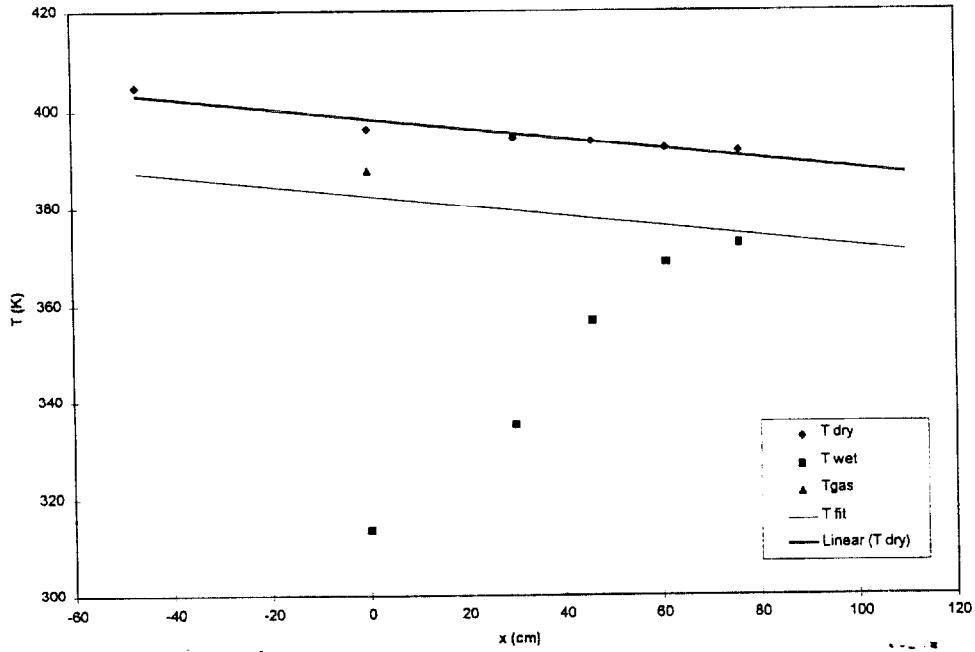


Figure 1. Steady-state temperatures along the duct.

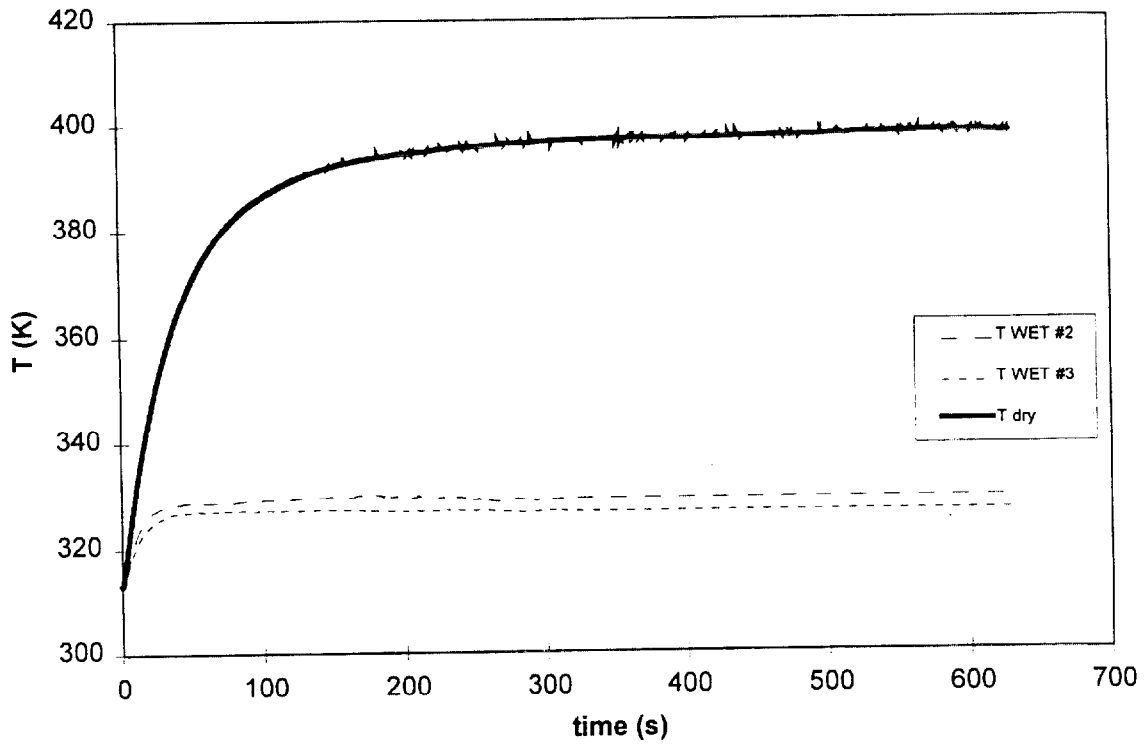


Figure 2. Transient probe temperature profiles during plunge tests.

4/12/99

Task: One PJ10 spray nozzle water injection
high air velocity (3.2 m/s)
high air temperature ($T_{\text{gas}} = 393 \text{ K}$).

Objectives: Calculate the response time index (RTI) of the probe and the parameter RHS.

Procedure: The test consists of two parts:

- 1) Steady-state conditions with water spray on. Plunge test of the probe, with initial temperature $T_0 = 300 \text{ K}$. Gas velocity and number of water droplets are measured in the test section. The procedure is repeated three times to verify repeatability.
- 2) Steady-state conditions with water spray off. Plunge test of the probe, with initial temperature $T_0 = 313$ and its transient heating is measured until it reaches steady-state.

	units	Wet conditions	Dry conditions
T_0	K	300	313
T before sprays	K	394	410
T rake #1	K	317	406
T rake #3	K	332	400
T rake #4	K	356	397
T rake #5	K	359	396
T rake #6	K	360	395

Table 1. Temperature at the seven recorded locations.

ΔT_0	K	33		
run #1 u	m/s	3.3 ± 0.1		
run #2 u	m/s	3.0 ± 0.1		
run #3 u	\bar{m}/s	3.3 ± 0.1		
$u_{\text{average}} \pm \sigma_{n-1}$	m/s	3.2 ± 0.1		
run #1 n (20 samples)		2.3 ± 2.1		
run #2 n (20 samples)		3.0 ± 3.0		
run #3 n (20 samples)		3.0 ± 2.7		
$n_{\text{average}} \pm \sigma_{n-1}$		2.8 ± 2.6		
n_0 [from $n_0(u)$ curve]		3.3		
D	m	$80 \cdot 10^{-6}$		
ϵ	s	1/1000		
A	m^2	$3 \cdot 10^{-5}$		
β		$(5.7 \pm 5.7) \cdot 10^{-6}$		
T_{gas}	K	379		
T_{s0} dry	K	313		
T_{s0} wet	K	300		
RTI		123 ± 6		
		hot/wet cond.#1	hot/wet cond.#2	hot/wet cond.#3
RHS		Not Valid	16.2 ± 0.1	16.2 ± 0.2
$\frac{T^{\text{DRY}} - T}{T^{\text{DRY}} - T_0}$		Not Valid	0.77 ± 0.05	0.77 ± 0.06

Table 2. Test parameters.

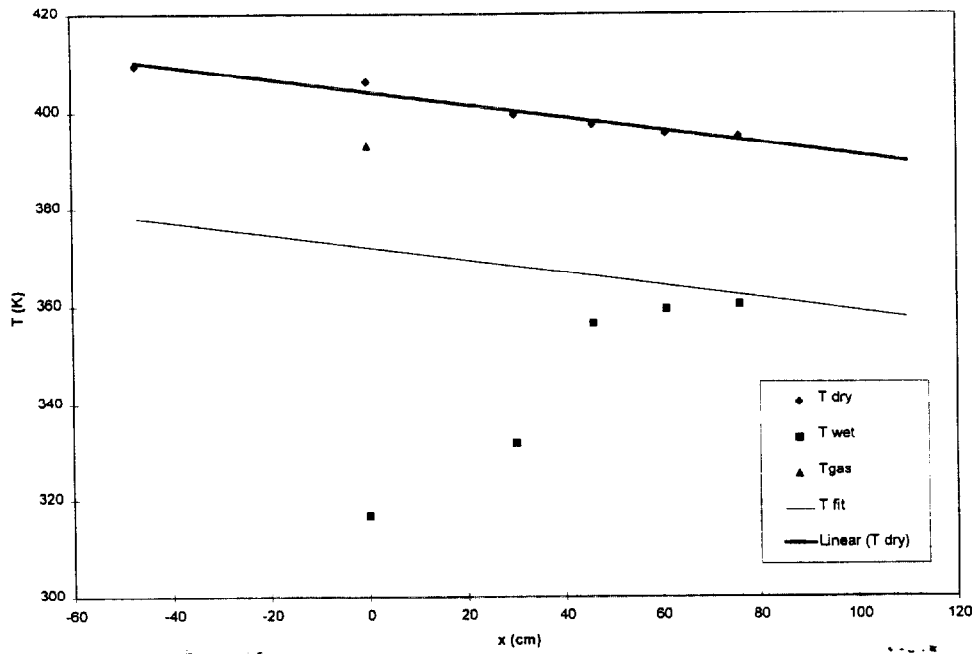


Figure 1. Steady-state temperatures along the duct.

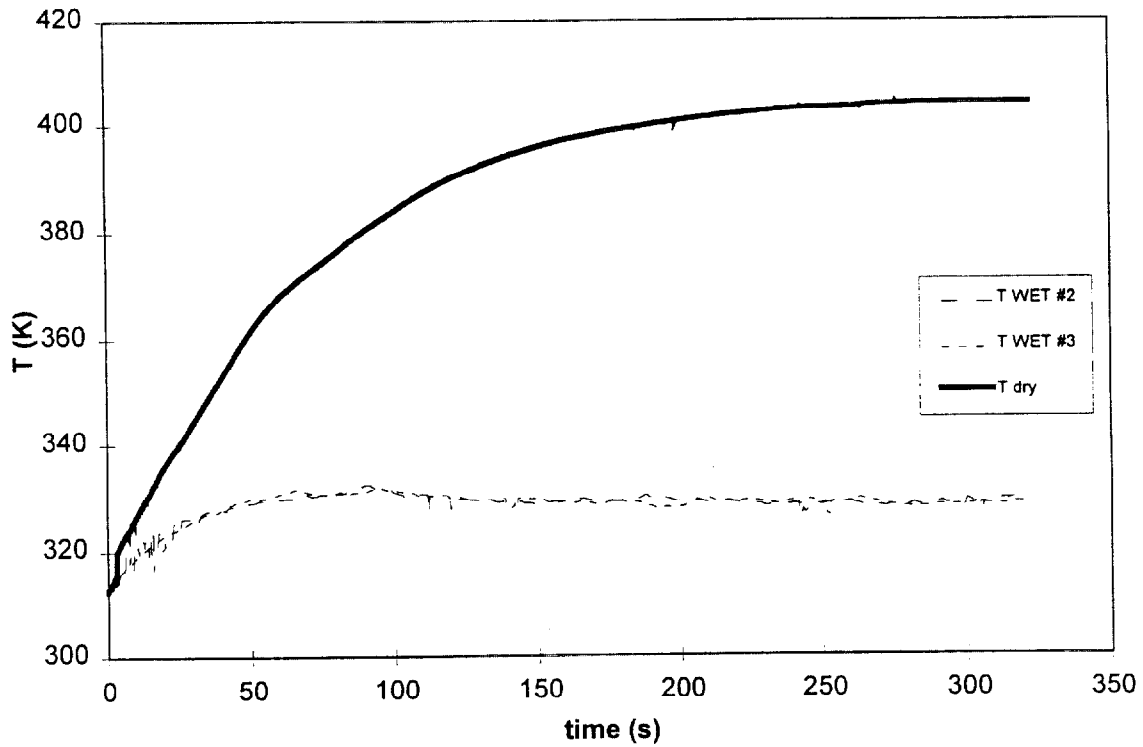


Figure 2. Transient probe temperature profiles during plunge tests.

4/12/99 test#2

Task:

One PJ10 spray nozzle water injection
high air velocity (3.6 m/s)
high air temperature ($T_{\text{gas}} = 434 \text{ K}$).

Objectives:

Calculate the response time index (RTI) of the probe and the parameter RHS.

Procedure:

The test consists of two parts:

- 1) Steady-state conditions with water spray on. Plunge test of the probe, with initial temperature $T_0=300 \text{ K}$. Gas velocity and number of water droplets are measured in the test section. The procedure is repeated three times to verify repeatability.
- 2) Steady-state conditions with water spray off. Plunge test of the probe, with initial temperature $T_0=308$ and its transient heating is measured until it reaches steady-state.

	units	Wet conditions	Dry conditions
T_0	K	300	308
T before sprays	K	459	459
T rake #1	K	348	444
T rake #3	K	375	435
T rake #4	K	378	432
T rake #5	K	380	429
T rake #6	K	380	429

Table 1. Temperature at the seven recorded locations.

ΔT_0	K	46		
run #1 u	m/s	4.2 ± 0.1		
run #2 u	m/s	3.2 ± 0.1		
run #3 u	m/s	3.6 ± 0.1		
$u_{\text{average}} \pm \sigma_{n-1}$	m/s	3.6 ± 0.1		
run #1 n (20 samples)		2.2 ± 1.9		
run #2 n (20 samples)		1.5 ± 1.2		
run #3 n (20 samples)		1.9 ± 1.9		
$n_{\text{average}} \pm \sigma_{n-1}$		2.9 ± 1.7		
n_0 [from $n_0(u)$ curve]		3.6		
D	m	$80 \cdot 10^{-6}$		
ϵ	s	1/1000		
A	m^2	$3 \cdot 10^{-5}$		
β		$(7.2 \pm 4.2) \cdot 10^{-6}$		
T_{gas}	K	434		
T_{s0} dry	K	308		
T_{s0} wet	K	300		
RTI		131 ± 24		
		hot/wet cond.#1	hot/wet cond.#2	hot/wet cond.#3
RHS		16.4 ± 0.1	16.3 ± 0.0	16.3 ± 0.1
$\frac{T^{\text{DRY}} - T}{T^{\text{DRY}} - T_0}$		0.72 ± 0.01	0.63 ± 0.02	0.65 ± 0.02

Table 2. Test parameters.

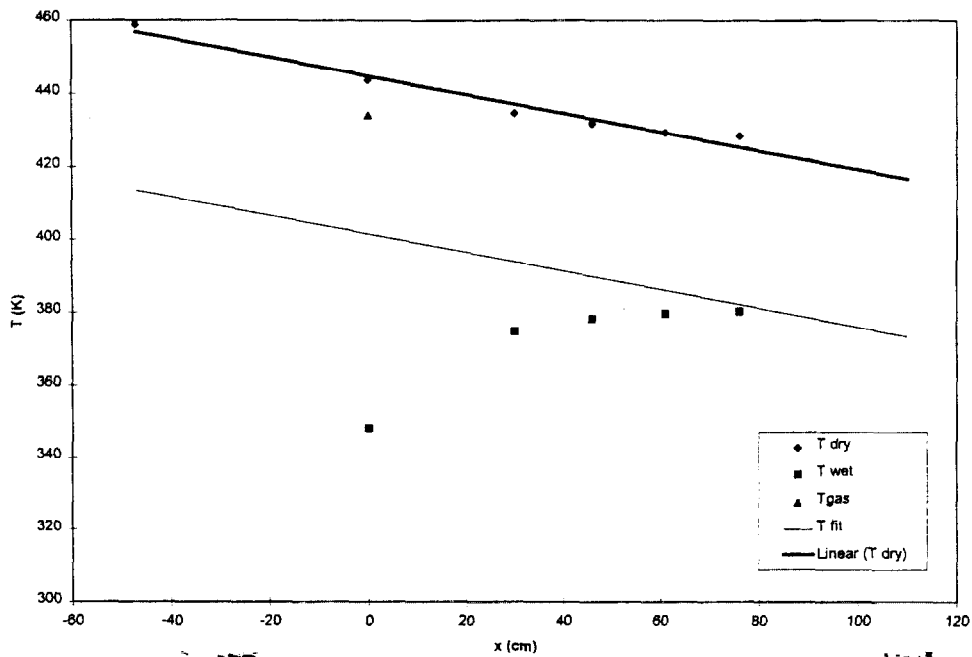


Figure 1. Steady-state temperatures along the duct.

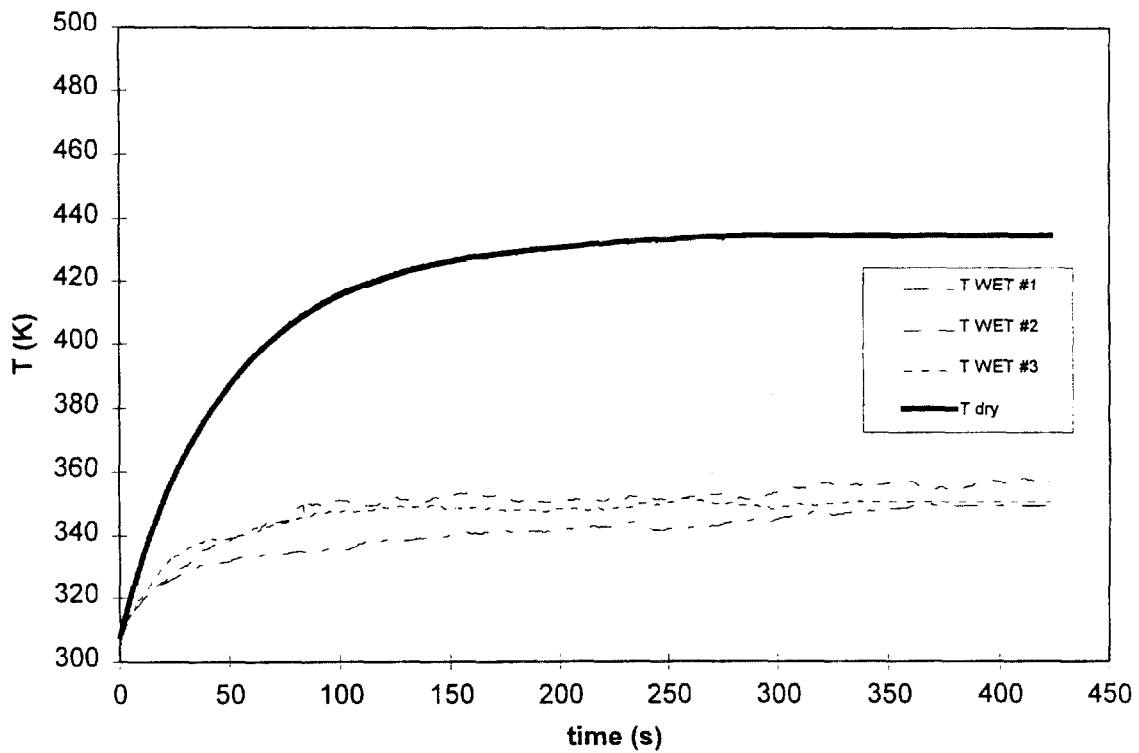


Figure 2. Transient probe temperature profiles during plunge tests.

4/14/99

Task: One PJ10 spray nozzle water injection
high air velocity (3.6 m/s)
high air temperature ($T_{\text{gas}} = 379 \text{ K}$).

Objectives: Calculate the response time index (RTI) of the probe and the parameter RHS.

Procedure: The test consists of two parts:

- 1) Steady-state conditions with water spray on. Plunge test of the probe, with initial temperature $T_0=300 \text{ K}$. Gas velocity and number of water droplets are measured in the test section. The procedure is repeated three times to verify repeatability.
- 2) Steady-state conditions with water spray off. Plunge test of the probe, with initial temperature $T_0=310$ and its transient heating is measured until it reaches steady-state.

	units	Wet conditions	Dry conditions
T_0	K	300	310
T before sprays	K	394	394
T rake #1	K	317	388
T rake #3	K	349	382
T rake #4	K	352	380
T rake #5	K	353	378
T rake #6	K	352	378

Table 1. Temperature at the seven recorded locations.

ΔT_0	K	24		
run #1 u	m/s	3.5 ± 0.1		
run #2 u	m/s	3.6 ± 0.1		
run #3 u	m/s	3.6 ± 0.1		
$u_{\text{average}} \pm \sigma_{n-1}$	m/s	3.6 ± 0.1		
run #1 n (20 samples)		2.4 ± 2.4		
run #2 n (20 samples)		2.1 ± 2.1		
run #3 n (20 samples)		2.4 ± 2.4		
$n_{\text{average}} \pm \sigma_{n-1}$		2.3 ± 2.3		
n_0 [from $n_0(u)$ curve]		3.6		
D	m	$80 \cdot 10^{-6}$		
ε	s	1/1000		
A	m ²	$3 \cdot 10^{-5}$		
β		$(5.7 \pm 5.7) \cdot 10^{-6}$		
T_{gas}	K	379		
T_{s0} dry	K	310		
T_{s0} wet	K	300		
RTI		76 ± 10		
		hot/wet cond.#1	hot/wet cond.#2	hot/wet cond.#3
RHS		16.2 ± 0.1	16.2 ± 0.1	16.3 ± 0.0
$\frac{T^{\text{DRY}} - T}{T^{\text{DRY}} - T_0}$		0.86 ± 0.05	0.87 ± 0.04	0.89 ± 0.03

Table 2. Test parameters.

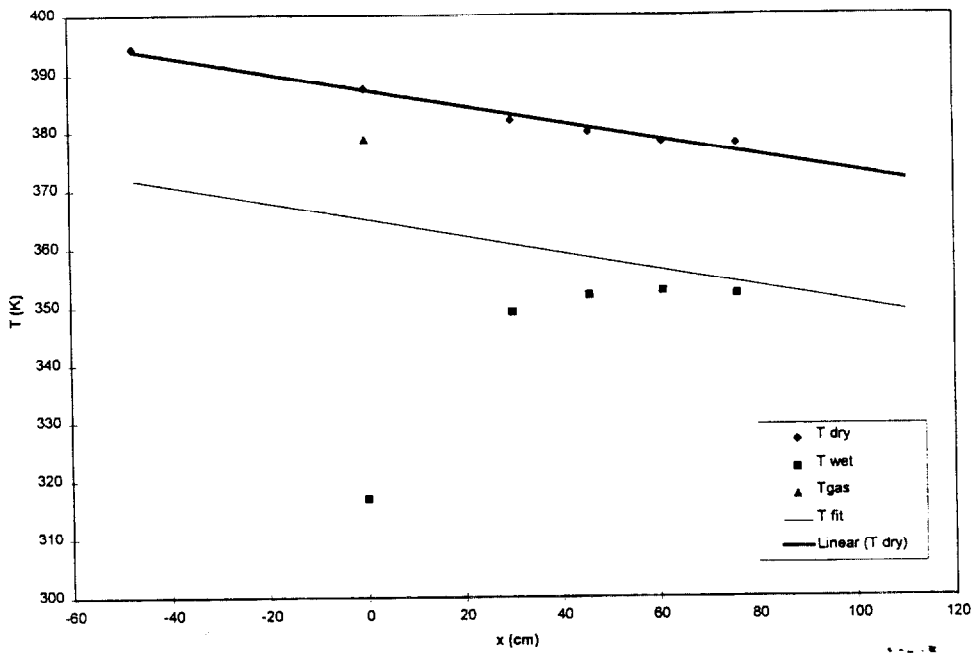


Figure 1. Steady-state temperatures along the duct.

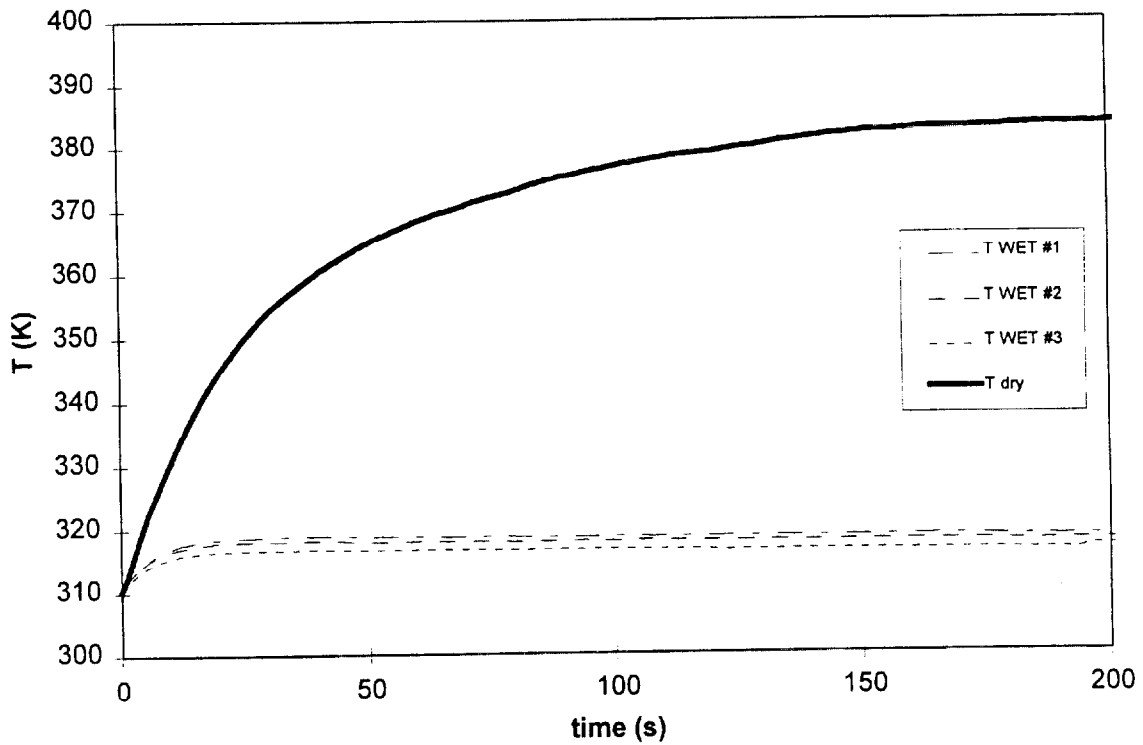


Figure 2. Transient probe temperature profiles during plunge tests.

4/15/99

Task: One PJ10 spray nozzle water injection
high air velocity (4.6 m/s)
high air temperature ($T_{\text{gas}} = 372 \text{ K}$).

Objectives: Calculate the response time index (RTI) of the probe and the parameter RHS.

Procedure: The test consists of two parts:

- 1) Steady-state conditions with water spray on. Plunge test of the probe, with initial temperature $T_0=300 \text{ K}$. Gas velocity and number of water droplets are measured in the test section. The procedure is repeated three times to verify repeatability.
- 2) Steady-state conditions with water spray off. Plunge test of the probe, with initial temperature $T_0=313$ and its transient heating is measured until it reaches steady-state.

	units	Wet conditions	Dry conditions
T_0	K	300	313
T before sprays	K	392	392
T rake #1	K	315	386
T rake #3	K	329	380
T rake #4	K	338	378
T rake #5	K	343	377
T rake #6	K	347	377

Table 1. Temperature at the seven recorded locations.

ΔT_0	K	22		
run #1 u	m/s	4.8 ± 0.1		
run #2 u	m/s	4.7 ± 0.1		
run #3 u	\bar{m}/s	4.4 ± 0.3		
$u_{\text{average}} \pm \sigma_{n-1}$	m/s	4.6 ± 0.2		
run #1 n (20 samples)		1.6 ± 1.6		
run #2 n (20 samples)		1.8 ± 1.8		
run #3 n (20 samples)		1.7 ± 1.7		
$n_{\text{average}} \pm \sigma_{n-1}$		1.7 ± 1.7		
n_0 [from $n_0(u)$ curve]		4.5		
D	m	$80 \cdot 10^{-6}$		
ϵ	s	1/1000		
A	m^2	$3 \cdot 10^{-5}$		
β		$(3.3 \pm 3.3) \cdot 10^{-6}$		
T_{gas}	K	372		
T_{s0} dry	K	315		
T_{s0} wet	K	300		
RTI		72 ± 8		
		hot/wet cond.#1	hot/wet cond.#2	hot/wet cond.#3
RHS		16.6 ± 0.3	16.6 ± 0.1	16.7 ± 0.1
$\frac{T^{\text{DRY}} - T}{T^{\text{DRY}} - T_0}$		0.79 ± 0.06	0.80 ± 0.06	0.83 ± 0.05

Table 2. Test parameters.

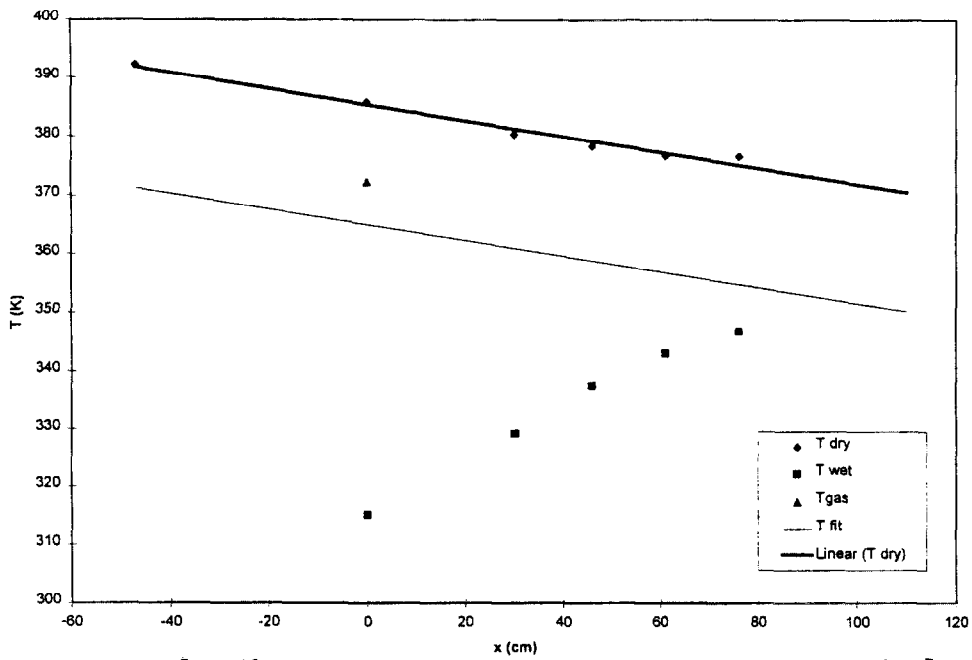


Figure 1. Steady-state temperatures along the duct.

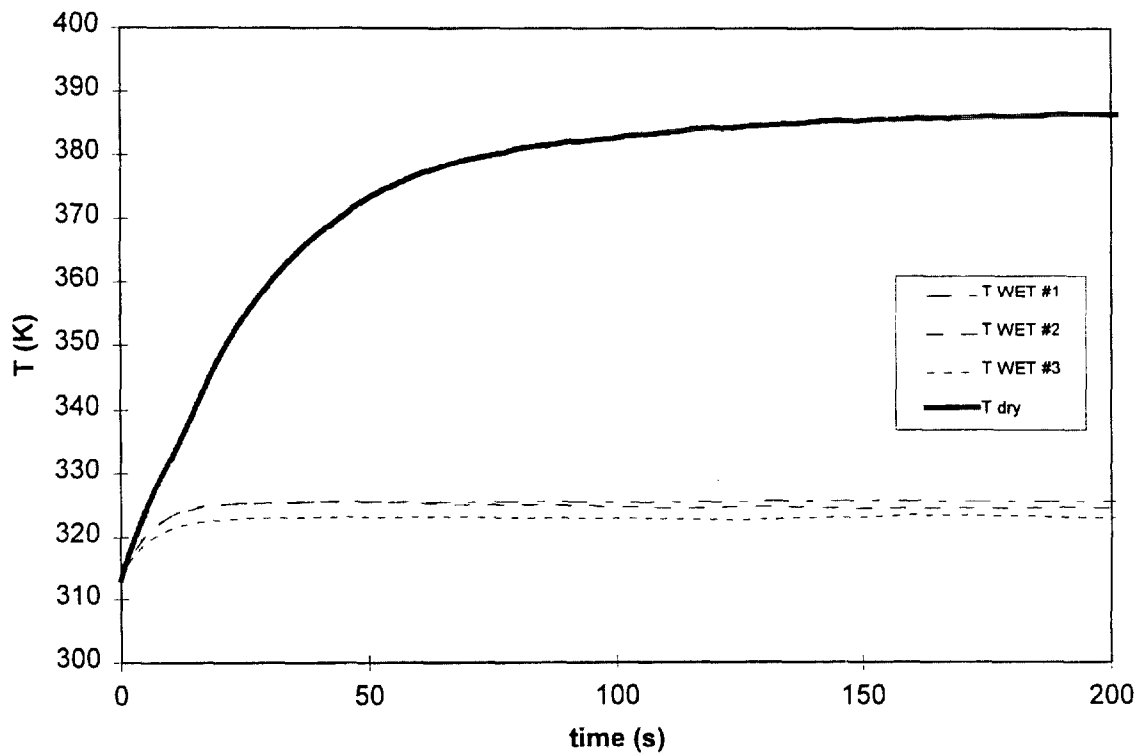


Figure 2. Transient probe temperature profiles during plunge tests.

4/16/99

Task: One PJ10 spray nozzle water injection
high air velocity (5.8 m/s)
high air temperature ($T_{\text{gas}} = 411 \text{ K}$).

Objectives: Calculate the response time index (RTI) of the probe and the parameter RHS.

Procedure: The test consists of two parts:

- 1) Steady-state conditions with water spray on. Plunge test of the probe, with initial temperature $T_0=300 \text{ K}$. Gas velocity and number of water droplets are measured in the test section. The procedure is repeated three times to verify repeatability.
- 2) Steady-state conditions with water spray off. Plunge test of the probe, with initial temperature $T_0=310$ and its transient heating is measured until it reaches steady-state.

	units	Wet conditions	Dry conditions
T_0	K	300	310
T before sprays	K	440	440
T rake #1	K	329	422
T rake #3	K	386	420
T rake #4	K	390	417
T rake #5	K	391	416
T rake #6	K	391	413

Table 1. Temperature at the seven recorded locations.

ΔT_0	K	19		
run #1 u	m/s	6.0 ± 0.1		
run #2 u	m/s	5.7 ± 0.1		
run #3 u	m/s	5.7 ± 0.1		
$u_{\text{average}} \pm \sigma_{n-1}$	m/s	5.8 ± 0.1		
run #1 n (20 samples)		2.7 ± 1.8		
run #2 n (20 samples)		2.2 ± 1.9		
run #3 n (20 samples)		2.3 ± 1.95		
$n_{\text{average}} \pm \sigma_{n-1}$		2.4 ± 1.9		
n_0 [from $n_0(u)$ curve]		5.4		
D	m	$80 \cdot 10^{-6}$		
ϵ	s	1/1000		
A	m^2	$3 \cdot 10^{-5}$		
β		$(3.7 \pm 2.9) \cdot 10^{-6}$		
T_{gas}	K	411		
T_{s0} dry	K	310		
T_{s0} wet	K	300		
RTI		68 ± 8		
		hot/wet cond.#1	hot/wet cond.#2	hot/wet cond.#3
RHS		Not Valid	16.6 ± 0.1	16.6 ± 0.1
$\frac{T^{\text{DRY}} - T}{T^{\text{DRY}} - T_0}$		Not Valid	0.83 ± 0.05	0.84 ± 0.05

Table 2. Test parameters.

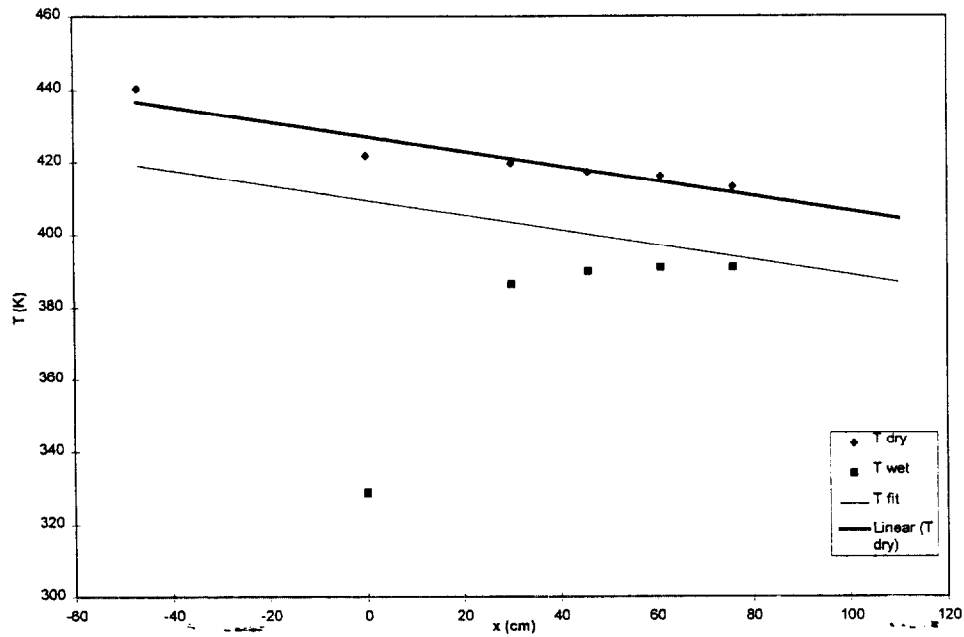


Figure 1. Steady-state temperatures along the duct.

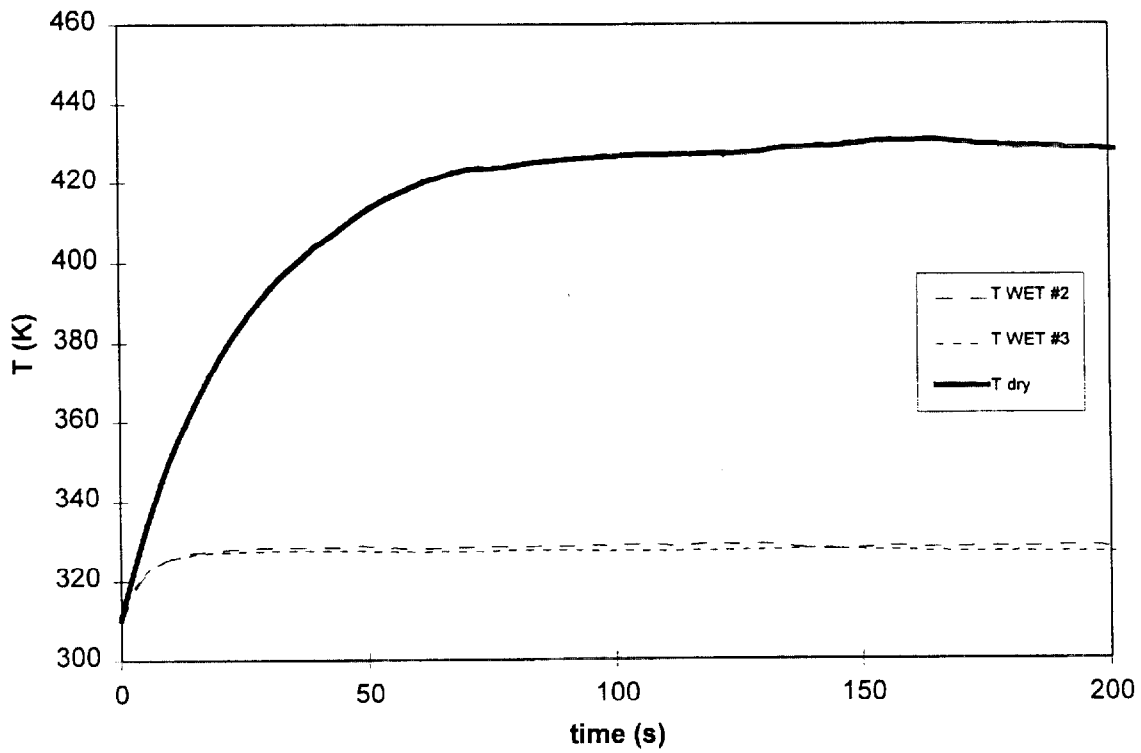


Figure 2. Transient probe temperature profiles during plunge tests.

4/19/99

Task: One PJ10 spray nozzle water injection
high air velocity (4.1 m/s)
high air temperature ($T_{\text{gas}} = 378 \text{ K}$).

Objectives: Calculate the response time index (RTI) of the probe and the parameter RHS.

Procedure: The test consists of two parts:

- 1) Steady-state conditions with water spray on. Plunge test of the probe, with initial temperature $T_0=300 \text{ K}$. Gas velocity and number of water droplets are measured in the test section. The procedure is repeated three times to verify repeatability.
- 2) Steady-state conditions with water spray off. Plunge test of the probe, with initial temperature $T_0=305 \text{ K}$ and its transient heating is measured until it reaches steady-state.

	units	Wet conditions	Dry conditions
T_0	K	300	305
T before sprays	K	388	388
T rake #1	K	311	382
T rake #3	K	357	378
T rake #4	K	362	376
T rake #5	K	364	374
T rake #6	K	364	374

Table 1. Temperature at the seven recorded locations.

ΔT_0	K	8		
run #1 u	m/s	4.3 ± 0.2		
run #2 u	m/s	4.0 ± 0.1		
run #3 u	m/s	4.1 ± 0.1		
$u_{\text{average}} \pm \sigma_{n-1}$	m/s	4.1 ± 0.1		
run #1 n (20 samples)		1.7 ± 1.7		
run #2 n (20 samples)		2.3 ± 2.5		
run #3 n (20 samples)		2.1 ± 1.5		
$n_{\text{average}} \pm \sigma_{n-1}$		2.0 ± 1.9		
n_0 [from $n_0(u)$ curve]		4.1		
D	m	$80 \cdot 10^{-6}$		
ε	s	1/1000		
A	m ²	$3 \cdot 10^{-5}$		
β		$(4.4 \pm 4.2) \cdot 10^{-6}$		
T_{gas}	K	378		
T_{s0} dry	K	305		
T_{s0} wet	K	300		
RTI		72 ± 4		
		hot/wet cond.#1	hot/wet cond.#2	hot/wet cond.#3
RHS		16.5 ± 0.3	16.6 ± 0.2	16.6 ± 0.2
$\frac{T^{\text{DRY}} - T}{T^{\text{DRY}} - T_0}$		0.80 ± 0.05	0.80 ± 0.04	0.88 ± 0.03

Table 2. Test parameters.

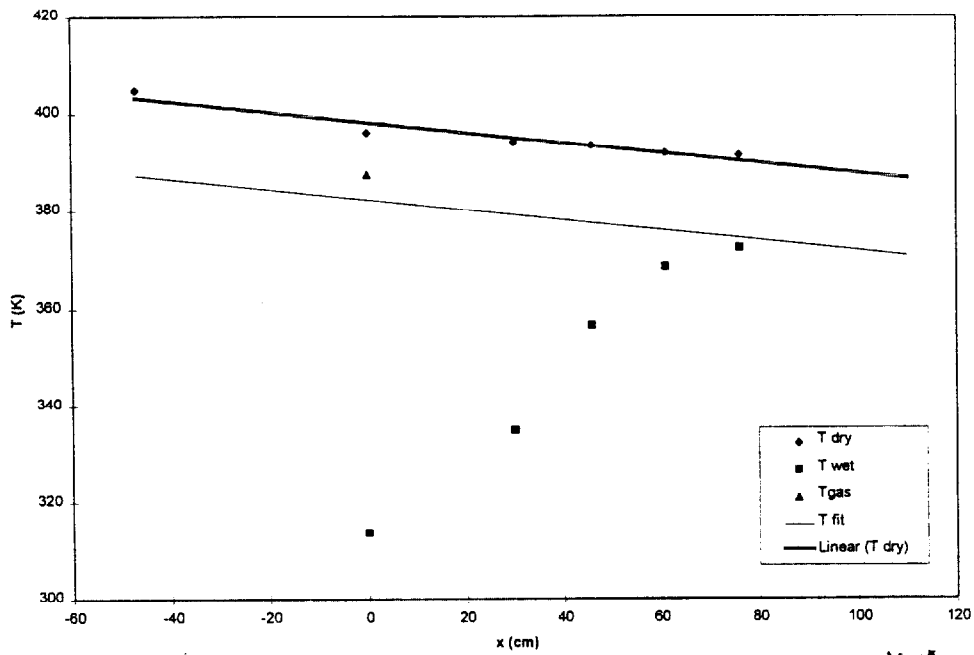


Figure 1. Steady-state temperatures along the duct.

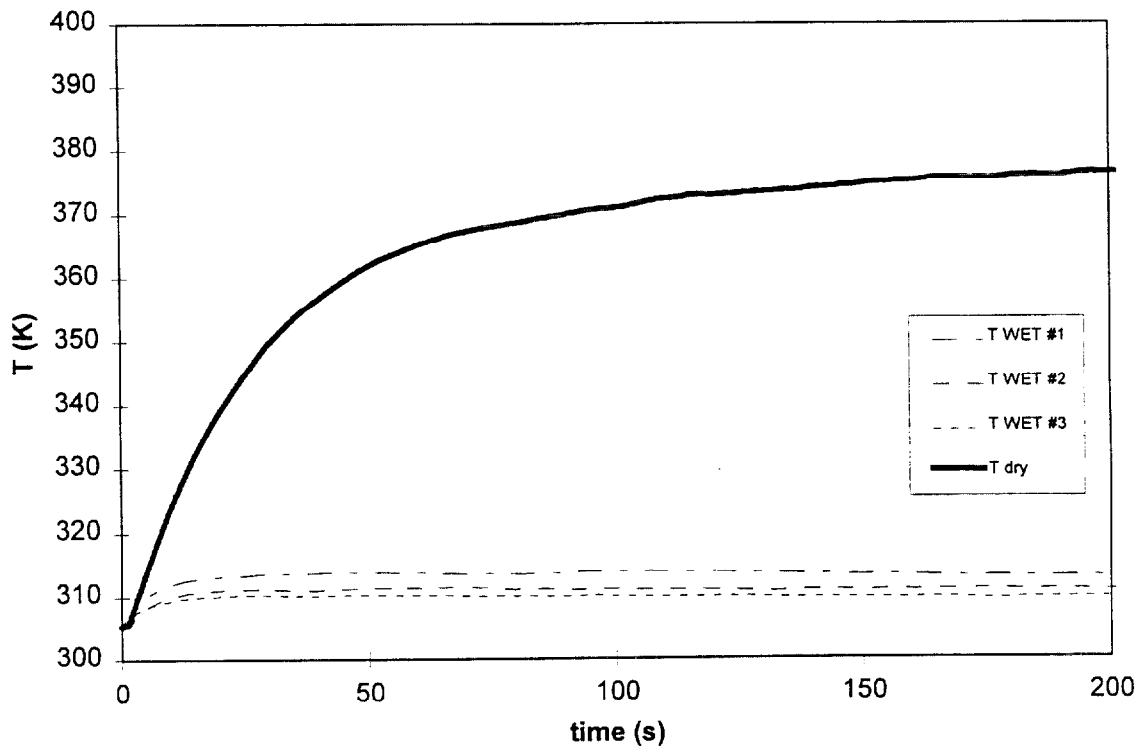


Figure 2. Transient probe temperature profiles during plunge tests.

4/19/99 test #2

Task:

One PJ10 spray nozzle water injection
high air velocity (5.3 m/s)
high air temperature ($T_{\text{gas}} = 427 \text{ K}$).

Objectives:

Calculate the response time index (RTI) of the probe and the parameter RHS.

Procedure:

The test consists of two parts:

- 1) Steady-state conditions with water spray on. Plunge test of the probe, with initial temperature $T_0=300 \text{ K}$. Gas velocity and number of water droplets are measured in the test section. The procedure is repeated three times to verify repeatability.
- 2) Steady-state conditions with water spray off. Plunge test of the probe, with initial temperature $T_0=308 \text{ K}$ and its transient heating is measured until it reaches steady-state.

	units	Wet conditions	Dry conditions
T_0	K	300	308
T before sprays	K	448	448
T rake #1	K	334	437
T rake #3	K	379	430
T rake #4	K	384	426
T rake #5	K	387	424
T rake #6	K	388	422

Table 1. Temperature at the seven recorded locations.

ΔT_0	K	29		
run #1 u	m/s	4.9 ± 0.2		
run #2 u	m/s	5.5 ± 0.1		
run #3 u	\bar{m}/s	5.6 ± 0.1		
$u_{\text{average}} \pm \sigma_{n-1}$	m/s	5.3 ± 0.1		
run #1 n (20 samples)		3.8 ± 2.8		
run #2 n (20 samples)		2.5 ± 2.5		
run #3 n (20 samples)		3.3 ± 3.0		
$n_{\text{average}} \pm \sigma_{n-1}$		3.3 ± 2.8		
n_0 [from $n_0(u)$ curve]		5.0		
D	m	$80 \cdot 10^{-6}$		
ϵ	s	1/1000		
A	m^2	$3 \cdot 10^{-5}$		
β		$(5.6 \pm 4.4) \cdot 10^{-6}$		
T_{gas}	K	427		
T_{s0} dry	K	308		
T_{s0} wet	K	300		
RTI		71 ± 9		
		hot/wet cond.#1	hot/wet cond.#2	hot/wet cond.#3
RHS		16.6 ± 0.2	16.6 ± 0.1	16.7 ± 0.2
$\frac{T^{\text{DRY}} - T}{T^{\text{DRY}} - T_0}$		0.82 ± 0.05	0.82 ± 0.05	0.83 ± 0.05

Table 2. Test parameters.

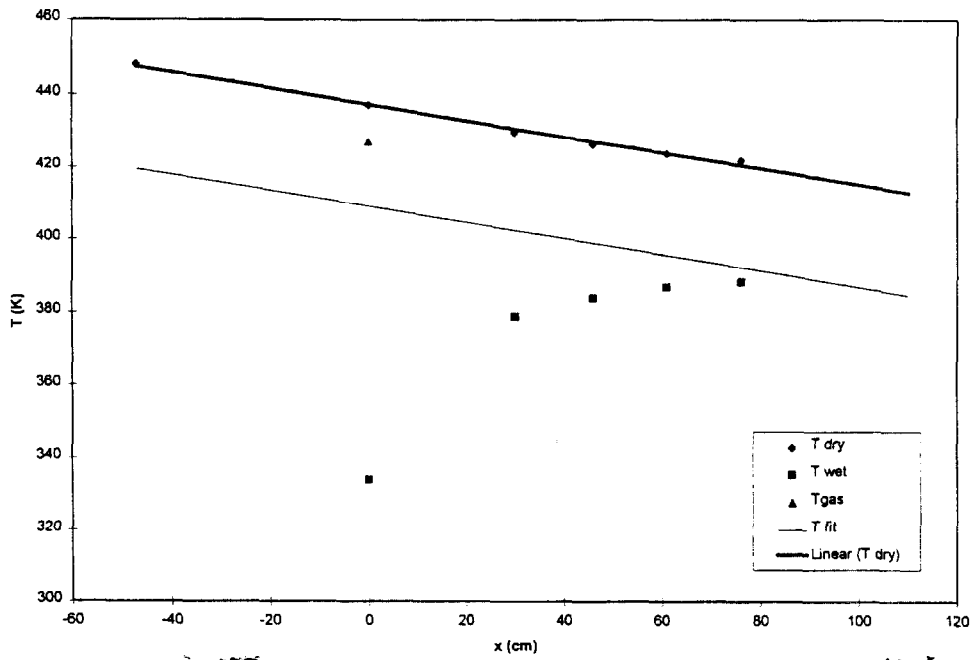


Figure 1. Steady-state temperatures along the duct.

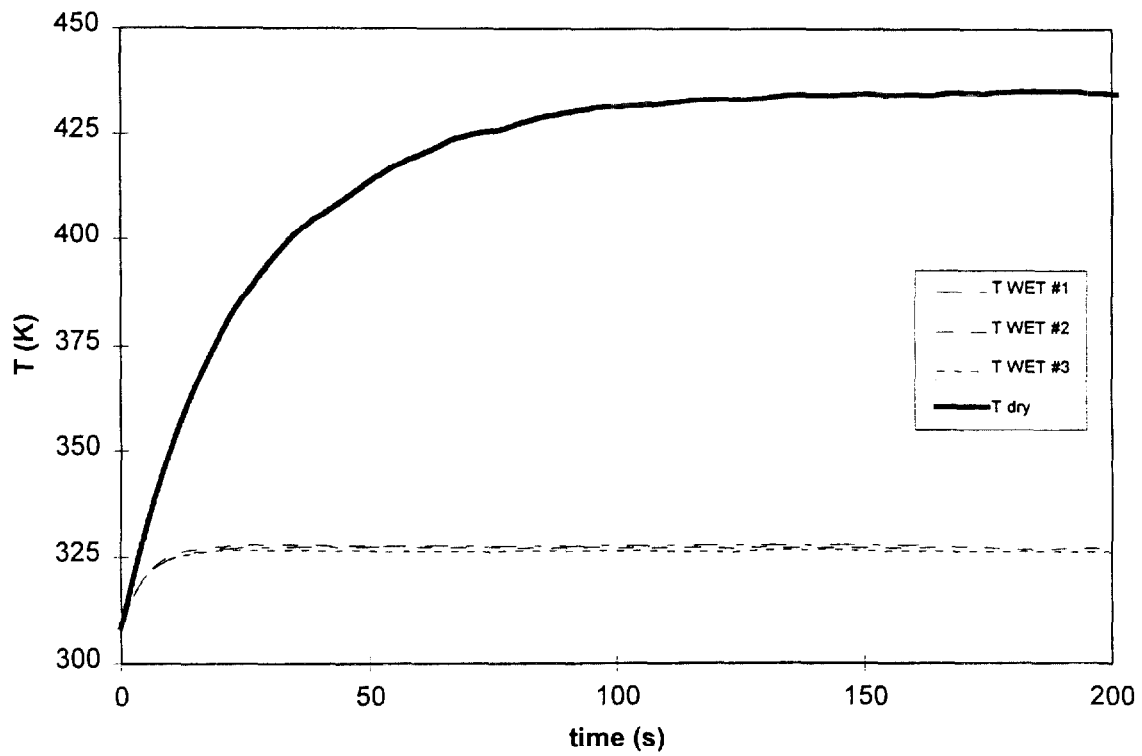


Figure 2. Transient probe temperature profiles during plunge tests.

NIST-114 (REV. 11-94) ADMAN 4.09	U.S. DEPARTMENT OF COMMERCE NATIONAL INSTITUTE OF STANDARDS AND TECHNOLOGY	(ERB USE ONLY) ERB CONTROL NUMBER DIVISION	
MANUSCRIPT REVIEW AND APPROVAL		PUBLICATION REPORT NUMBER	CATEGORY CODE
		NIST GCR 99-776	NUMBER PRINTED PAGES
INSTRUCTIONS: ATTACH ORIGINAL OF THIS FORM TO ONE (1) COPY OF MANUSCRIPT AND SEND TO THE SECRETARY, APPROPRIATE EDITORIAL REVIEW BOARD.		PUBLICATION DATE	NUMBER PRINTED PAGES
TITLE AND SUBTITLE (CITE IN FULL)		July 1999	
The Effect of Minute Water Droplets on a Simulated Sprinkler Link Thermal Response			
CONTRACT OR GRANT NUMBER 60NANB8D0012	TYPE OF REPORT AND/OR PERIOD COVERED Final Report		
AUTHOR(S) (LAST NAME, FIRST INITIAL, SECOND INITIAL) Gavelli, F., Ruffino, P., Anderson, G., and di Marzo, M.	PERFORMING ORGANIZATION (CHECK (X) ONE BLOCK) <input checked="" type="checkbox"/> NIST/GAITHERSBURG <input type="checkbox"/> NIST/BOULDER <input type="checkbox"/> JILA/BOULDER		
LABORATORY AND DIVISION NAMES (FIRST NIST AUTHOR ONLY)			
BFRL/Fire Safety Engineering Division			
SPONSORING ORGANIZATION NAME AND COMPLETE ADDRESS (STREET, CITY, STATE, ZIP)			
Department of Commerce National Institute of Standards and Technology, Gaithersburg, MD 20899			
PROPOSED FOR NIST PUBLICATION			
<input type="checkbox"/> JOURNAL OF RESEARCH (NIST JRES) <input type="checkbox"/> J. PHYS. & CHEM. REF. DATA (JPCRD) <input type="checkbox"/> HANDBOOK (NIST HB) <input type="checkbox"/> SPECIAL PUBLICATION (NIST SP) <input type="checkbox"/> TECHNICAL NOTE (NIST TN)	<input type="checkbox"/> MONOGRAPH (NIST MN) <input type="checkbox"/> NATL. STD. REF. DATA SERIES (NIST NSRDS) <input type="checkbox"/> FEDERAL INF. PROCESS. STDS. (NIST FIPS) <input type="checkbox"/> LIST OF PUBLICATIONS (NIST LP) <input type="checkbox"/> NIST INTERAGENCY/INTERNAL REPORT (NISTIR)	<input type="checkbox"/> LETTER CIRCULAR <input type="checkbox"/> BUILDING SCIENCE SERIES <input type="checkbox"/> PRODUCT STANDARDS <input checked="" type="checkbox"/> OTHER NIST GCR	
PROPOSED FOR NON-NIST PUBLICATION (CITE FULLY)	<input type="checkbox"/> U.S.	<input type="checkbox"/> FOREIGN	PUBLISHING MEDIUM <input type="checkbox"/> PAPER <input type="checkbox"/> DISKETTE (SPECIFY) _____ <input type="checkbox"/> OTHER (SPECIFY) _____ <input type="checkbox"/> CD-ROM
SUPPLEMENTARY NOTES			
ABSTRACT (A 2000-CHARACTER OR LESS FACTUAL SUMMARY OF MOST SIGNIFICANT INFORMATION. IF DOCUMENT INCLUDES A SIGNIFICANT BIBLIOGRAPHY OR LITERATURE SURVEY, CITE IT HERE. SPELL OUT ACRONYMS ON FIRST REFERENCE.) (CONTINUE ON SEPARATE PAGE, IF NECESSARY.)			
This report presents the derivation of an improved model for the prediction of the transient thermal response of a ceiling-mounted fire detection sprinkler link in the event of a fire. The model expands the range of applicability of the current approach to include the presence of minute water droplets being carried by the hot gas plume. This situation has been observed experimentally in situations where a fire develops in an enclosed space equipped with an array of sprinklers: the activation of the first sprinkler releases a fine water spray, part of which is entrained by the rising plume and affects the operation of the surrounding devices.			
KEY WORDS (MAXIMUM OF 9; 28 CHARACTERS AND SPACES EACH; SEPARATE WITH SEMICOLONS; ALPHABETIC ORDER; CAPITALIZE ONLY PROPER NAMES)			
ceilings; droplets; fire models; fire plumes; heat transfer; thermal analysis; water sprays			
AVAILABILITY <input checked="" type="checkbox"/> UNLIMITED <input type="checkbox"/> FOR OFFICIAL DISTRIBUTION - DO NOT RELEASE TO NTIS <input type="checkbox"/> ORDER FROM SUPERINTENDENT OF DOCUMENTS, U.S. GPO, WASHINGTON, DC 20402 <input checked="" type="checkbox"/> ORDER FROM NTIS, SPRINGFIELD, VA 22161			NOTE TO AUTHOR(S): IF YOU DO NOT WISH THIS MANUSCRIPT ANNOUNCED BEFORE PUBLICATION, PLEASE CHECK HERE. <input type="checkbox"/>